Excitatory Amino Acid Transporters: Structural and Functional Insights Achieved through Thiol-modification of Cysteine Substitutions

By

Rebecca Pauline Seal

A DISSERTATION

Presented to the Neuroscience Graduate Program and the Oregon Health Sciences University School of Medicine in partial fulfillment of the requirements for the degree of Doctor of Philosophy

December 1998

School of Medicine
Oregon Health Sciences University

CERTIFICATE OF APPROVAL

This is to certify that the Ph.D. thesis of

Rebecca Pauline Seal

has been approved

[redacted]

Advisor

[redacted]

Committee Chair

[redacted]

Member

[redacted]

Member

[redacted]

Member

Associate Dean for Graduate Studies

Acknowledgments

I am thankful to everyone who contributed something to my life during graduate school whether it was in the lab, in the classroom, at home or in a pub.

I am extremely grateful to my advisor Susan Amara, who was always supportive and who went well beyond my greatest hopes for a mentor. I am proud to have been under her tutelage and to have shared an interest not only in our research, but in business and the world of biotech/pharmaceuticals. I hope that we continue to share in them through the years.

A big thank you to all of the scientists in the Amara lab with whom I shared ideas and/ or reagents, and who graciously gave me their time and their thoughts: Tien Ngyen, Jeff Arriza, Eva Shannon, Mark Sonders, Wendy Fairman, Krishna Prasad, Peter Poerzgen, Spencer Watts, Kevin Poth, Mary Chalmers, Sonal Das and Gursh Khatra. A special thanks to Gloria Ellis for her help and encouragement through the years.

The one who I am most indebted to is Barbara Leighton, who has worked with me in the last couple of years trying to answer the question of topology and in the process always showing enthusiasm for her work. Her contribution to this thesis is beyond words. I wish her all the best in her future scientific endeavors.

I would like to thank my Committee members for their time and input: Mike Forte, Jack Kaplan, Mike Kavanaugh and Scott Landfear.

Sue Povlock (the maid of honor for my thesis) for her awesome friendship and for being my "Surrogate Susan" when I need someone to give me input on writing my grant or practicing for a presentation.

Gwynn Daniels for agreeing to take on and succeed at the side project of cloning excitatory amino acid transporters from Drosophila.

My dear friends from the "real world" who were always teasing and encouraging me: Allie Cichocki, Carolyn Church, Arthur Daret, Jon Quick and Kelly Brown (who recently entered the real world).

I'd also like to acknowledge friends that I met at OHSU, who were always supportive whether it be in a carpool going each morning to Starbucks for coffee and a Panini Dolce or at the mall getting my ears pierced or staying up until 2am talking: Stephanie Starr, Liz Klamo, Armando Lagrutta, Bethan Jones, Monika Stein, and Martin Kohler.

Lastly and most importantly, I am grateful to my family: my parents and my brother, who were always asking me if I was working hard and who always gave me love and encouragement.

This body of work was supported by a pre-doctoral grant from the National Institute of Mental Health to RPS, a National Institutes of Health grant to SGA, and the Howard Hughes Medical Institute.

Table of Contents

Summary

Sodium-dependent excitatory amino acid (EAA) transporters located in both neurons and glial cells are responsible for clearing synaptically released glutamate from the extracellular milieu and for maintaining glutamate concentrations below neurotoxic levels. The primary structure of the cloned EAA carriers has been the basis for initial models of transporter structure and subsequent experiments have continued to address the transmembrane topology and the structural determinants that underlie transporter function. A detailed examination of the function of the carriers expressed in heterologous systems has revealed additional properties of the transporters, including the mediation of uncoupled, substrate-dependent and substrate-independent ion conductances. This information, together with the functional and pharmacological characterization of the EAA carriers will ultimately provide a basis for understanding the mechanism of transport.

The studies described in this dissertation are aimed at resolving the transmembrane topology of the EAA carriers and at examining the functional role of residues located in a highly conserved domain that has been implicated in substrate and co-transported ion interactions. To address these questions, we chemically-modified individual cysteines substituted into functional, surface-expressed carriers in intact cultured cells. By using this system we were able to take advantage of the fact that cysteine substitution is a minor alteration that appears to be very well tolerated and the availability of an expanding array of thiol-specific compounds that exhibit a wide range of chemical properties.

In the first series of experiments, a functional, cysteine-less version of EAAT1 [Cys(-)] was used to examine twenty-four highly conserved residues, P392 through Q415, for their contribution to the transport mechanism. It was determined that a majority of the functional cysteine mutants react with MTSEA, which suggests that much of this domain is in an aqueous environment. Also, cysteines substituted for one residue at each end of the domain (A395C and A414C), react with membrane impermeant reagents MTSET and

MTSES, supporting a model that places these residues near the extracellular surface. In addition, transporter substrates and inhibitors block the reaction between MTS-derivatives and A395C, while the co-substrate sodium slows the reaction of MTSEA with the Y405C and E406C residues, consistent with their suggested role in co-transported cation interactions. From these results, we propose that this domain forms a re-entrant membrane loop at the cell surface similar to ones found in a number of ion channels and thus, may comprise part of pore for the translocation of substrates and co-transported ions or for the uncoupled flux of ions.

A second goal of this work was to evaluate the transmembrane topology. Previous studies have established the presence of six α-helical transmembrane domains (TMs) in the first half of the carrier, but the number and orientation of TMs in the latter half remains unclear. To address the topology of this domain, individual residues in the C-terminus of Cys(-) were mutated to cysteine and their extracellular accessibility evaluated in only those mutants which were functional and surface-expressed. Cysteine substitutions were labeled with membrane impermeant and then biotin-containing derivatives of thiol-reactive compounds in intact COS-7 cells. A number of residues were reactive with the impermeant compounds, suggesting that they reside either in the extracellular space or in an aqueous intermembrane compartment that is accessible to the extracellular milieu. Based on these residues, it appears that unlike the sodium and chloride-dependent neurotransmitter transporter family, which are presumed to have six α-helical TMs in their C-terminal domain, the EAA carriers have several short TM segments that could be modeled as β-strands or as non-periodic, including a re-entrant loop as was suggested by the experiments examining the effects of thiol-modification on function.

Our analysis of EAAT1 has demonstrated the importance of residues in the C-terminal region to transporter function and has revealed a complex topology for this region, which includes a re-entrant loop domain similar to those identified in ion channels. Although a detailed model of the structure of the entire C-terminal region has not yet been

attained, we have developed in these studies several tools with which to further delineate the topology, as well as the structural determinants that underlie substrate transport and the ion conductances.

A re-entrant loop domain in the glutamate carrier EAAT1 participates in substrate binding and translocation

Rebecca P. Seal† and Susan G. Amara*
†Program in Neuroscience and *Howard Hughes Medical Institute, Vollum Institute, Oregon Health Sciences University, Portland, Oregon 97201

Running Title: Cysteine-scanning mutagenesis of EAAT1

Corresponding Author:
Susan G. Amara
Vollum Institute L- 474
Oregon Health Sciences University
3181 S.W. Sam Jackson Park Rd.
Portland, OR 97201
amaras@ohsu.edu
Tel: (503) 494-6723
Fax: (503) 494-8320

Published in Neuron, Vol. 21, 1487-1498 (1998)

Summary

To investigate the structural determinants underlying transport by Na^+-dependent glutamate carriers, we examined the contribution of twenty-four highly conserved residues of EAAT1, P392 through Q415, using the Substituted Cysteine Accessibility Method (SCAM). When substituted with cysteine the majority of the residues are accessible to the sulfhydryl modifying reagent MTSEA suggesting that much of this domain is in an aqueous environment. The membrane impermeant reagents, MTSES and MTSET react with only one residue at each end of the domain (A395C and A414C), supporting a model that places these residues near the extracellular surface. Substrates and inhibitors of the carrier block the reaction between MTS-derivatives and the side-chain of A395C, but not A414C. Sodium ions slow the rate of the MTSEA reaction of the side-chains of Y405C and E406C consistent with their suggested role in cation interactions. Finally, the extent to which MTS-derivatives inhibit the transport activity of A414C is dependent on the size of the substituent that is added to the side-chain. From these results, we propose that this domain forms a re-entrant membrane loop at the cell surface and may comprise part of the translocation pore for substrates and/or co-transported ions.

Introduction

Sodium-dependent glutamate transporters contribute to the process of excitatory transmission by buffering and removing synaptically released glutamate (Tong and Jahr, 1994; Mennerick and Zorumski, 1994; Otis et al., 1996; Diamond and Jahr, 1997). By maintaining extracellular glutamate concentrations at low micromolar levels, they also contribute to the prevention of excitotoxic mechanisms of cell death (Szatkowki and Attwell, 1994). The electrogenic uptake of excitatory amino acids (EAAs) by these carriers is coupled to the electrochemical gradient of sodium ions (Kanner and Sharon, 1978). Although the transport of substrates appears to occur by a classical carrier-mediated co-transport mechanism, application of substrates to these carriers also appears to elicit a chloride conductance that is thermodynamically uncoupled from substrate movement (Eliasof and Werblin, 1993; Wadiche et al., 1995a; Fairman et al., 1995; Picaud et al., 1995a). The ability to mediate a substrate-activated chloride conductance suggests that these molecules may also modulate cell excitability (Picaud et al., 1995b). Thus, as mediators of both transport and ion channel activities, EAA transporters (EAATs) have the potential to modulate synaptic transmission through the simultaneous execution of multiple functions.

Although several members of the EAAT family have been cloned and characterized (Pines et al., 1992; Kanai and Hediger, 1992; Storck et al., 1992; Arriza et al., 1994; Fairman et al., 1995; Arriza et al., 1997), the structural elements of the carrier that contribute to ion binding, substrate transport and anion permeation have not yet been resolved. Several lines of evidence point to the functional importance of a putative membrane-spanning region (TM) from residues P392 through Q415 (TM 8 by hydropathy analysis). This highly conserved region contains a motif (AAXFIAQ) that is found in all members of this carrier family, including an invertebrate sodium-dependent EAA carrier from *D. melanogaster* (dEAAT) (Seal et al., 1998a), a proton-dependent glutamate transporter from E. coli (GltP) (Tolner et al., 1992) and a dicarboxylate carrier from R.

meliloti (DctA) (Bolton et al., 1986). Experimental evidence to support the importance of this region in substrate and co-transported ion interactions has come from studies of chimeric and site-directed mutant transporters. Chimeras made between kainate sensitive (EAAT2) and insensitive (EAAT1) subtypes of the human EAAT carriers demonstrated that kainate, a constrained analog of glutamate that acts as a competitive inhibitor, appears to interact with this domain (Vandenberg et al., 1995). Additional evidence highlighting the importance of this region has come from the evaluation of site-directed mutants of the GLT-1 transporter (rat homolog of EAAT2) that appear to influence substrate interactions with the carrier, including D398, Y403 and E404 (Pines et al., 1995; Kavanaugh et al., 1997; Zhang et al., 1998). Finally, although several groups have investigated the transmembrane topologies for members of this family, the C-terminal half of the carrier, which includes this domain remains ambiguous (Jording and Puhler, 1993; Wahle and Stoffel, 1996; Slotboom et al., 1996). For these reasons, we have systematically evaluated twenty-four amino acid residues from P392 to Q415 in the human EAAT1 transporter by the Substituted Cysteine Accessibility Method (SCAM) (Akabas et al., 1992; Akabas et al., 1994) to examine their accessibility to the extracellular milieu and for their contributions to the binding and/or translocation of carrier substrates.

We employed SCAM because, unlike typical mutagenesis paradigms, this approach allows for transporter function to be evaluated both before and after modification of specific residues with cysteine-reactive reagents. Interactions between individual residues and substrates of the transporter can be examined by determining whether the presence of EAA or ion co-substrates alters the kinetics of the reaction of cysteine residues with thiol-modifying reagents. Methanethiosulfonate (MTS)-derivatives react rapidly and specifically with the sulfhydryl moiety of the cysteine residue to create a covalent attachment that introduces either a positively charged ethylamine (MTSEA), a negatively charged ethylsulfonate (MTSES) or a bulkier ethyl trimethylammonium (MTSET) group (Akabas, et al., 1992). These compounds have been shown to react at least a billion times faster with

the unprotonated form of the sulfhydryl moiety (Roberts et al., 1986). Because the ionized, or more reactive form is strongly disfavored by the low dialectric constant of the lipid environment, it is assumed that modification of the side-chains occurs in an aqueous environment (Karlin and Akabas, 1998) .

In this study, we show that one residue at each end of the scanned region, A395C and A414C, is accessible to both of the membrane impermeant reagents, MTSES and MTSET, that membrane permeant MTSEA inhibits the transport activity of a majority of the cysteine substitution mutants, and that the modification rates of three cysteine mutants, A395C, Y405C and E406C are altered by substrates and co-transported ions. These results suggest that, at the cell surface, this region of the carrier has the topological configuration of a re-entrant loop. Like the re-entrant loops found in a number of ion channels, residues in this domain may participate in forming an aqueous pore through which substrates and co-transported ions travel and may directly facilitate their binding and/or translocation during the transport cycle.

Results

Although application of the MTS-derivatives to the wild-type EAAT1 transporter did not alter its transport activity (data not shown), a carrier devoid of cysteine residues (Cys(-)) eliminated the possibility that one or more endogenous cysteine residues would become reactive when other residues were mutated. Conservative substitutions for the three endogenous cysteine residues, C186S, C252A and C375G (Figure 1A) resulted in a Cys(-) carrier with similar transport properties. An apparent affinity value (K_m) for L-Glu transport was obtained by measuring the uptake of radiolabeled L-Glu in COS-7 cells. As shown in Table 1, a slightly lower K_m value was observed for the Cys(-) carrier (K_m = 37± 3μM; n = 9) than for the EAAT1 carrier (K_m = 70 ± 5μM; n = 3). This difference was also observed when the potency to elicit substrate-activated transport currents (EC_{50}) was measured for the Cys(-) transporter (EC_{50} = 8 ± 2μM; n = 4) and the EAAT1 transporter (EC_{50} = 20 ± 2μM; n = 4) using the two-electrode voltage-clamp technique in the *Xenopus* oocyte expression system. Examination of individual cysteine mutants in oocytes indicated that the higher apparent affinity is linked with the C375G mutation because the C186S (EC_{50} = 21 ± 4μM; n = 4) and C252A (EC_{50} = 25 ± 5μM; n = 4) mutants have EC_{50} values similar to EAAT1, while the C375G (EC_{50} = 7 ± 1μM; n = 4) mutant has an EC_{50} value closer to the Cys(-) carrier. No differences were observed between the wild-type and Cys(-) carriers in either the current-voltage relationships determined in oocytes nor in the maximum velocity (V_{max}) of radiolabeled L-Glu uptake in COS-7 cells (data not shown). Also, the plasma membrane levels of the two proteins were comparable when they were evaluated in COS-7 cells using a cell-surface biotinylation protocol (data not shown; see Experimental Procedures). Thus, the activity of the Cys(-) transporter appears to be similar to the wild-type EAAT1 and therefore, provides an excellent background in which to introduce single cysteine substitutions for analysis by SCAM.

A

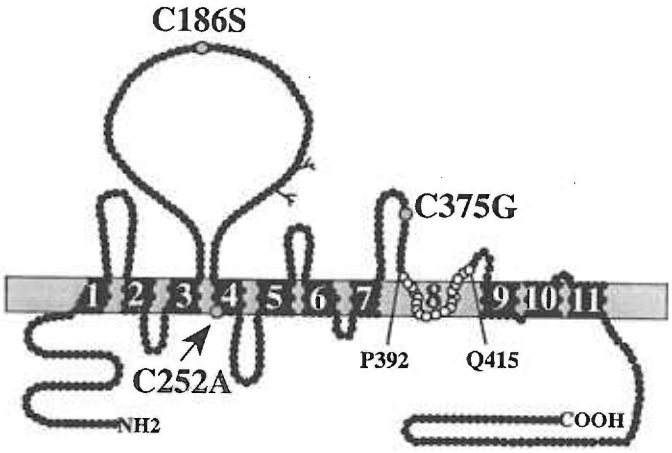

B

	392												405									415
EAAT 1	P	V	G	A	T	I	N	M	D	G	T	A	L	Y	E	A	L	A	A	I	F	I	A	Q
EAAT 2	P	V	G	A	T	V	N	M	D	G	T	A	L	Y	E	A	V	A	A	I	F	I	A	Q
EAAT 3	P	V	G	A	T	I	N	M	D	G	T	A	L	Y	E	A	V	A	A	V	F	I	A	Q
EAAT 4	P	V	G	A	T	I	N	M	D	G	T	A	L	Y	E	A	L	A	A	I	F	I	A	Q
EAAT 5	P	V	G	A	T	I	N	M	D	G	T	A	L	Y	E	A	V	A	A	I	F	I	A	Q

C

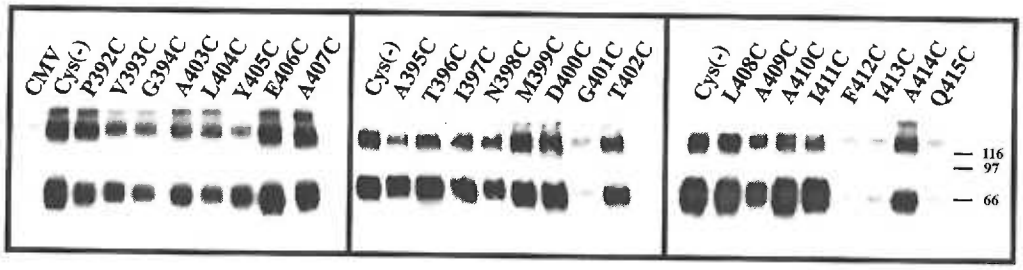

Figure 1. Location of the cysteine substitutions in EAAT1

(A) Topological model of the human EAAT1 carrier. Hydrophobic stretches are drawn as numbered membrane-associated domains with the eighth TM configured as a re-entrant membrane loop. Arrows indicate the three endogenous cysteine residues (C186S, C252A and C375G) conservatively mutated to create the Cys(-) carrier, and the residues P392 through Q415, that span the domain analyzed by SCAM.

(B) Alignment of the residues of TM 8 of the cloned human EAATs 1-5, that were individually substituted to cysteine in the Cys(-) form of EAAT1. Residues in white boxes are not conserved with EAAT1.

(C) Cell-surface expression of EAAT mutants in COS-7 cells. Western blots of transiently expressed carriers labeled with membrane impermeant NHS-biotin in intact COS-7 cells. Blots were probed with a polyclonal antibody raised to the C-terminus of EAAT1. CMV denotes the vector-transfected control. EAAT1 expressed in COS-7 cells appears as two bands that run at ~ 120kDa and 66kDa.

Cysteine substitution mutants show transport activity similar to Cys(-)

To evaluate whether residues in the eighth hydrophobic domain of the carrier (Figure 1A) interact with substrates or co-transported ions, twenty-four consecutive amino acid residues (P392 through Q415; Figure 1B) were individually substituted with cysteine using the Cys(-) carrier as the template. Functional characterization of each mutant transporter was determined by measuring the accumulation of radiolabeled L-Glu in COS-7 cells. Fifteen of the twenty-four mutants show significant accumulation of L-Glu over that observed for mock-transfected cells and all have K_m values for L-Glu transport that are similar to the Cys(-) carrier (Table1). V_{max} values for the functional mutants were greater than 20% of the V_{max} of the Cys(-) carrier (data not shown). To determine whether the loss of transport activity observed with nine of the cysteine substitution mutants was due to an absence of the transporter at the cell-surface, the plasma membrane levels of the mutant proteins were evaluated by cell surface biotinylation. Four of the nine mutants appear to be severely reduced at or absent from the plasma membrane (G401C, F412C, I413C and Q415C), while the remaining five mutants are expressed at levels comparable to or slightly lower than the Cys(-) carrier (G394C, N398C, M399C, D400C, T402C; Figure 1C).

Extracellularly applied MTS-derivatives react with the cysteine substitutions.

The accessibility of each cysteine residue to an aqueous milieu was determined in the fifteen functional mutants by measuring the uptake of radiolabeled L-Glu with and without the extracellular application of the MTS-derivatives, in intact COS-7 cells. While MTSES and MTSET are thought to be membrane impermeant, MTSEA permeates the membrane under some conditions (Holmgren et al., 1996). Regardless of whether they cross the membrane, reaction of these compounds with cysteine residues only occurs to an appreciable extent when the sulfhydryl moiety is in an aqueous environment. Therefore, we assume that a cysteine side-chain reactive with MTSEA faces either the extracellular or intracellular milieu

or an aqueous-filled intra-membrane compartment such as a pore, while a cysteine side-chain reactive with MTSES or MTSET faces either the extracellular milieu or an aqueous intra-membrane compartment, accessible from the extracellular space (Javitch, 1998).

While no change in uptake was observed after the application of 2.5mM MTSEA to the Cys(-) carrier, significant inhibition was observed for all of the cysteine substituted carriers, except A407C, L408C and I411C (Figure 2A). As shown in Figure 2B, a lower concentration of MTSEA (1mM) still markedly inhibited L-Glu transport by the P392C through I397C, Y405C, and A414C transporters. The functional effects induced by the extracellular application of the membrane impermeant MTS-derivatives, MTSES and MTSET were also evaluated. MTSET is positively charged and has a trimethylammonium group, which is bulkier than the amine of MTSEA. At 1mM, this reagent significantly inhibited the uptake of the A395C and A414C transporters (Figure 2C). MTSES (10mM), a negatively charged molecule that has a similar size to MTSET, also significantly inhibited the uptake of L-Glu by these two transporters (Figure 2D). The positioning of these two reactive residues at opposite ends of this relatively hydrophobic domain, which has been implicated in the binding of intracellular potassium ions (Pines et al., 1995; Kavanaugh et al., 1997), suggests that this region could form a re-entrant loop, similar to what has been postulated for a number of proteins that transport ions across cell membranes (see Discussion).

Effects of MTS-derivatives on transport by A414C

Although all three of the MTS-derivatives tested appear to inhibit transport of the A414C carrier, the percent of inhibition conferred by a maximal concentration of MTSEA is less than with MTSET or MTSES (Figure 2). Initially it was observed that application of 2.5mM MTSEA (37 ± 3%; n = 5) reduced transport by approximately the same percentage as with 1mM MTSEA (35 ± 4%; n = 3) (Figure 2). To confirm that the A414C carrier is

Table 1. Apparent Affinity Values of L-glutamate Transport by the Single Cysteine Mutants Expressed in COS-7 Cells.

Mutant	K_m (μM)	n	Mutant	K_m (μM)	n
EAAT1	70 +/- 5	3	A403C	35 +/- 4	2
Cys(-)	37 +/- 3	9	L404C	26 +/- 11	2
P392C	46 +/- 6	2	Y405C	36 +/- 4	2
V393C	26 +/- 5	2	E406C	27 +/- 7	3
G394C	N.F.		A407C	39 +/- 5	3
A395C	39 +/- 6	3	L408C	43 +/- 8	4
T396C	58 +/- 11	3	A409C	39 +/- 4	2
I397C	49 +/- 4	3	A410C	38 +/- 11	3
N398C	N.F.		I411C	46 +/- 12	2
M399C	N.F.		F412C	N.F.	
D400C	N.F.		I413C	N.F.	
G401C	N.F.		A414C	44 +/- 6	2
T402C	N.F.		Q415C	N.F.	

Each transporter was transiently expressed in COS-7 cells and the accumulation of radiolabeled L-glutamate measured at concentrations ranging from 1 to 1000 μM. K_m values were derived by fitting the data to the Michaelis-Menten equation. Errors are presented as SEM for n independent determinations. Non-functional carriers are denoted by N.F.

maximally inhibited by these concentrations, cells expressing the transporter were incubated with additional concentrations of MTSEA (0.5 to 5mM). As shown in Figure 3A, the percent inhibition of L-Glu uptake observed was approximately the same at all concentrations tested and was never greater than 50%. These findings imply that while MTSES and MTSET can abolish greater than 90% of the L-Glu transport activity, the maximum inhibition conferred by MTSEA at this residue appears to be only 30-40%. Using concentrations of MTSEA ranging from 0.05 to 2.5mM, a second order rate constant of $104 \pm 15\ M^{-1}s^{-1}$ (n = 2) was calculated. To better understand the nature of the interaction of the MTS-derivatives with the cysteine at this position, the effects of two neutral MTS-derivatives were evaluated. MMTS (methyl methanethiosulfonate) with a single methyl group is small, while MTSACE (2-(aminocarbonyl)ethyl methanethiosulfonate) is approximately the same size as MTSET and MTSES. Maximal concentrations of these compounds appeared to inhibit transport of L-Glu by $16 \pm 4\%$ (n = 5) and $64 \pm 6\%$ (n = 2), respectively (Figure 3B). These data suggest that A414C is readily accessible to the extracellular aqueous environment and that the extent of the inhibition observed depends on the chemical properties of the MTS-derivative used.

Inhibition of transport by these compounds may depend on their ability to react to completion with the cysteine side-chain or it may depend on the size and/or electrostatic properties of the substituent once it has been linked to the sulfhydryl group. To examine this, cells expressing the A414C carrier were incubated with a saturating concentration of MTSEA (2.5mM; Figure 3C), MMTS (1mM; Figure 3D) or MTSACE (2.5mM; Figure 3E) alone or followed by incubation with MTSES. If after the sequential application of both the test compound and MTSES, the fractional inhibition of uptake reflects that observed with the test compound alone, it implies that the compound was able to react to completion with the residue, and thus prevent subsequent modification by MTSES. This result was observed with each compound tested, indicating that they react to completion with the same cysteine side-chains as MTSES. Thus, it appears that the size and possibly the charge of

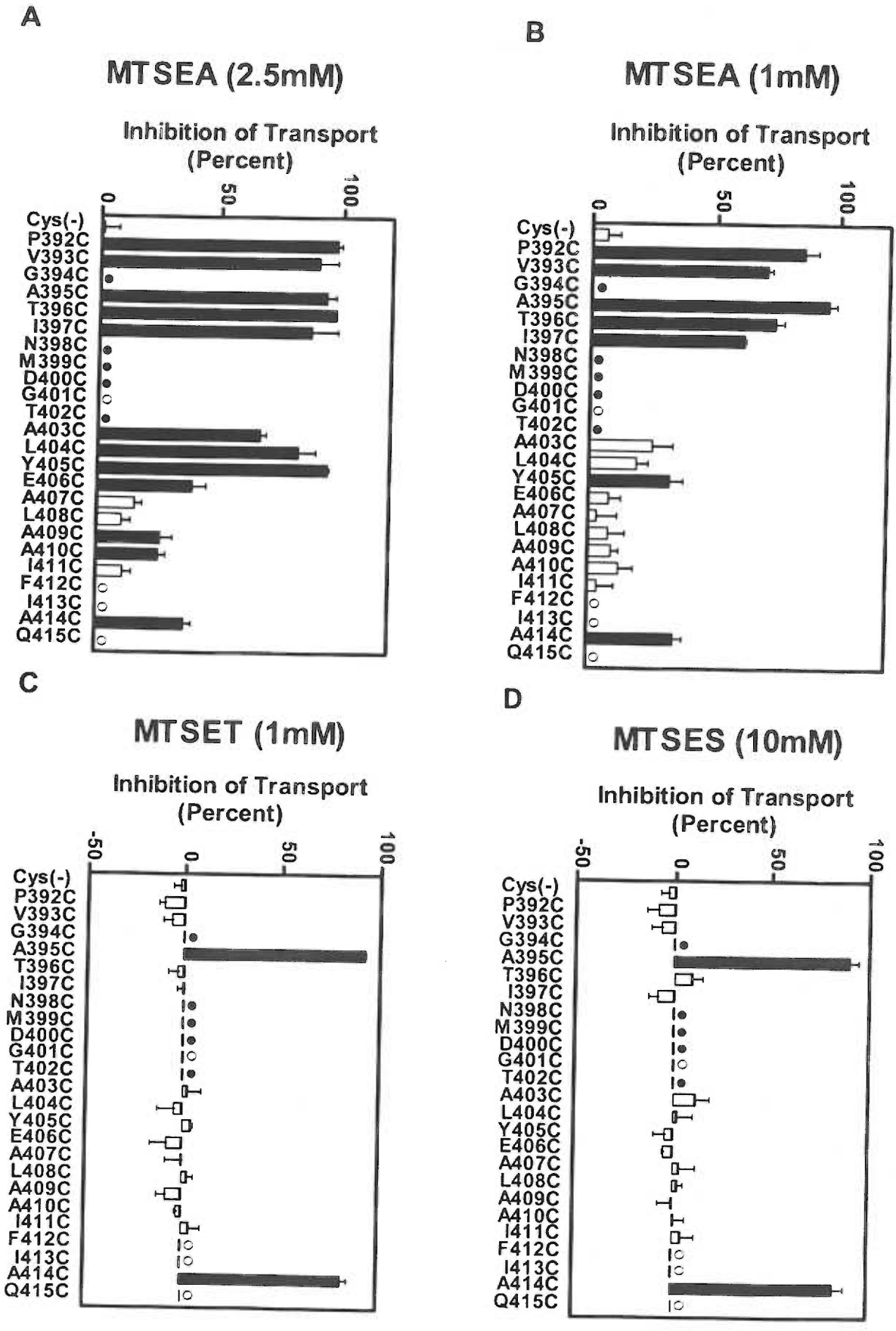
A
MTSEA (2.5mM)
Inhibition of Transport
(Percent)
0
50
100
Cys(-)
P392C
V393C
G394C
A395C
T396C
I397C
N398C
M399C
D400C
G401C
T402C
A403C
L404C
Y405C
E406C
A407C
L408C
A409C
A410C
I411C
F412C
I413C
A414C
Q415C
B
MTSEA (1mM)
Inhibition of Transport
(Percent)
0
50
100
Cys(-)
P392C
V393C
G394C
A395C
T396C
I397C
N398C
M399C
D400C
G401C
T402C
A403C
L404C
Y405C
E406C
A407C
L408C
A409C
A410C
I411C
F412C
I413C
A414C
Q415C
C
MTSET (1mM)
Inhibition of Transport
(Percent)
-50
0
50
100
Cys(-)
P392C
V393C
G394C
A395C
T396C
I397C
N398C
M399C
D400C
G401C
T402C
A403C
L404C
Y405C
E406C
A407C
L408C
A409C
A410C
I411C
F412C
I413C
A414C
Q415C
D
MTSES (10mM)
Inhibition of Transport
(Percent)
-50
0
50
100
Cys(-)
P392C
V393C
G394C
A395C
T396C
I397C
N398C
M399C
D400C
G401C
T402C
A403C
L404C
Y405C
E406C
A407C
L408C
A409C
A410C
I411C
F412C
I413C
A414C
Q415C

Figure 2. Inhibition of L-Glu transport by covalent modification of MTS-derivatives.

COS-7 cells transiently transfected with Cys(-) or the various mutants were incubated with and without either 2.5mM MTSEA (A), 1mM MTSEA (B), 1mM MTSET (C), or 10mM MTSES (D). L-Glu uptake is expressed as the percent inhibition of transport. Black bars show residues that were inhibited to a significantly greater extent than the Cys(-) carrier ($p < 0.05$; one-way ANOVA). Each bar is the mean ± S.E.M from 3 or more independent experiments. Mutants unable to transport L-Glu are denoted by either an open circle (not at cell surface) or filled circle (at cell surface).

A

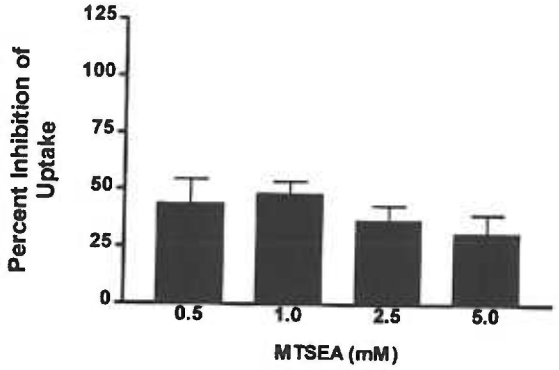
Percent Inhibition of Uptake
125
100
75
50
25
0
0.5
1.0
2.5
5.0
MTSEA (mM)

B

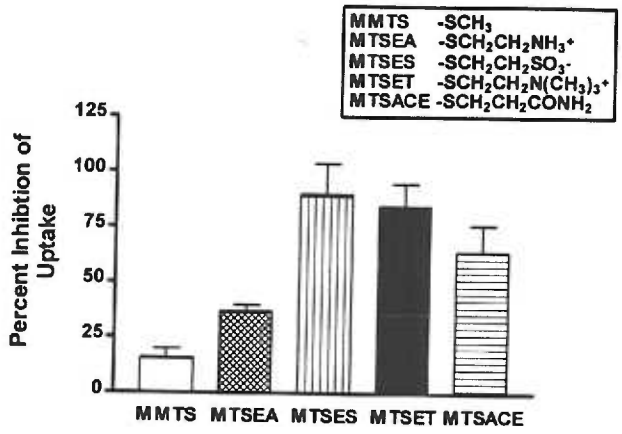
MMTS -SCH3
MTSEA -SCH2CH2NH3+
MTSES -SCH2CH2SO3-
MTSET -SCH2CH2N(CH3)3+
MTSACE -SCH2CH2CONH2
Percent Inhibtion of Uptake
125
100
75
50
25
0
MMTS MTSEA MTSES MTSET MTSACE

C

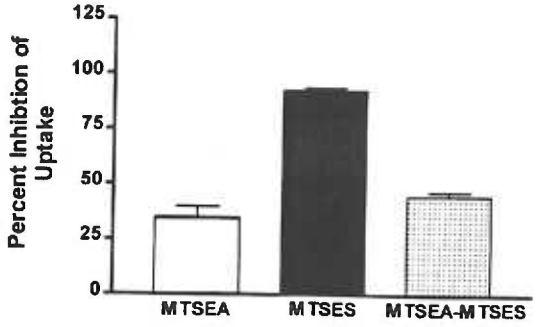
Percent Inhibtion of Uptake
125
100
75
50
25
0
MTSEA
MTSES
MTSEA-MTSES

D

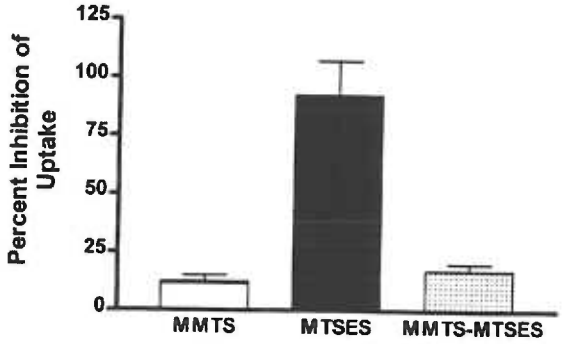
Percent Inhibtion of Uptake
125
100
75
50
25
0
MMTS
MTSES
MMTS-MTSES

E

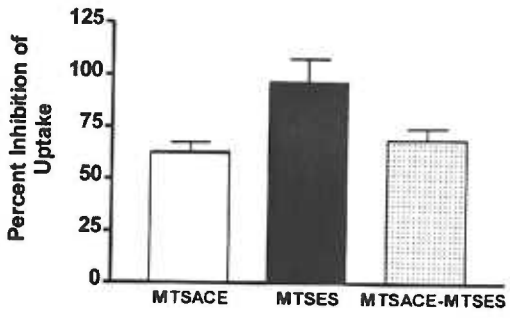
Percent Inhibtion of Uptake
125
100
75
50
25
0
MTSACE
MTSES
MTSACE-MTSES

Figure 3. MTS-derivatives differentially affect A414C transport activity.

(A) Cells expressing the A414C transporter were incubated with concentrations of MTSEA (0.5mM to 5mM). L-Glu uptake is plotted as the percent inhibition of uptake and the data presented are the means ± S.E.M. of 3-5 independent experiments.

(B) Cells expressing the A414C transporter were incubated with 1mM MMTS, 2.5mM MTSEA, 10mM MTSES, 1mM MTSET, or 2.5mM MTSACE. L-Glu uptake is plotted as the percent inhibition of uptake and the data presented are the means ± S.E.M. of 2-7 independent experiments done in triplicate.

(C) Cells expressing the A414C transporter were incubated with 2.5mM MTSEA or 10mM MTSES alone or with 2.5mM MTSEA followed by incubation with 10mM MTSES. L-Glu uptake is plotted as the percent inhibition of uptake and the data presented are the means ± S.E.M. of 3 independent experiments done in triplicate.

(D) Same as in C, but with 1mM MMTS rather than MTSEA.

(E) Same as in C, but with 2.5mM MTSACE rather than MTSEA.

the modifying group, rather than limitations in the ability of the compound to react to completion with the residue, determine the reduction in L-Glu transport by the A414C carrier.

Carrier substrates protect engineered cysteine residues from modification by the MTS-derivatives.

To examine whether substrates of the carrier could protect the reactive cysteine substitutions from modification by the MTS-derivatives, a saturating concentration of L-Glu was incubated with each compound (Figure 4). MTSET (1mM), MTSES (10mM) or MTSEA (2.5mM) was applied in the presence and absence of 10mM L-Glu. Transport of L-Glu was plotted as the percent inhibition of uptake. Although both the A395C and A414C transporters are greatly inhibited by the membrane impermeant MTS-derivatives, only the A395C carrier was protected from MTSES and MTSET by the presence of substrate (Figure 4A). Interestingly, when the A395C carrier was incubated with a relatively high concentration of MTSEA (2.5mM), L-Glu did not effectively block the reaction between the cysteine residue and the modifying reagent. However, as shown in subsequent experiments, a significant protective effect of substrates could be observed with lower concentrations of MTSEA.

To further examine the protective effect of L-Glu on the A395C transporter, concentration curves of each MTS-derivative were carried out with and without a saturating concentration of L-Glu. In the absence of L-Glu, increasing concentrations of MTSET (Figure 4B), MTSES (Figure 4C) and MTSEA (Figure 4D) led to complete inhibition of the transport activity. The fraction of uptake activity was plotted as a function of the MTS-derivative concentration and fitted to generate the second order rate constants (k_{MTSET} = 3.0 $\pm$ 0.3 $M^{-1}s^{-1}$, k_{MTSES} = 0.72 $\pm$ 0.05 $M^{-1}s^{-1}$ and k_{MTSEA} = 10 $\pm$ 2 $M^{-1}s^{-1}$). L-Glu prevented the inhibition of transport by MTSET and MTSES at concentrations several fold above those required to abolish the transport activity (10mM and 50mM, respectively). This is in

contrast to what is observed with MTSEA. In the presence of L-Glu, the level of transport activity remained high until the concentration of MTSEA reached ~ 1.3mM, at which point it decreased sharply and was abolished by 2.5mM. Although these data could not be fit to generate a second order rate constant, the IC_{50} for MTSEA was approximately 3-fold greater ($IC_{50} = 1.8 \pm 0.3$; n = 4) than when the experiment was carried out in the absence of L-Glu ($IC_{50} = 0.5 \pm 0.1$; n = 4).

Because the second order rate constant is a function of both the concentration of the reagent and the duration of the incubation, the ability of L-Glu to protect A395C in the presence of 2.5mM MTSEA was also examined as a function of time (Figure 4E). As expected, a similar relationship was observed between the transport activity and exposure to MTSEA. In the absence of L-Glu, MTSEA inhibited transport completely and with a second order rate constant of $12 \pm 2\ M^{-1}s^{-1}$ (n = 3). In the presence of L-Glu, the transport activity diminished over time and was abolished by 5 min. These data also could not be fit to generate a second order rate constant, however, the modification reaction was slowed more than 5-fold by L-Glu ($t_{0.5} > 200$ sec versus $t_{0.5} = 25 \pm 5$ sec; n = 3). Therefore, a saturating concentration of L-Glu protects the A395C residue from modification by high concentrations of the membrane impermeant compounds MTSES and MTSET, as well as, from MTSEA at concentrations less than ~ 1.3mM. The unique behavior of MTSEA on the transport activity of the A395C carrier in the presence of L-Glu may be because MTSEA can be membrane permeant under some conditions (see Discussion) (Holmgren, et al., 1996). L-Glu (10mM) had no effect on the MTSEA modification observed with the other cysteine substituted carriers (data not shown).

Protection occurs with a physiologically relevant concentration of L-Glu. We also examined whether L-Glu limits modification of the A395C carrier at concentrations of L-Glu that are physiologically relevant to the transport mechanism. Cells expressing the A395C carrier were incubated with a low concentration of MTSEA (0.25mM) and concentrations of L-Glu ranging from 0 to 1000μM. Radiolabeled L-Glu uptake was

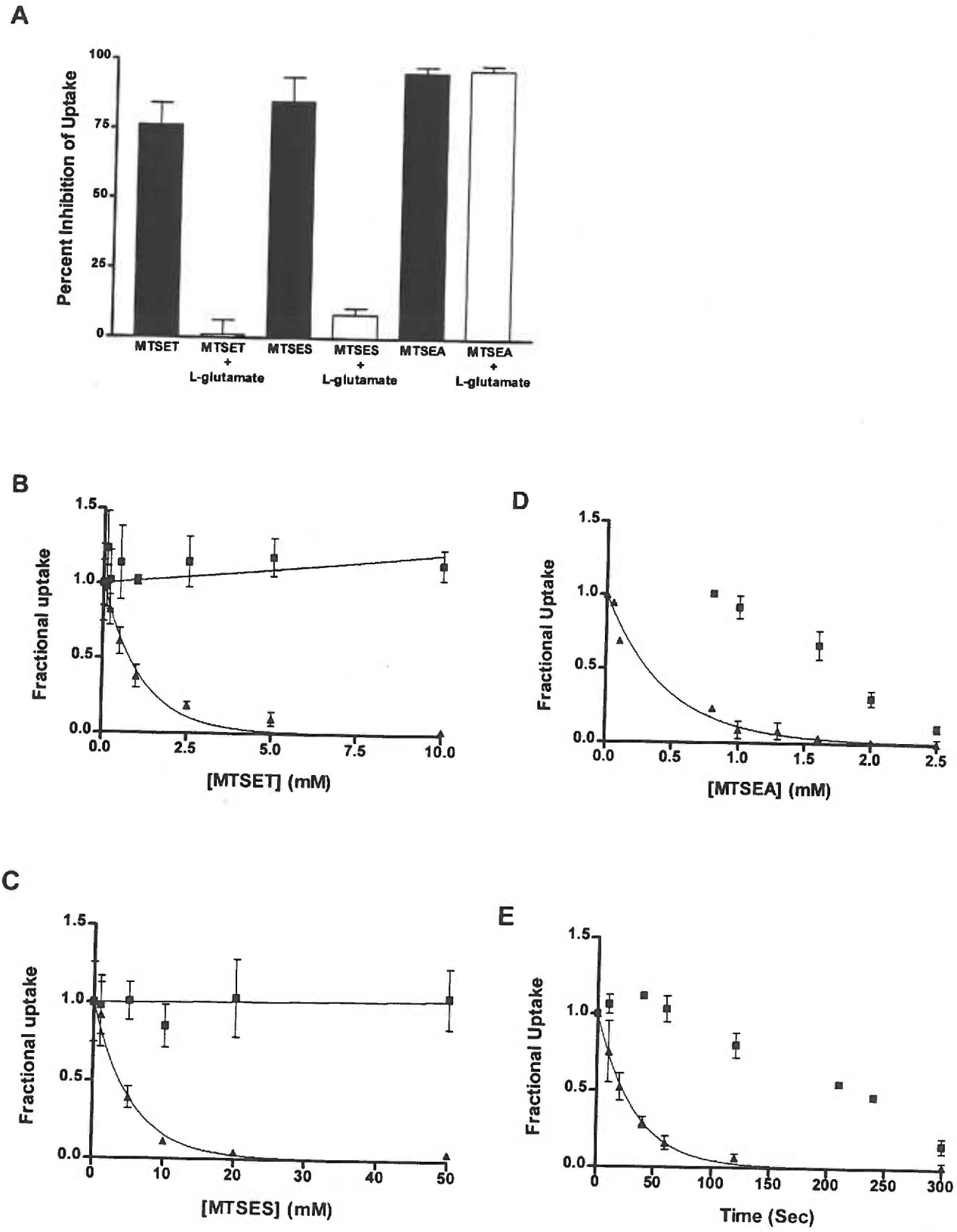
A
Percent Inhibition of Uptake
100
75
50
25
0
MTSET
MTSET + L-glutamate
MTSES
MTSES + L-glutamate
MTSEA
MTSEA + L-glutamate
B
Fractional uptake
[MTSET] (mM)
C
Fractional uptake
[MTSES] (mM)
D
Fractional Uptake
[MTSEA] (mM)
E
Fractional Uptake
Time (Sec)

Figure 4. Effect of L-Glu on thiol-modification of the A395C transporter.

(A) COS-7 cells transiently transfected with the A395C transporter were incubated with 1mM MTSET, 10mM MTSES, or 2.5mM MTSEA in the presence (white bars) and absence (black bars) of 10mM L-Glu. Data are plotted as percent inhibition of L-Glu uptake.

(B) Cells expressing the A395C transporter were incubated with concentrations of MTSET ranging from 0.1 to 10mM in the presence (squares) and absence (triangles) of 10mM L-Glu. Data are plotted as the fraction of L-Glu uptake as a function of the MTSET concentration and are the means ± S.D. of 2 independent experiments done in triplicate.

(C) Cells expressing the A395C transporter were incubated with concentrations of MTSES ranging from 1 to 50mM in the presence (squares) and absence (triangles) of 10mM L-Glu. Data are plotted as the fraction of L-Glu uptake as a function of the MTSES concentration and are the means ± S.D. of 2 independent experiments done in triplicate.

(D) Cells expressing the A395C transporter were incubated with concentrations of MTSEA ranging from 0 to 2.5mM in the presence (squares) and absence (triangles) of 10mM L-Glu. Data are plotted as the fraction of L-Glu uptake as a function of MTSEA concentration and are the means ± S.D. of 4 independent experiments done in triplicate.

(E) Cells expressing the A395C transporter were incubated with 2.5mM MTSEA in the presence (squares) and absence (triangles) of 10mM L-Glu for times ranging from 10 to 300 seconds. Data are plotted as the fraction of L-Glu uptake as a function time and are the means ± S.E.M. for 3 independent experiments done in triplicate.

measured and fitted to the Michaelis-Menten equation (Figure 5A). The calculated EC_{50} value is similar to the K_m value for L-Glu uptake by this carrier in COS-7 cells (EC_{50} = 35± 5μM; n= 3, K_m = 37± 3μM; n = 9). To determine whether this relationship holds true for other MTS-derivatives, we also carried out the experiment with MTSES and obtained a similar EC_{50} value (data not shown). The similarity in the affinity values for the protection mechanism and the uptake activity suggests that protection of the residue occurs at a step within the transport process.

Binding of the competitive, non-transported inhibitor, DL-TBOA also blocks modification of the A395C residue.

To further explore the relationship between A395C and transport, we tested whether a high affinity, non-transported, competitive inhibitor of EAAT1, DL-*threo*- β-Benzyloxyaspartate (DL-TBOA) (Shimamoto et al., 1998), could protect the A395C residue from modification by MTSES. Non-transported competitive inhibitors are thought to bind at substrate binding sites and may have the ability to induce conformational changes in the carrier. However, because they are not translocated, the profile of conformation states and binding events that occur with these compounds are likely to be more restricted than with substrates. Cells were incubated with 10mM MTSES and concentrations of DL-TBOA ranging from 1 to 1000μM. DL-TBOA was able to protect the A395C residue from modification by MTSES with an EC_{50} of 29 ± 8μM (n = 3; Figure 5B), a value similar to its affinity to inhibit the uptake of L-Glu by this carrier (IC_{50} of 19 ± 4μM; n = 2). As was observed with L-Glu, DL-TBOA also completely blocked modification by MTSET, but not by MTSEA (data not shown). These results are consistent with protection of the A395C transporter taking place at a step in the transport cycle closely linked to L-Glu binding.

Protection of the A395C residue by L-Glu is not temperature-sensitive.

We took advantage of the temperature-dependence of transport to help identify at which step(s) in the transport cycle L-Glu acts to block the modification of A395C. L-Glu transport is highly temperature-sensitive such that at temperatures approaching 0°C, translocation is severely reduced (Stallcup et al., 1979), although binding of substrate remains relatively unaffected (Wadiche and Kavanaugh, 1998). The observed temperature-dependence is consistent with protein conformational changes required for translocation (Wadiche and Kavanaugh, 1998). Therefore, we tested the ability of L-Glu to protect the A395C residue from modification at a temperature that severely impairs substrate translocation (Figure 5C). A time course for the modification of the A395C carrier by 10mM MTSES was carried out in the presence and absence of 10mM L-Glu, at 22°C and at 2-4°C. At 22°C, MTSES irreversibly inhibited the transport activity of the carrier with a reaction rate constant of 0.80 ± 0.05 $M^{-1}s^{-1}$ (n = 3) in the absence of L-Glu and at a rate approximately 20-fold slower in the presence of L-Glu, $k = 0.047 \pm 0.009$ $M^{-1}s^{-1}$ (n = 3). This result is consistent with the ability of L-Glu to protect the residue from modification over a range of MTSES concentrations (see Figure 4C). At 2-4°C and in absence of L-Glu, the reactivity rate ($k = 0.21 \pm 0.03$ $M^{-1}s^{-1}$ n = 3) was 25% of the rate measured at 22°C. The reduction in the reaction rate at the lower temperature ($Q_{10} \cong 2$) is consistent with previous estimates of the temperature-dependence of the rate of the chemical reaction between the sulfhydryl group and the MTS-derivative ($Q_{10} = 2$, A. Karlin, personal communication). As was observed at 22°C, L-Glu completely protected A395C from modification when the reaction was carried out at 2-4°C ($k = 0.033 \pm 0.003$ $M^{-1}s^{-1}$; n = 3). Thus, L-Glu protects the residue from modification when the reaction is carried out at temperatures that dramatically slow the transport cycle, suggesting that block by L-Glu occurs at a step prior to the temperature-sensitive conformational changes that the carrier undergoes as a result of its interaction with substrate.

Sodium ions affect the modification rate of two cysteine substitution mutants.

The L-Glu transport is thought to proceed through the ordered binding of substrates, with sodium binding before substrate (Kanner and Bendahan, 1982), though the sites may or may not be closely related. To determine whether sodium interacts with residues P392 through Q415, we evaluated the reactivity of the cysteine substitution mutants with MTS-derivatives in the presence and absence of extracellular sodium. Only E406C (Figure 6A) and Y405C (Figure 6B) show altered modification rates when sodium is replaced with equimolar choline, and only with MTSEA but not MTSES or MTSET.

COS-7 cells expressing the E406C transporter were incubated with concentrations of MTSEA ranging from 0.05 to 2.5mM in the presence of either sodium or choline. As shown in Figure 6A, MTSEA had a significantly greater effect on transport in 120mM choline. The second order rate constant was increased ~ 6-fold ($k_{choline} = 3.0 \pm 0.6\ M^{-1}s^{-1}$; n = 2 and $k_{sodium} = 0.51 \pm 0.08\ M^{-1}s^{-1}$; n = 2) and the concentration of MTSEA that resulted in a 50% inhibition of the transport activity was decreased from ~5mM to <1mM.

With the Y405C transporter, only a small increase in the modification rate was observed in the absence of sodium (data not shown). Because the reaction rate is dependent on both the reaction time and the concentration of reagent, we explored this small increase by measuring the rate as a function of time, at two different concentrations of MTSEA (0.5mM and 1mM) and in the presence of either sodium or choline. Under these conditions, replacement with choline significantly increased the reaction rate at both concentrations of MTSEA, suggesting that sodium also retards the modification of this residue (Figure 6B). The fractional inhibition of transport observed for the A395C and A414C carriers after application of sub-maximal concentrations of MTSES (5mM) or MTSET (0.5mM) did not change with sodium replacement (data not shown).

A

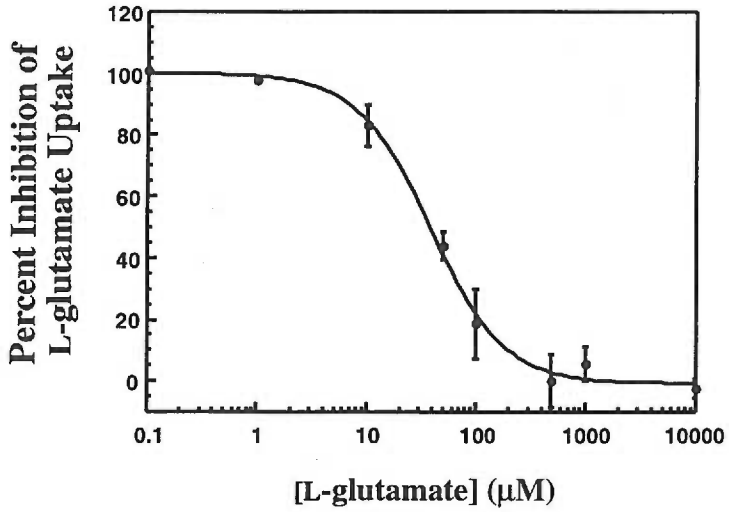
Percent Inhibition of L-glutamate Uptake
120
100
80
60
40
20
0
0.1
1
10
100
1000
10000
[L-glutamate] (μM)

B

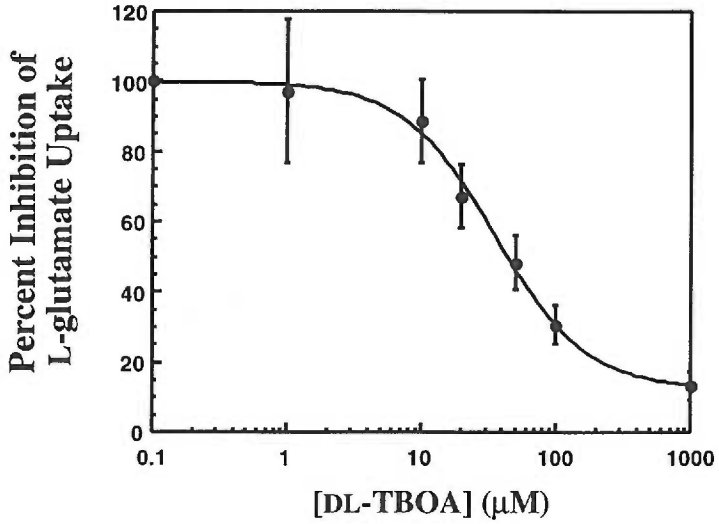
Percent Inhibition of L-glutamate Uptake
120
100
80
60
40
20
0
0.1
1
10
100
1000
[DL-TBOA] (μM)

C

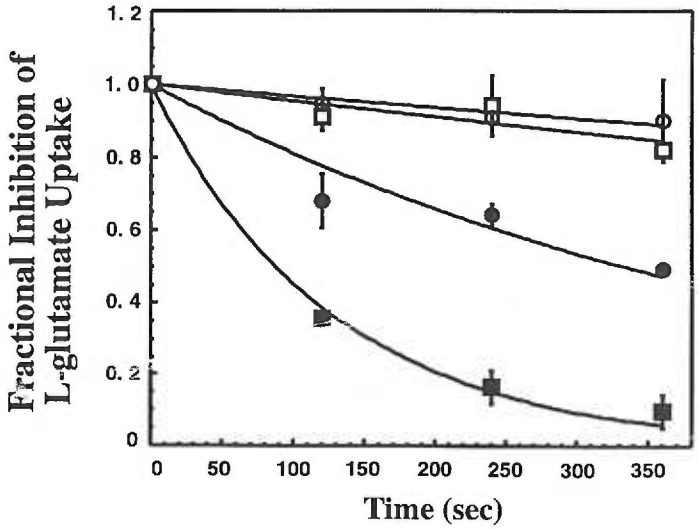
Fractional Inhibition of L-glutamate Uptake
1.2
1.0
0.8
0.6
0.4
0.2
0
0
50
100
150
200
250
300
350
Time (sec)

A

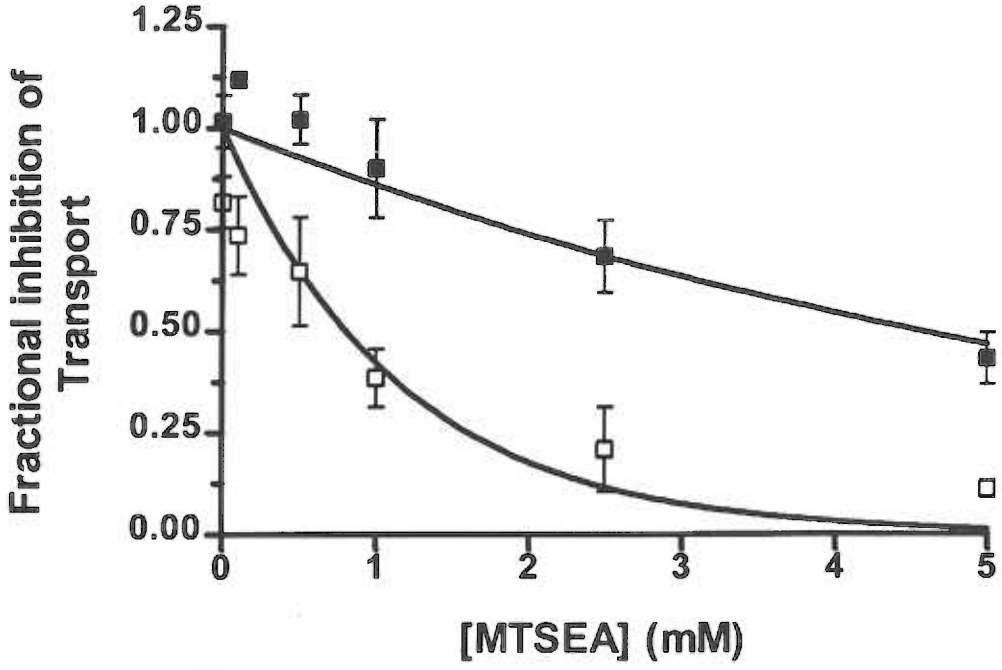
Fractional inhibition of Transport
1.25
1.00
0.75
0.50
0.25
0.00
0
1
2
3
4
5
[MTSEA] (mM)

B

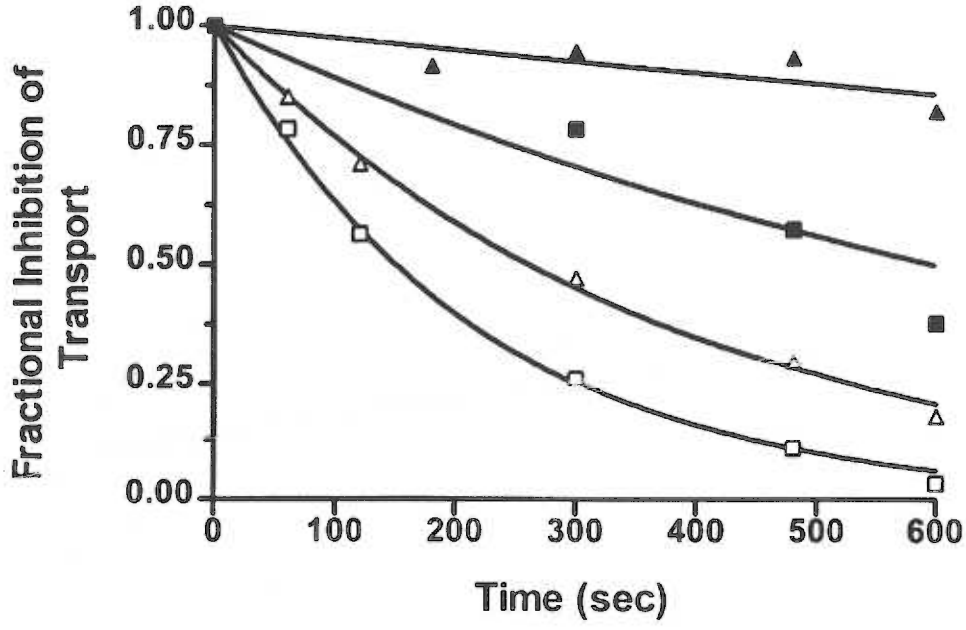
Fractional Inhibition of Transport
1.00
0.75
0.50
0.25
0.00
0
100
200
300
400
500
600
Time (sec)

Figure 6. Sodium affects the rate of MTSEA modification.

(A) Cells transiently expressing the E406C transporter were incubated with concentrations of MTSEA ranging from 0 to 5mM in buffer containing 120mM of either sodium (filled squares) or choline (open squares). Data are plotted as the fractional inhibition of L-Glu transport as a function of the MTSEA concentration. Data are the means ± S.E.M. of 3 experiments done in triplicate. Second order rate constants are 3.0 ± 0.6 $M^{-1}s^{-1}$ (choline) and 0.51 ± 0.01 $M^{-1}s^{-1}$ (sodium).

(B) Cells transiently expressing the Y405C transporter were incubated with 0.5mM (filled symbols) or 1mM (open symbols) MTSEA for times ranging from 60 to 600 sec in the presence of sodium (triangles) or choline (squares). Data are the means of 2 independent experiments performed in triplicate. Second order rate constants are 2.4 ± 0.4 $M^{-1}s^{-1}$ (choline) and 0.5 ± 0.1 $M^{-1}s^{-1}$ (sodium) at 0.5mM MTSEA and 4.6 ± 0.1 $M^{-1}s^{-1}$ (choline) and 2.67 ± 0.01 $M^{-1}s^{-1}$ (sodium) at 1mM MTSEA.

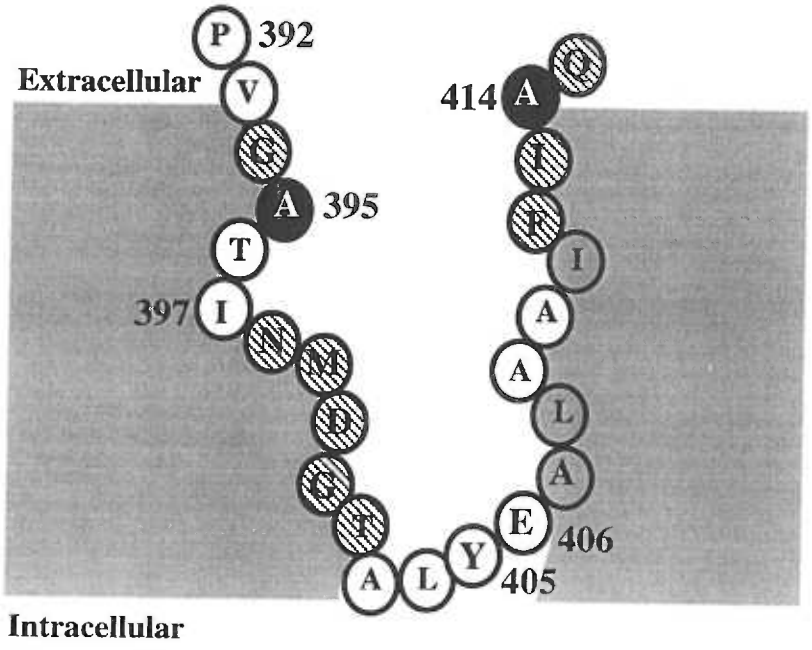

Figure 7. Topological model of the region P392 through Q415 in EAAT1. Residues that when substituted to cysteine react with all three MTS-derivatives are black, those that react only with MTSEA are white, those that did not react significantly with the MTS-derivatives are gray, and those that result in a non-functional transporter are striped.

Discussion

Our studies suggest a model for the topological organization of the region from P392 through Q415 based on the accessibility of these residues to the various MTS reagents in functional, surface-expressed transporters. Analysis of hydropathy profiles as well as several proposed topological models (Jording and Puhler, 1993; Wahle and Stoffel, 1996; Slotboom et al., 1996) suggested that this domain would be predominantly membrane-associated. Interestingly, we observed that MTSEA, a compound known to react only with residues in an aqueous environment, inhibited the transport activity of nearly all of the cysteine substitutions (Figure 2A). This result combined with our findings on the reactivity of other cysteine-substituted residues is more consistent with a model in which this region lines an aqueous pore within the membrane. In addition, the pattern of reactivity suggests a non-periodic secondary structure. Although one can not exclude a β-stranded or an α-helical conformation, the accessibility pattern makes it highly unlikely that this region exists in either of these conformations with one side facing into a pore. If that were the case, then every other residue (β-strand) or every third or fourth residue (α-helix) would have been accessible.

Two residues located at opposite ends of the domain, A395C and A414C, react with the impermeant compounds, MTSET (Figure 2C) and MTSES (Figure 2D). Additionally, their modification rates with MTSEA are the highest when compared to the other residues, suggesting that they are quite accessible. Thus, both residues are likely positioned near the extracellular side of the membrane (Figure 7). A lower concentration of MTSEA (1mM) still inhibits the functional mutants clustered around the A395C residue (P392C through I397C), as well as the more centrally located Y405C residue, but does not inhibit the mutants A403C through A410C, that are also near the center of this domain (Figure 2B). The reduced reactivity of these latter residues is consistent with their placement deeper within a crevice, so that they are sterically and possibly electrostically less

reactive with extracellularly applied MTSEA. Y405 may be accessible to both the extracellular and intracellular environments (Figure 7) as has been suggested by studies that implicate the analogous residue in GLT-1 in the binding of internal potassium ions (Zhang et al., 1998). MTSEA can permeate the membrane in its uncharged form and thus under some conditions could react with residues from either side of the membrane (Holmgren et al., 1996). We have shown in COS-7 cells that MTSEA gains access to the intracellular side of the membrane and reacts with a cysteine substituted in a known cytoplasmic domain in the C-terminus of EAAT1 (RPS, unpublished). Thus, inhibition of some cysteine mutants with MTSEA may be explained by modification from the cytoplasmic side of the membrane.

Together these data support the idea that this region forms a re-entrant loop that may be part of a translocation pore for substrates and co-transported ions. A similar topology was proposed for this domain in a study using microsomal membranes to examine the folding of truncations of GLAST-1 (rat homolog of EAAT1) fused to a glycosylation reporter domain. Wahle et al. (1996) proposed that the region is re-entrant but was modeled as two b-strands within the membrane. Evidence was not yet available, however, to experimentally confirm this secondary structure or to implicate it in the formation of a pore.

In a recent report, the membrane orientation of individual cysteine residues substituted into the GLT-1 transporter was evaluated using thiol-specific modifying reagents (Grunewald et al., 1998). The results of this study were the basis for a model with seven α-helical TMs, followed by three shorter membrane-associated segments, and ending with an eighth α-helical TM. This model interprets the region of our proposed P-loop as a membrane spanning α-helix (TM7) with the preceding residues as intracellular. Our data, contradict this aspect of the model because we have shown here in a functional assay that A395C in EAAT1, which would correspond to the cytoplasmic side of the putative GLT-1 TM7, can be readily modified with the membrane impermeant reagents MTSES and MTSET (Figure 2). In addition, a larger molecule, MTSEA-biotin, labels

A395C, and this reaction can be blocked by MTSES and MTSET (data not shown). Moreover, we have found that the transport activity of two cysteine mutants made in the EAAT1 domain analogous to the putative intracellular loop before TM7, can be abolished by the extracellular application of the membrane-impermeant reagents, MTSES and MTSET (data not shown). Together, these data argue that at least a portion of the region before P392 faces the extracellular milieu, consistent with our model of a re-entrant loop for this domain. The reason for the differences in the two models is not clear, but may reflect differences in the experimental approaches used.

Re-entrant loops have been postulated for a number of ion channels (reviewed in MacKinnon, 1995), including the M2 segment of ionotropic glutamate receptors (Hollmann et al., 1994; Wo and Oswald, 1994; Bennett and Dingledine, 1995), the P-loop of cyclic nucleotide-gated channels (Sun et al., 1996) and the P-loop of voltage-gated potassium (Yellen et al., 1991) and sodium channels (Sather et al., 1994; Perez-Garcia et al., 1996). X-ray crystallographic analysis of an S. lividans potassium channel that has similarity in both sequence and function to the mammalian voltage-gated potassium channels, provides additional evidence that residues of such P-loops participate in forming the aqueous pore and selectivity filter for ions (Doyle et al., 1998). Many examples in both recombinant and *in vivo* systems, illustrate that transporters mediate both substrate-gated ion conductances as well as substrate-independent ("leak") conductances (reviewed in Lester et al., 1994; Sonders and Amara, 1996; DeFelice and Blakely, 1996). Thus, although solute-dependent transporters translocate substrates and coupled-ions with a fixed stoichiometry, many of these carriers also appear to mediate the flux of uncoupled ions in a manner similar to ion channels. Based on these findings, mechanistic models of solute-dependent transporters have expanded from simple alternating-access models to ones that also incorporate gating mechanisms and pore domains akin to those in ion channels (Lester et al., 1994; Cammack et al., 1994; Su et al., 1996; Sonders and Amara, 1996; DeFelice and Blakely, 1996). The

presence of a re-entrant loop in this family of carriers is consistent with the existence of a channel-like pore that could mediate the translocation of substrates and/or the flux of ions.

Protection of the A395C residue is independent of substrate translocation

Several experiments suggest the involvement of this domain in substrate binding and/or translocation. Analysis of the A395C residue revealed that L-Glu protects the residue from modification by MTSES, MTSET and low concentrations of MTSEA with an affinity that is similar to its apparent transport affinity (Figure 5A). This could occur because the binding of L-Glu blocks access of the reagents to the cysteine side-chain or because it stabilizes a particular conformation that restricts access to the side-chain. Biochemical evidence for substrate-induced conformational changes in the N-terminal half of GLT-1 has been obtained by comparing the size of transporter fragments generated by limited proteolysis in the presence and absence of substrates (Grunewald and Kanner, 1995).

Non-transported, competitive inhibitors are thought to bind to similar sites as substrates, but not to induce a complete transport cycle. Although DL-TBOA is not transported, it may induce or stabilize particular conformations upon binding the carrier, as shown with kainate, a non-transported, competitive inhibitor that appears to increase the accessibility of the Y403C residue in GLT-1 (Zarbiv et al., 1998). Thus, the ability of DL-TBOA to protect the A395C residue from modification by MTSES (and MTSET, but not MTSEA; data not shown) with an affinity similar to its affinity to block the transport of L-Glu (Figure 5B), suggests that protection of the residue is similar to that observed with L-Glu and takes place prior to substrate translocation.

Measurement of transport rates at lowered temperatures has been used to distinguish substrate binding from translocation because the transport of substrates appears to be highly temperature-dependent, whereas the binding of substrates remains unaffected (Wadiche and Kavanaugh, 1998). The finding that L-Glu protects the A395C residue at temperatures where transport does not occur (Figure 5C) also supports the idea that substrates block the modification at a step prior to substrate translocation. The results from

these experiments are again consistent with the idea that protection of the residue occurs at a step closely linked to substrate binding, but independent of translocation, and could support a model in which the A395C residue lies near a glutamate binding site.

The A395C residue was not protected by L-Glu when MTSEA was applied at concentrations greater than approximately 2mM (Figure 4). It could not be determined whether covalent attachment of MTSEA effectively competes with the reversible binding of L-Glu from the extracellular side of the membrane or if MTSEA reacts with the residue using an alternative route that involves crossing the cell membrane. The latter explanation seems more likely because L-Glu can still protect the A395C residue from modification by the membrane impermeant reagents MTSES and MTSET at concentrations that are effectively greater than 2.5mM MTSEA once the reactivity rates have been normalized. Thus, the A395C residue, like Y405C, may be modified by MTSEA from either side of the membrane.

The A414 residue may reside at the entrance of a translocation pore.

Another intriguing observation is that the transport inhibition observed with modifications of A414C roughly correlates with the size of the added substituent group (Figure 3). Modification by bulky MTS-derivatives, MTSES (negative charge), MTSET (positive charge) or the large MTSACE (neutral) resulted in dramatically reduced transport activity, whereas the smaller MTSEA (positive charged) or MMTS (neutral) reagents resulted in only minor inhibition. Because all of the MTS-derivatives reacted to completion with this residue, it is likely that MTSEA and MMTS exert a limited effect on the transport activity of the carrier because they introduce smaller substituents. Inhibition by the MTS-derivatives could arise from a decrease in the ability of L-Glu or sodium ions to bind to the carrier or from steric limitations placed on conformational changes required for substrate transport. In the scheme shown in Figure 7, we position A414C at the extracellular entrance of a translocation pore formed by this region of the carrier, to reflect its accessibility to all MTS-

derivatives tested and to position it where it could interfere with the access of substrates or co-transported ions when it is modified by MTS-derivatives of sufficient size.

Accessibility of two residues is influenced by extracellular sodium ions

SCAM analysis also revealed that extracellular sodium ions limit the modification of cysteine substitutions at Y405 and at E406 (Figure 6). This may occur by direct occlusion, or alternatively by stabilizing a conformation that restricts access to the side-chain. A similar decrease in the accessibility of Y403C and E404C in GLT-1 to MTSEA in the presence of external sodium ions was observed (Zarbiv et al., 1998). Although we have not observed MTSET modification of Y405C in EAAT1, it does appear to react with the Y403C mutant of GLT-1 (Zarbiv et al., 1998). In earlier site-directed mutagenesis studies of GLT-1, aromatic substitutions at the Y403 position altered the ion dependence and the increased affinity of sodium binding to the carrier (Zhang et al., 1998). It has been hypothesized that the quadrupole moment of aromatic amino acids influence the binding of cations in some channels by a weak electrostatic interaction (Dougherty, 1996) and an interaction of this type may influence the binding of sodium and/or potassium ions to the glutamate transporters as well. Because the modification rates of these residues with MTSEA are increased in the absence of extracellular sodium ions, we propose that they reside within an aqueous translocation pore and are positioned such that they can be accessed from the extracellular milieu (Figure 7).

In conclusion, this study provides evidence that residues P392 through Q415 of EAAT1 are important to several aspects of transporter structure and function. The existence of a re-entrant membrane loop with both ends exposed to the extracellular milieu suggests that, by analogy the to the P-loops of ion channels, this domain may participate in the formation of an aqueous translocation pore. Examination of other domains in the carrier by SCAM should bring insight into the tertiary structure of the carrier and provide a more

detailed model of the structural determinants underlying the translocation and ion-flux processes executed by these molecules.

Experimental Procedures

Construction of the Cys(-) and single cysteine carriers

A Cys(-) transporter was engineered by making conservative substitutions of the three endogenous cysteine residues in the EAAT1 transporter (C186S, C252A and C375G), using the ALTERED SITES II site-directed mutagenesis kit and recommended protocol (Promega, Madison, WI). Cys(-) was sequenced on both strands and subcloned into pOTV for expression in *Xenopus* oocytes and into pCMV5 for expression in COS-7 cells (Arriza et al., 1994). Single cysteine carriers were made using a PCR-based mutagenesis strategy. Two primers were designed to flank the mutagenesis region. One was made to a unique Pst1 restriction site in the 5' end of the coding sequence (5'Pst1), and the other one to the last nucleotides of the coding sequence and included an Xba1 site (3'Xba1). Twenty-four mutant primers were designed to substitute each residue in the region P392 through Q415 with cysteine. For each reaction, 1mg each of the 5'Pst1, 3'Xba1 and a mutant primer were added to a tube containing 10 units of Vent polymerase, 10 units of Taq thermostable ligase (both from New England Biolabs, Beverly, MA), 0.25mM of each of dATP, dCTP, dGTP, dTTP, 1X Taq thermostable ligase buffer and 100ng of the Cys(-)OTV plasmid in a final volume of 100ml. Cycling conditions were: 95°C for 5 min (1 cycle), 95°C for 30 sec, 50°C for 30 sec, 65°C for 10 min (25 cycles), and a 15 min final extension at 65°C. The 1.2Kb products were subcloned into Cys(-)OTV and Cys(-)CMV5 plasmids using the Pst1 and Xba1 sites and sequenced by Dye Terminator Cycle Sequencing (ABI PRISM, Perkin Elmer).

Functional characterization of the Cys(-) and single cysteine transporters

Transport affinity values (K_m) for L-Glu uptake into COS-7 cells were determined for each carrier. Cells were transiently-transfected using the DEAE-dextran method and 48 hrs later a radiolabeled L-Glu transport assay performed, as previously described (Arriza et al.,

1994). K_m values were derived by nonlinear regression analysis (Kaleidagraph, Synergy Software, Reading, PA).

Two-electrode voltage-clamp was used in Xenopus oocytes to measure the transport affinity (EC_{50}) (-60mV) and current-voltage relationships for L-Glu from substrate-elicited steady-state currents as described previously (Arriza et al., 1997).

Cell-surface expression levels of the carriers in COS-7 cells

Cell-surface expression of transiently-transfected transporters was assayed as previously described (Daniels and Amara, 1998). Briefly, cells were washed with PBS and then incubated with 1.5 mg/ml NHS-biotin (Pierce, Rockford, IL) in PBS for 40 min at 4°C. A glycine-containing buffer was used to quench the reaction. Cells were lysed on ice with a 1% Triton X-100 buffer, transferred to a 1.5 µl microfuge tube and spun at 14,000 rpm. Ultralink™ Immobilized NeutrAvidin beads (Pierce, Rockford, IL) were added to the supernatants, and the components were mixed overnight at 4°C. The beads were then washed, 2X SDS loading buffer was added, and the sample incubated at 37°C for 30 min. The proteins were separated on an 8.5% polyacrylamide gel, transferred to Immobilon-P (Millipore Corp., Bedford, MA), probed with a polyclonal antibody raised to the C-terminus of EAAT1 (1:3,000 dilution), and visualized with a horseradish peroxidase (HRP)-conjugated secondary antibody (1:10,000; Amersham, Arlington Heights, IL) and chemiluminescent detection (Dupont NEN, Boston, MA).

Application of MTS-derivatives and measurement of the transport activity in COS-7 cells

MTS-derivatives (Toronto Research Chemicals Inc.) were solublized in water as 50X stocks immediately prior to use. Cells were washed once with PBS before the MTS-derivatives were added to their final concentrations. To compensate for the different rates of covalent modification with free sulfhydryls in solution, the MTS-derivatives were applied in most experiments at the following concentrations: 2.5mM MTSEA, 10mM MTSES and

1mM MTSET (Stauffer and Karlin, 1994). Unless otherwise stated, in all experiments incubations with MTS-derivatives were done at RT for 5 min. Following the incubation, cells were washed 3X with PBS and assayed for uptake of 10mM radiolabeled L-Glu (9.9μM non-labeled L-Glu and 100nM [^{3}H]-L-Glu (24 Ci/mmol); 10 min at RT).

The effect of the MTS-derivatives on uptake is expressed as either the percent inhibition (PI = 100- (100*uptake after /uptake before)) or the fraction of uptake remaining (F = uptake after/ uptake before). Second order rate constants (k) were calculated by plotting F as a function of time (t) in sec or of concentration of MTS-derivative (c) in moles/liter and then fitting the data to the equation: F = exp(-ktc), in the case where F goes to zero at very large t or c. Otherwise, the data were fitted to the equation F = Fmax *exp(-ktc) + Fmin. Significance was determined by one-way ANOVA ($p < 0.05$) using statistical software (SPSS, Inc., Chicago, IL).

To examine the effects of sodium on sulfhydryl modification, cells were washed 1X with KRH buffer containing either sodium chloride or choline chloride (each at 120mM). MTS-derivatives were incubated in the same buffer. After the incubation, the cells were washed 1X with the corresponding buffer and then 2X with PBS.

For experiments in which DL-TBOA or non-labeled L-Glu were included in the reaction, the compounds were added 2 min prior to the MTS-derivatives. The percent inhibition of uptake was plotted as a function of the L-Glu or DL-TBOA concentration and fitted to the Michaelis-Menten equation using non-linear regression analysis to determine the half-maximal concentration (EC_{50}) that protects the residue from modification (Kaleidagraph).

To examine the effect of low temperature on protection by substrate, cells were placed on ice and then washed twice with ice cold PBS. L-Glu was added, followed 2 min later by the modifying reagent. After five min, the cells were washed 1X with ice cold PBS and 2X with PBS at RT. Radiolabeled uptake of L-Glu was assayed as described.

Acknowledgments

We are very grateful to Dr. Keiko Shimamoto for the generous gift of DL-TBOA. We also thank Jonathan Javitch, Wendy Fairman, Peter Poerzgen, Geoff Murdoch and Kevin Poth for their comments and helpful insights. This work was supported by National Institutes of Health grants NS33273 to S.G.A. and MH11673 to R.P.S. and by the Howard Hughes Medical Institute.

Topology of the glutamate transporter as defined by the extracellular accessibility of cysteine substitutions in EAAT1

Rebecca P. Seal*, Barbara H. Leighton†, and Susan G. Amara†
*Program in Neuroscience and the †Howard Hughes Medical Institute, Vollum Institute, Oregon Health Sciences University, Portland, OR 97201

Running title: Topology of the glutamate transporter

Corresponding Author:
Susan G. Amara
Vollum Institute L-474
Oregon Health Sciences University
3181 S.W. Sam Jackson Park Rd.
Portland OR 97201
Tel: (503) 494-6723
Fax: (503) 494-8230
Amaras@ohsu.edu

Summary

Excitatory amino acid (EAA) transporters are polytopic membrane proteins expressed in neurons and glial cells that serve to buffer and remove extracellular glutamate during synaptic transmission. Previous studies have established the presence of six α-helical transmembrane domains (TMs) 1-6 in the N-terminal portion of the EAA carriers, but the number and orientation of TMs in the C-terminal end remains ambiguous. To address this, individual residues in the C-terminus of a cysteine-less version of EAAT1 [Cys(-)] were individually mutated to cysteine and their extracellular accessibility evaluated by labeling with membrane impermeant and then biotin-containing derivatives of thiol-reactive compounds in intact COS-7 cells. A number of cysteine substitutions were reactive with the impermeant compounds, suggesting that they reside either in the extracellular space or in an aqueous intermembrane compartment that is accessible to the extracellular milieu. From these analyses, we confirm the presence of α-helical TMs 5 and 6 and propose that there are at least four additional TMs, including one that forms a re-entrant membrane loop. This model for the EAA transporter structure is novel and is clearly distinct from the six α-helical TMs postulated for the C-terminal domain of the sodium and chloride-dependent neurotransmitter transporter family.

Introduction

High affinity, sodium-dependent glutamate transporters, expressed in neurons and glial cells, buffer and remove synaptically released glutamate (Tong and Jahr, 1994; Mennerick and Zorumski, 1994; Otis et al., 1996; Diamond and Jahr, 1997) and serve to limit the excitotoxic actions of glutamate that lead to neuronal death (Choi, 1994; Szatowski and Attwell, 1994). The unidirectional transport of substrates by these carriers is driven by the co-transport of two or three sodium ions (Kanner and Sharon, 1978; Zerangue and Kanvanaugh, 1996) and one proton (Zerangue and Kavanaugh, 1996) and the counter-transport of one potassium ion (Szatkowski et al., 1990). In addition to the electrogenic flux of coupled-ions, transporter substrates also elicit an associated chloride conductance that is thermodynamically uncoupled from transport (Eliasof, 1993; Fairman et al., 1995; Wadiche et al., 1995). The presence of the anion conductance together with an observed substrate independent "leak" conductance (Vandenberg et al., 1995) suggests that these carriers may have a broader role in neurotransmission than previously thought, and that they may operate by mechanisms more similar to ion channels than to classic carrier models, as has recently been proposed (Lester et al., 1994; Defelice and Blakely, 1996; Sonders and Amara, 1996).

Initial insight into the structure of this transporter family came from the isolation of genes that encode both eukaryotic: GLAST1 (Storck et al., 1992), GLT-1 (Pines et al., 1992), EAAC1 (Kanai and Hediger, 1992), EAAT 4 (Fairman et al., 1995) and EAAT 5 (Arriza et al., 1997) and prokaryotic: DctA (Engelke et al., 1989), GltP (Tolner et al., 1992a), GltT (Tolner et al., 1992b) members. High amino acid conservation of the mammalian subtypes with each other (50-60%) and with the bacterial subtypes (30-40%), suggests that they share a similar overall structure. Comparisons of the five mammalian subtypes, which are each comprised of ~ 500-600 amino acid residues, indicate that the N- and C-termini, which have been shown experimentally to reside intracellularly (Slotbloom

et al., 1996, Wahle and Stoffel, 1996), are the least conserved. Hydropathy analyses indicate that the first six hydrophobic stretches which also show a fair degree of amino acid conservation, likely form α-helical transmembrane domains (TMs). This model is supported by the results of a study that experimentally demonstrated the ability of these domains to act as membrane-spanning (Wahle and Stoffel, 1995). Demonstration of N-linked glycosylation at residues in this loop between TMs three and four indicates that it resides extracellularly (Conradt et al., 1995). Interestingly, there is a short segment of hydrophilic residues located in this loop that are uniquely conserved amongst the eukaryotic members of this family.

Residues in the C-terminal half of the carrier show a high degree of conservation and have been implicated in substrate, inhibitor, and co-transported ion interactions, based on studies of chimeras (Vandenberg et. al., 1995), site-directed mutagenesis (Pines et al., 1995; Kavanaugh et al., 1997; Zhang et al., 1998), and substituted cysteine accessibilities (Zarbiv et al., 1998; Seal and Amara, 1998). However, unlike the N-terminal ~350 amino acid residues of EAAT1, hydropathy analysis does not clearly define the number and orientation of transmembrane segments in the remaining ~200 residues. Experimental investigation of the C-terminal domain topology has not yet resolved this ambiguity. Studies of GLAST1, the rat homolog of EAAT1 (Wahle and Stoffel, 1996), GltT, a glutamate transporter from E. coli (Slotbloom et. al, 1996), and DctA, a dicarboxylic transporter from R. melioti (Jording and Puhler, 1993), all employed strategies that assess the orientation of a reporter epitope fused to sequential C-terminal deletions of the transporter. Despite the use of similar strategies, topological models for the carriers were proposed describing four β-strands (GLAST1), four α-helices (GltT) or six α-helices (DctA). Moreover, conclusions about these models were based on the analyses of non-functional transporters and therefore, from carrier structures that may not accurately reflect that of the native carrier. Recently, Grunewald et al. reported the topology of GLT-1, the rat homolog of human EAAT2, using thiol-modification of functional cysteine substitution

mutants expressed in HeLa cells (Grunewald et al., 1998). Although this approach is similar to the one employed here to evaluate the topology of the EAAT1 subtype, we provide both biochemical and functional evidence for an alternative topological model for several residues in last half of the carrier.

In this study, the topology of the C-terminal ~240 residues of the human EAAT1 transporter was evaluated in only functional, surface-expressed carriers. Residues in this region were individually substituted with cysteine and their accessibility to the extracellular space was evaluated by labeling with membrane impermeant and then biotin-containing derivatives of cysteine-reactive compounds in intact COS-7 cells. Additionally, in the case of a few mutants, the effect of modification by impermeant reagents on the transport activity was examined. The observed reactivity of several of the cysteine substitutions with the membrane impermeant reagents defines these residues as accessible to the extracellular milieu and suggests a topology in which TMs 6 and 7 span the membrane, residues in the loops following TMs 5, 7 and 8 are extracellular and TM 8 forms a re-entrant loop. Finally, although we identified in the last conserved domains of the carrier (domains 9-12) several residues that appear to be exposed to the extracellular space, additional methods will be required to determine whether or not they are membrane associated

Results

For reference purposes, EAAT1 was partitioned into twelve domains (1-12), based on hydropathy analyses (Figure 1) and amino acid conservation amongst the five cloned human subtypes (EAATs 1-5). Because TMs are often highly hydrophobic and conserved, a region in EAAT1 was designated as a domain if it showed either or both of these characteristics. As mentioned previously, there are six hydrophobic domains located in the first ~350 amino acid residues, that are generally considered to form α-helical TMs (Storck et al., 1992; Pines et al., 1992; Kanai and Hediger, 1992; Slotbloom et al. 1996; Wahle and Stoffel, 1996; Grunewald et al., 1998) and were thus designated as domains 1-6. Within the remaining ~200 amino acid residues there appear to be six highly conserved domains, three of these score strongly as hydrophobic (domains 7, 9, 10) while the other three score only weakly as hydrophobic (domains 8, 11, and 12; Figure 1). To determine the precise number and orientation of membrane-spanning segments in the last ~250 amino acid residues, we evaluated the extracellular accessibilities of individual cysteine substitutions to sulfhydryl modification in functional carriers expressed at the plasma membrane of intact cultured cells.

Cysteine was substituted for individual residues in the C-terminal half of EAAT1 and the resulting carriers were tested for their ability to mediate the accumulation of L-glutamate when expressed in COS-7 cells. A previously characterized functional version of EAAT1, in which all three endogenous cysteine residues were conservatively replaced [Cys(-)], was used as the template to create the single cysteine mutants (Seal and Amara, 1998). As shown in Table 1, each mutant was able to mediate the transport of L-glutamate.

The membrane orientation of the single cysteine substitutions was evaluated in two similar assays (Figure 2). In one assay, cells expressing the mutant carriers were incubated in the presence and absence of membrane impermeant stilbene disulfonate maleimide (SM) or the methanethiosulfonate (MTS) –derivative, [2-(Trimethylammonium) ethyl]

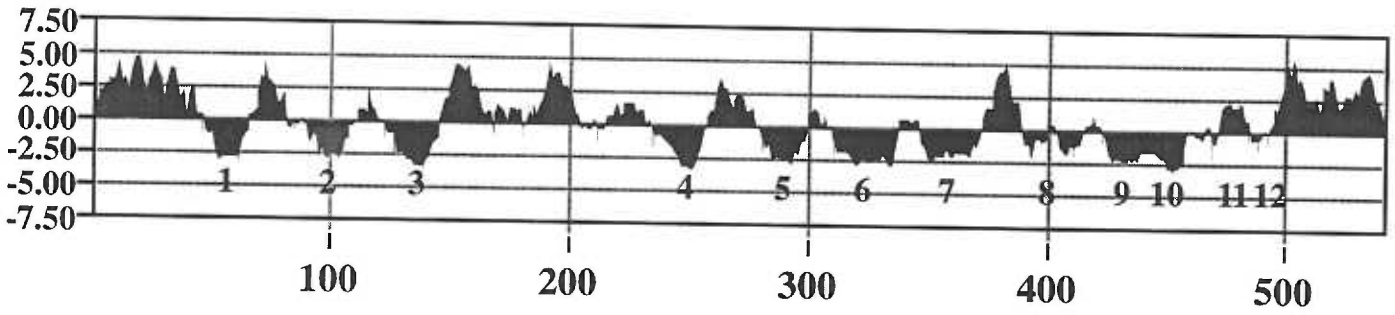

Figure 1. Hydropathy analysis of the EAAT1 Transporter.

Hydropathy plot of EAAT1 generated by the Goldman, Engelman, Steitz algorithm with a window size of 10 (MacVector^{TM}). Hydrophobicity increases as values of the index decrease. Five domains score strongly as hydrophobic (1-5) in the first half (~ 300 residues) of the carrier. In the second half (~240 residues), four conserved domains score strongly as hydrophobic (6, 7, 9, 10), two conserved domains score weakly as hydrophobic (8 and 12), and one conserved domain scores strongly hydrophilic (11).

Table 1.

Substitution Mutant	Vmax*
M307C	17+/-2
G308C	56+/-2
S366C	27+/-6
A367C	95+/-11
A395C	65+/-7
A414C	23+/-4
F423C	54+/-5
T428C	29+/-8
T432C	78+/-10
G442C	16+/-4
I453C	25 +/-5
T462C	59+/-10
T466C	77+/-1
R477C	32+/-3*
A527C	93+/-4

Radiolabeled uptake was measure in COS-7 cells expressing the transporters. Vmax are expressed as a percent of Cys(-) transporter Vmax. Values are averages for n >3 experiments performed in triplicate. *Uptake for R477C was performed once in triplicate.

methanethiosulfonate (MTSET), followed by incubation with the membrane permeant biocytin maleimide (BM). The structures of these sulfhydryl-reactive compounds are shown in Figure 3. Transporter mutants were immunoprecipitated using a polyclonal antibody raised to the C-terminus and then probed on western blots with strepavidin conjugated to horseradish peroxidase (HRP) to detect biotin labeling. The absence of labeling after treatment with SM indicates that the residue is located extracellularly. As a control, blots were re-probed with the C-terminal antibody to EAAT1 to demonstrate the presence of the transporter protein.

In a second assay, methanethiosulfonate (MTS) derivatives were used to identify residues that are exposed to the extracellular side of the membrane (Figure 2). MTS-derivatives react specifically and rapidly with the sulfhydryl group of cysteine and are a billion times more reactive in an aqueous environment than a lipid one (Roberts et al., 1986). Because the MTS-derivatives are smaller than the maleimide derivatives (Figure 3), they may react with residues that the larger maleimides cannot access, including residues that may reside in an aqueous compartment within the membrane. Cells expressing the mutant transporters were incubated in the presence and absence of the membrane impermeant MTS-derivatives, (2-sulfonatoethyl)methanethiosulfonate (MTSES) and MTSET, and then incubated with N-Biotinylaminoethyl methanethiosulfonate (MTSEA-biotin). Biotinylated proteins were isolated with NeutrAvidin beads and western blots probed for the presence of the biotin-isolated transporter with the EAAT1 C-terminal antibody. The inability to detect a mutant carrier after pre-incubation with the impermeant reagents, indicates that the residue is extracellular or is exposed to the extracellular milieu from an intermembrane compartment.

A

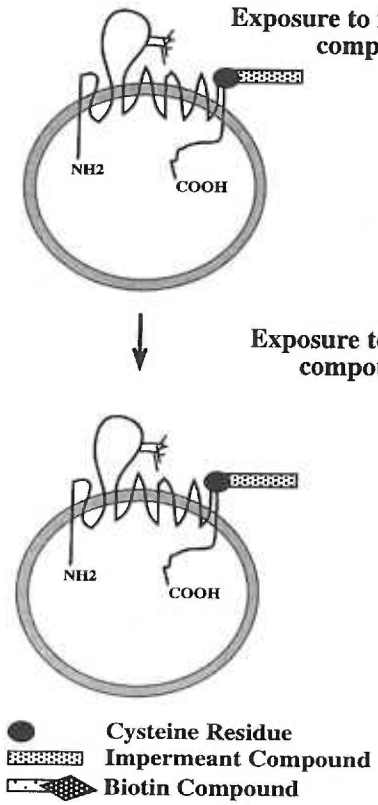

B

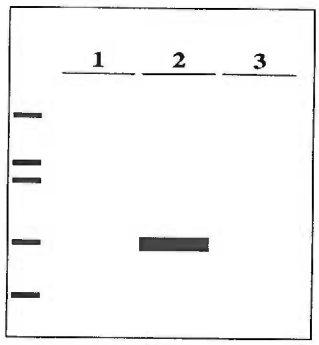

1. No Treatment
2. Biotin Compound Only
3. Impermeant Compound and Biotin Compound

Figure 2. Strategy to resolve the membrane orientation of individual cysteine substitutions in EAAT1.

(A) Intact COS-7 cells expressing a carrier mutant are first incubated either in the presence and absence of membrane impermeant derivatives of maleimides and methanethiosulfonates followed by an incubation with biotin-linked derivatives of these sulfhydryl reactive reagents.

(B) Carriers in which the cysteine is accessible to membrane impermeant reagents from the extracellular milieu will not be detected on the western blot.

Methanethiosulfonate Derivatives:

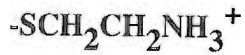

MTSEA

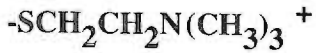

MTSET

MTSES

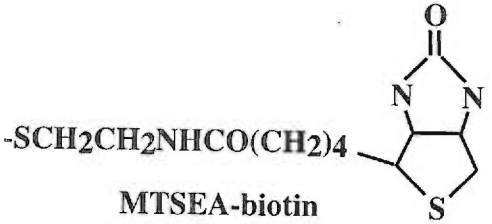

MTSEA-biotin

Maleimide Derivatives:

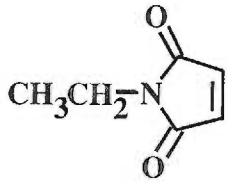

NEM

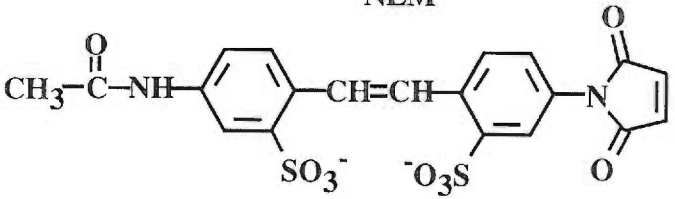

SM

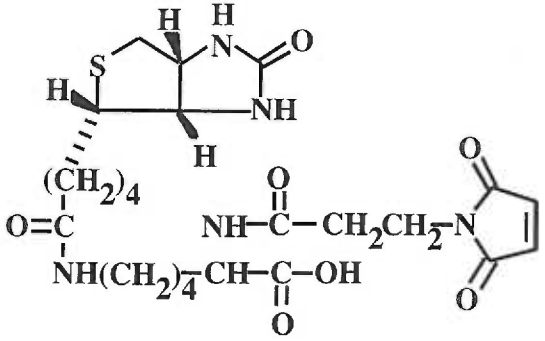

BM

Figure 3. Structures of the thiol-reactive compounds.

Structures of the methanethiosulfonate derivatives: (2-aminoethyl) methanethiosulfonate (MTSEA), [2-(Trimethylammonium) ethyl] methanethiosulfonate (MTSET), (2-sulfonatoethyl) methanethiosulfonate (MTSES), and N-Biotinylaminoethyl methanethiosulfonate (MTSEA-biotin), and of the maleimide derivatives: N-ethyl maleimide (NEM), stilbene disulfonate maleimide (SM), biocytin maleimide (BM).

Membrane impermeant compounds do not block labeling of an intracellular residue

A preponderance of evidence has established an intracellular localization for the C-terminus (Slotbloom et al., 1996; Wahle et al., 1996; Arriza et al., 1997). For this reason, a cysteine substitution mutant (A527C) created in this domain of the carrier was used to test whether MTSES, MTSET and SM, which are considered to be membrane impermeant based on other studies (Loo and Clarke, 1995; Holmgren et al., 1996), could gain access to an intracellular residue of the transporter in this system. As shown in the top panel of Figure 4A, when cells expressing A527C were pre-incubated with SM at concentrations of 0.2mM or 1mM, BM labeling of a 66 kDa transporter band is detected to approximately the same extent as without SM pre-treatment. The bottom panel shows the presence of the transporter protein in each lane. MTSES (10mM) and MTSET (1mM) also appear unable to affect BM labeling of the A527C transporter (Figure 4B). In contrast, N-ethylmaleimide (NEM) (0.2mM) and (2-aminoethyl) methanethiosulfonate MTSEA (1mM), compounds known to be membrane permeant (Holmgren et al., 1996), readily blocked biotin labeling (Figures 4C and 4D). Again, the bottom panel shows the presence of the transporter in each lane. These results demonstrate that the membrane impermeant compounds, MTSES, MTSET and SM, do not gain access to an intracellular residue when applied to the extracellular side of intact COS-7 cells, whereas compounds that are known to permeate the membrane, NEM, MTSEA and BM, readily react with this residue.

Extracellular localization of cysteine substitutions

We began our evaluation of the number and orientation of membrane spanning domains in the C-terminus of the carrier by determining the extracellular accessibility of residues in the hydrophilic loop following domain 5. Two cysteine substitutions, M307C and G308C, in this loop, were reactive with BM and could be blocked by pre-incubation with the

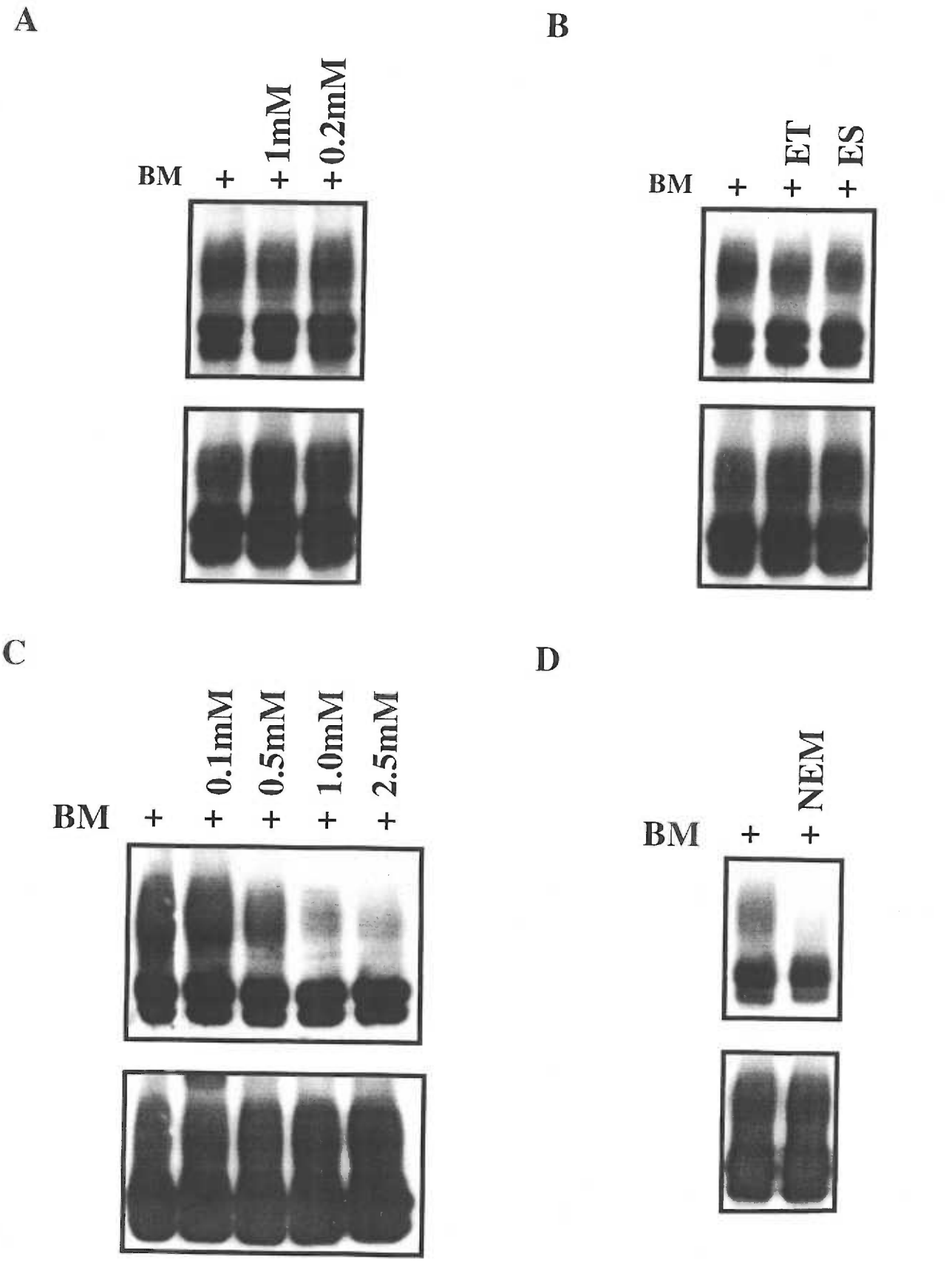
A
BM
+
+ 1mM
+ 0.2mM
B
BM
+
+ ET
+ ES
C
BM
+
+ 0.1mM
+ 0.5mM
+ 1.0mM
+ 2.5mM
D
BM
+
+ NEM

Figure 4. Membrane permeant but not impermeant reagents modify an intracellular residue of EAAT1 (A527C) in intact COS-7 cells.

(A) Top Panel: Cells expressing the A527C carrier were pre-incubated with impermeant SM at 1mM and 0.2mM, followed by incubation with 1mM BM. Blot was probed with strepavidin-HRP to detect biotin labeling of the 66 kDa A527C transporter. Bottom Panel: Same blot reprobed with C-terminal antibody (Ab) to EAAT1 shows the presence of the 66 kDa A527C transporter. Both blots show the presence of the EAAT1 Ab IgGs.

(B) Top Panel: Cells expressing the A527C carrier were pre-incubated with the membrane impermeant compounds MTSET (1mM) and MTSES (10mM) followed by incubation with 1mM BM. Blot was probed with strepavidin-HRP to detect biotin labeling of the 66 kDa A527C transporter. Bottom Panel: Same blot reprobed with C-terminal antibody (Ab) to EAAT1 shows the presence of the 66 kDa A527C transporter. Both blots show the presence of the EAAT1 Ab IgGs.

(C) Top Panel: Cells expressing the A527C carrier were pre-incubated with concentrations of the membrane permeant MTSEA ranging from 0.1 to 2.5mM and then incubated with 0.2mM BM. Blot was probed with strepavidin-HRP to detect biotin labeling of the 66 kDa A527C transporter. Bottom Panel: Same blot reprobed with C-terminal antibody (Ab) to EAAT1 shows the presence of the 66 kDa A527C transporter. Both blots show the presence of the EAAT1 Ab IgGs.

(D) Top Panel: Cells expressing the A527C carrier were incubated with 0.1mM of the membrane permeant NEM and then incubated with 0.2mM BM. Blot was probed with strepavidin-HRP to detect biotin labeling of the 66 kDa A527C transporter. Bottom Panel: Same blot reprobed with C-terminal antibody (Ab) to EAAT1 shows the presence of the 66 kDa A527C transporter. Both blots show the presence of the EAAT1 Ab IgGs.

impermeant SM (Figure 5) or MTSET (Figure 6 and data not shown) compounds. The bottom panels demonstrate that the transporter protein is present in each lane. Similar to the results obtained with BM, these two cysteines were also labeled with MTSEA-biotin and this could be blocked by pre-incubation with the membrane impermeant MTSES and MTSET (Figure 7). Thus, the cysteine residues substituted for M307 and G308 appear to be easily accessed from the extracellular milieu (Figure 9).

There is a region of several consecutive serine residues S363 to S366 that by hydropathy analysis appears to reside within or just after domain 7 (Figure 1). Substitution of S366 with cysteine resulted in a carrier mutant that could be labeled with BM. Pre-incubation with either SM (Figure 5) or MTSET (Figure 6) blocked labeling of this residue. In addition another residue, A367C was also reactive with BM and could be blocked by incubation with SM (Figure 5) or MTSET (Figure 6). Again, the presence of the transporter was detected in each lane. As shown in Figure 7, pre-incubation of both S366C and A367C with the impermeant compounds, MTSES or MTSET, prevented labeling by MTSEA-biotin. Furthermore in a functional assay, incubation of cells expressing the S366C or the A367C carriers with either MTSES or MTSET completely inhibits their transport activity (Figure 8). These findings strongly suggest that S366C and A367C residues are accessed from the extracellular space in carriers that are present at the plasma membrane.

Evidence that domain 8 is involved in the transport process has come from both chimera (Vandenberg et al., 1995) and site-directed mutagensis studies (Pines et al., 1995; Kavanaugh et al., 1997; Zhang et al., 1998), as well as from studies that employed cysteine modification to evaluate the functional role of residues in this domain (Zarbiv et al., 1998; Seal and Amara, 1998). It was previously demonstrated that the modification of cysteines substituted for one residue at each end of the domain, A395C and A414C, with the impermeant compounds MTSES and MTSET, resulted in the inhibition of L-glutamate transport (Seal and Amara, 1998). In the present study, both residues are readily labeled by

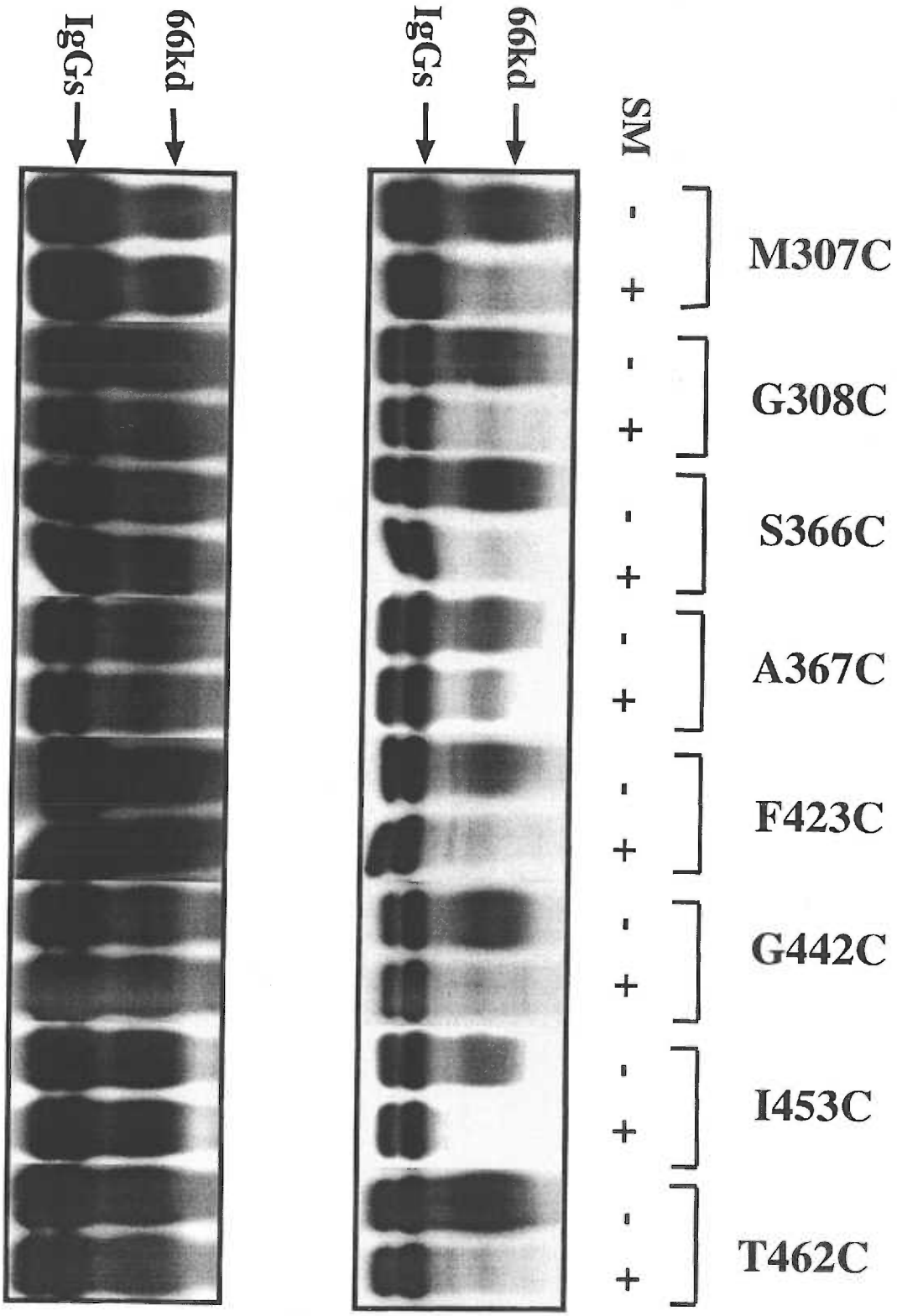
IgGs
66kd
IgGs
66kd
SM
-
+
M307C
-
+
G308C
-
+
S366C
-
+
A367C
-
+
F423C
-
+
G442C
-
+
I453C
-
+
T462C

Figure 5. BM labeling of single cysteine substitution mutants is prevented by SM.

Top Panel: Cells expressing the cysteine substitution mutants were pre-incubated with and without the membrane impermeant SM compound for 30 min and then incubated with BM for 30 min. Concentration of reagents for each mutant were 0.2mM SM and 0.2mM BM (M307C, S366C, T462C), 1mM SM and 1mM BM (A367C, F423C, G442C, I453C), or 0.2mM SM and 2mM BM (G308C). The blot was probed with strepavidin-HRP to detect biotin labeling. Bottom Panel: Same blot reprobed with a C-terminal Ab to EAAT1.

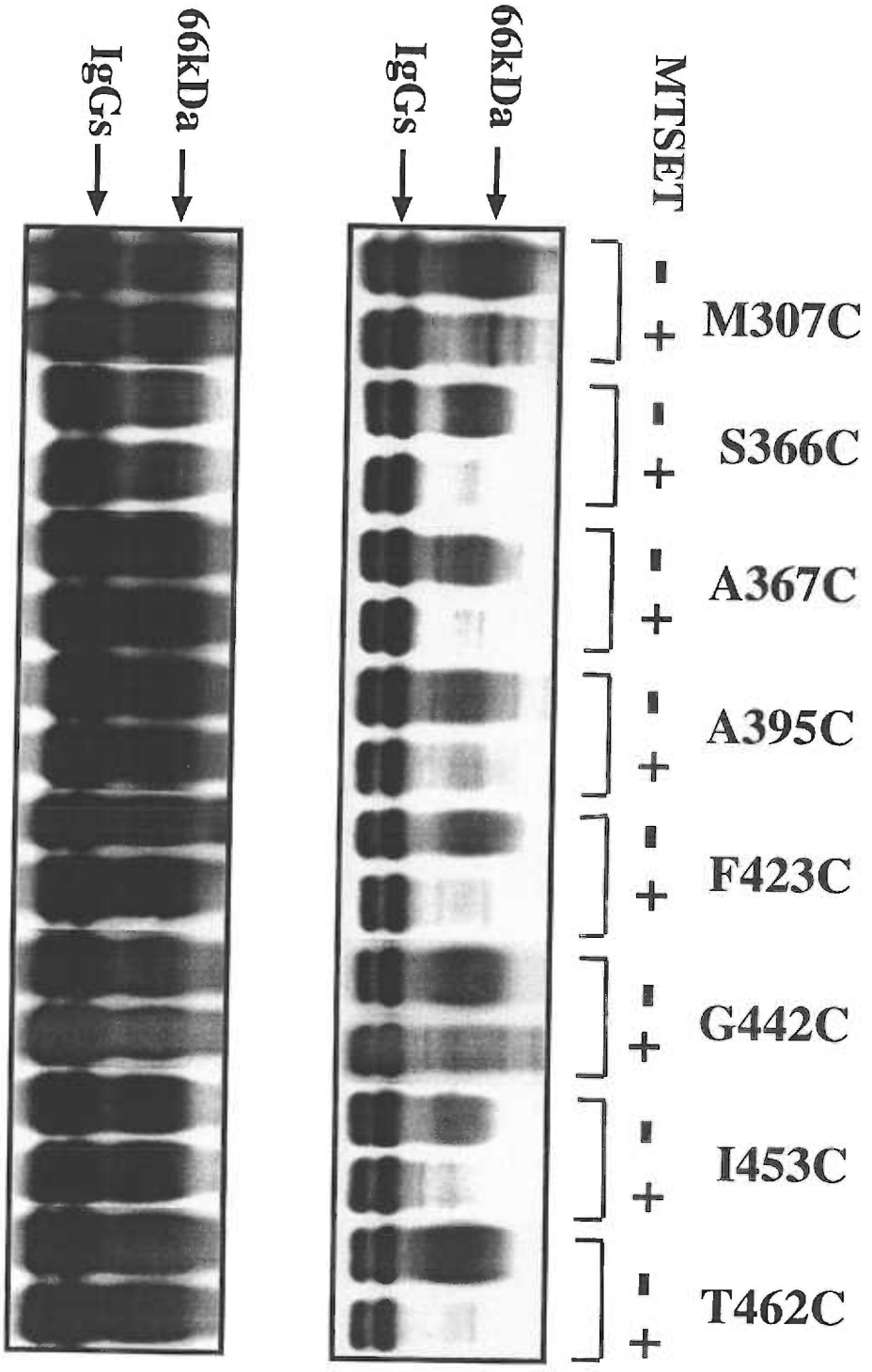
IgGs
66kDa
IgGs
66kDa
MTSET
-
+
M307C
S366C
A367C
A395C
F423C
G442C
I453C
T462C

Figure 6. BM labeling of cysteine substitutions is prevented by MTSET.

Top Panel: Cells expressing the cysteine substitution mutants were pre-incubated with and without the impermeant MTSET compound at 1mM for 5 min and then incubated with BM for 30 min. Concentrations of the BM compound for each mutant were: 0.02mM BM (S366C), 0.2mM BM (T462C) or 1mM BM (M307C, G308C, A367C, F423C, G442C, I453C). The blot was probed with strepavidin-HRP. Bottom Panel: Same blot reprobed with a C-terminal Ab to EAAT1.

MTSEA-biotin and this is prevented by pre-incubation with MTSES and MTSET (Figure 7). Also, A395C, but not A414C could be labeled by the larger BM compound and this labeling could be blocked by MTSET (Figure 6). These findings demonstrate that the A395C and A414C residues are exposed to the extracellular space and support the contention that this domain forms a re-entrant membrane loop (Figure 9; see Discussion).

An extracellular location for the hydrophilic loop following domain 8 is supported by the labeling pattern of another mutant, F423C. The site of the substitution is located just 9 amino acids downstream of the A414. BM was able to label the cysteine substituted at this position and SM (Figure 5) and MTSET (Figure 6) blocked this labeling. Similarly, MTSES and MTSET blocked labeling of the residue with MTSEA-biotin (Figure 7). Thus, the extracellular accessibility of a cysteine substituted for F423 to a range of thiol-modifying reagents supports its placement in the extracellular milieu.

A span of ~ 39 residues (G424 to T462) that follows this loop (domains 9 and 10) is highly conserved, scores strongly as hydrophobic and thus, is likely to be membrane associated (Figure 1). Five residues in this region were accessible to MTS-biotin or BM. T428C, at the beginning of the domain, was labeled with MTS-biotin and this labeling could be blocked by pre-incubation with MTSES and MTSET (Figure 7). Just four residues away is another residue, T432C, that labeled with MTS-biotin but did not react with either MTSES and MTSET (Figure 7). In contrast, G442C and I453C were reactive with both MTSEA-biotin and BM. The reactivity with BM could be blocked by pre-incubation with SM (Figure 5) and MTSET (Figure 6) and the reactivity with MTSEA-biotin could be blocked by both MTSET and MTSES (Figure 7). Another residue, T462C, could also be labeled with all of the sulfhydryl-reactive compounds used in this study (Figures 3, 4 and 5). Thus, we identified four residues in this domain (T428C, G442C, I453C and T462C) that reside in an aqueous environment and are accessible to the extracellular space.

M307C
G308C
S366C
A367C
A395C
A414C
MTS-Biotin
+ ET ES
F423C
T428C
T432C
G442C
I453C
T462C
T466C
R477C
A527C

Figure 7. MTSEA-biotin labeling is prevented by MTSES and MTSET.

Cells expressing the cysteine substitution mutants were pre-incubated with membrane impermeant MTS-derivatives, 1mM MTSET or 10mM MTSES for 5 min at RT and then incubated with 2mM MTSEA-biotin for 20 min. Blots were probed with a C-terminal Ab to EAAT1.

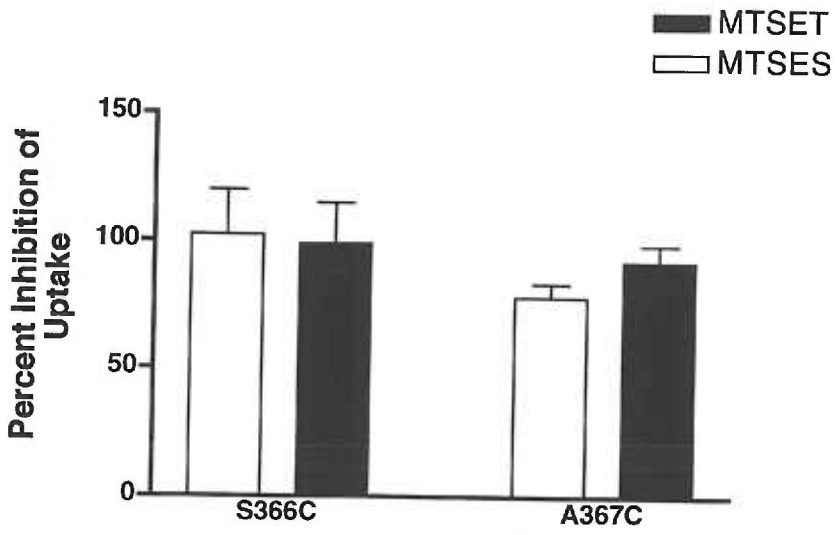
MTSET
MTSES
Percent Inhibition of Uptake
150
100
50
0
S366C
A367C

Figure 8. Transport activity of S366C and A367C carriers is abolished by MTSES and MTSET.

Cells expressing the S366C and A367C transporters were incubated in the presence and absence of 10mM MTSES or 1mM MTSET for 5min at RT. Radiolabeled L-glutamate uptake was measured and plotted as the percent inhibition of uptake. Data are expressed as the means +/- S.D. of 2-3 independent experiments.

Another highly conserved domain in the carrier (domain 11), which spans from T466 to D487 contains several polar and charged residues and thus has some hydrophilic character. Previous studies have shown that the individual mutation of residues in this region, R479 in GLAST1 (Conradt and Stoffel, 1995) and D470 in GLT-1 (Pines et al., 1995) results in abolished transporter function. Substitution of the threonine at position 466 with cysteine resulted in a functional carrier that could be labeled by MTSEA-biotin and pre-incubation with either MTSES or MTSET blocked MTSEA-biotin labeling (Figure 7). Moreover, BM labeled this residue and SM and MTSET prevented the labeling (data not shown). Another residue in this region (R477) is accessible to MTSEA-biotin, but not to BM or to MTSES or MTSET. We have not yet identified a residue in domain 12 that could be labeled with either MTSEA-biotin or BM.

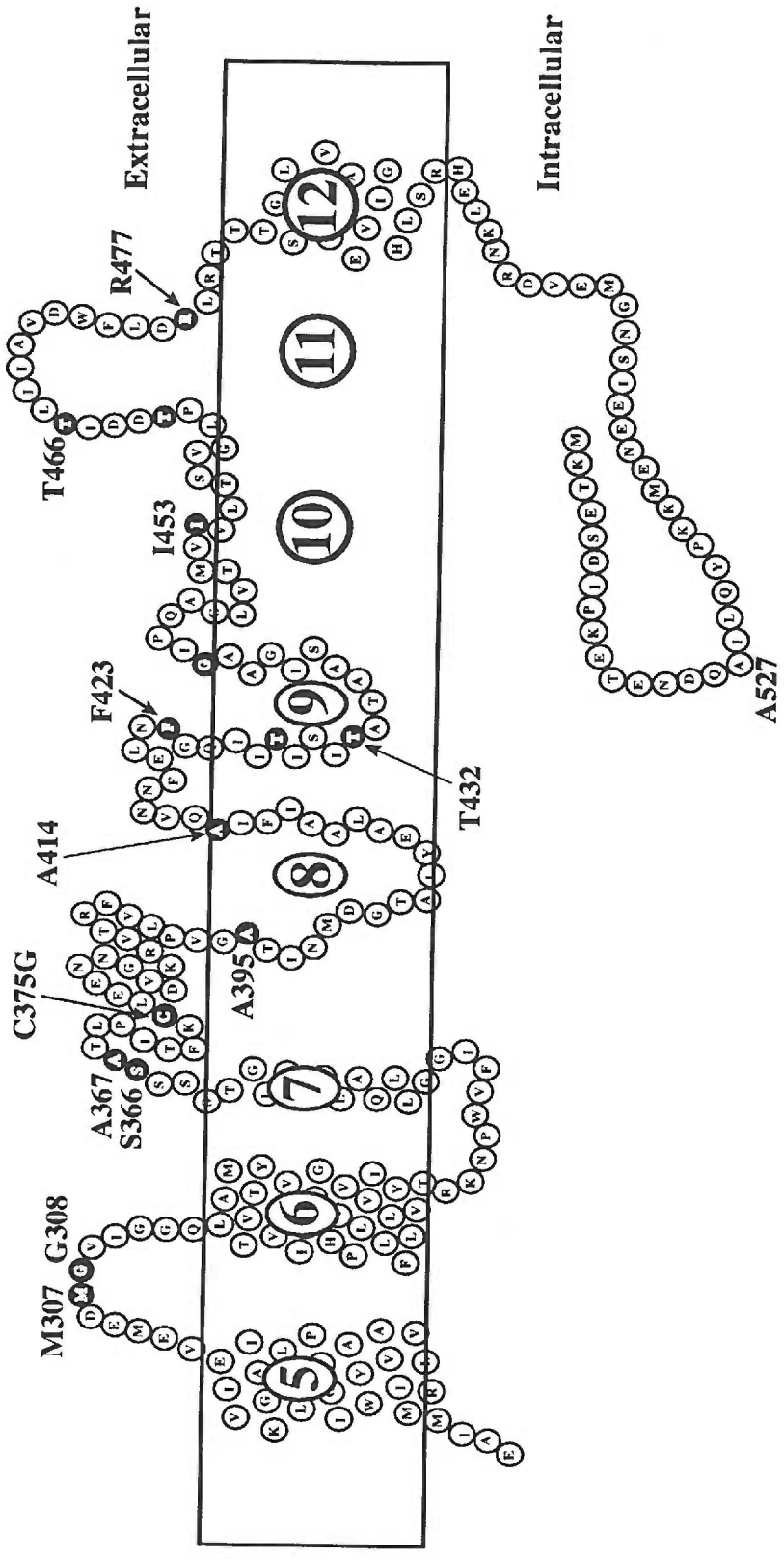
Extracellular
Intracellular
R477
T466
I453
F423
A414
T432
C375G
A395
A367
S366
M307
G308
A527
5
6
7
8
9
10
11
12

Figure 9. Schematic representation of the topology of the C-terminal half of EAAT1.

The proposed topological orientation of residues from E374 (domain 5) to M543 (C-terminal end) in EAAT1 are illustrated. Residues shaded black were accessible to modification from the extracellular space when mutated to cysteine and thus are positioned either extracellularly or in an aqueous compartment within the membrane. C375G is an endogenous cysteine that was mutated to glycine in Cys(-). EAAT1 was partitioned into twelve domains based on hydropathy analysis and on amino acid conservation amongst the EAAT family. Hydrophobic domains 5, 6 and 12 are modeled as transmembrane α–helices, hydrophobic domains 7 and 9 are drawn as β-strands, domain 8 is modeled as re-entrant loop, and hydrophobic domain 10 is membrane associated.

Discussion

Cysteine substitution of residues in the C-terminal half of EAAT1 was very well tolerated and thus, the topology of this carrier was examined by analyzing only functional, surface-expressed carriers (Table 1). Our model is based on the identification of residues that are exposed to the extracellular space, as defined by the ability of membrane impermeant compounds to block labeling observed with the biotin-containing compounds in intact cells. Although, a large number of the single cysteine mutants (>85%) did not react with either of the biotin-conjugated compounds, a sufficient number were accessible as to provide a detailed picture of the topology.

Residues between TMs 5 and 6 are extracellular

We identified two residues in the loop between domains 5 and 6 (M307C and G308C) that were reactive with all of the membrane impermeant compounds and thus, clearly reside in the extracellular milieu. These results are consistent with hydropathy analyses and with all of the experimentally derived topological models that have been proposed thus far. In a study of GLT-1, cysteines substituted for residues in the same loop (E306, A309 and R310) were shown biochemically to be accessible to MTSET in intact HeLa cells (Grunewald et al., 1998). In another study, it was demonstrated that a glycosylation reporter domain fused to the residues of this loop in a C-terminal truncation of the GLAST1 transporter, was glycosylated when expressed in *Xenopus* oocytes or in an in vitro translation system coupled to microsomal membranes. These results are again consistent with an extracellular location for these residues (Wahle and Stoffel, 1996).

The sixth hydrophobic domain spans the membrane

The hydrophilic loop after TM 6 is short (~9 residues) and is highly conserved (Figure 9). Because we could not find a residue from L339 to I349 (but not P345) that reacts with the

biotin-containing derivatives, the location of this loop with respect to the membrane could not be determined experimentally. Nevertheless, we propose that domain 6 spans the membrane (now designated TM 6), based on its strongly hydrophobic nature and on the results of previous studies that have demonstrated its capacity to span the membrane (Wahle and Stoffel, 1996). In an earlier study, it was observed that cysteine substitutions thought to lie close to the lipid bilayer were not accessible to BM, presumably due to steric restrictions (Loo and Clarke, 1995). Thus, it may be that residues of the loop after TM 6 are not accessible to the reagents because they are too closely associated with the lipid bilayer, are in a particularly inaccessible secondary structure, or because they are involved in protein-protein contacts with other domains in the carrier or with a separate protein.

The seventh hydrophobic stretch is a short membrane-spanning domain. The finding that two residues in the loop following hydrophobic domain 7 (S366C and A367C) were reactive with membrane impermeant compounds (Figures 3, 4 and 5), provides compelling evidence to support a model in which domain 7 (now designated as TM7) acts as a short membrane spanning segment with the residues that follow it residing in the extracellular milieu. Moreover, the inhibition of transport activity by the carrier mutants following exposure to MTSES or MTSET establishes that these carriers were labeled at the plasma membrane rather than in an intracellular compartment (Figure 8). Based on the findings presented here, we suggest a model in which residues G350 through S363 reside in the membrane and serines S364 through S366 reside in the extracellular milieu near the membrane interface (Figure 9). The hydroxyl group of serine and threonine residues often plays a critical role in either substrate binding or ion channel permeation of neurotransmitter receptors and transporters (Akabas et al., 1992; Sur et al, 1997). Placement of the serine residues at the extracellular membrane interface (Figure 9) rather than in an intracellular loop (Grunewald et al., 1998), better positions them where they could mediate a similar role in transport of EAAs.

Biochemical and functional evidence supports domain 8 as a re-entrant loop

A re-entrant loop structure for domain 8 (designated TM8) is supported by the experimentally determined extracellular membrane orientation of several cysteine substitutions that flank this region (Figure 9). It was previously shown that reaction of A395C and A414C with either MTSES or MTSET abolishes the transport activity of these mutant carriers (Seal and Amara, 1998). Here, we provide biochemical evidence which demonstrates the extracellular accessibility of the A395C and A414C residues as well as residues that both precede (S366C and A367C) and directly follow (F423 and T428) this domain. These data strongly support the contention that domain 8 forms a re-entrant loop. Re-entrant membrane loops have been identified as participating in the ion pathway of channels (MacKinnon, 1995) and may form part of the pathway for the translocation of substrates and co-transported ions or for the flux of uncoupled ions by these carriers.

Our model (Figure 9), which shows TM7 as a short membrane spanning domain, the residues after it as an extracellular loop, and TM8 as a re-entrant loop is in contrast to the model proposed for GLT-1 using a similar strategy (Grunewald et al., 1998). Their model places residues that span from the C-terminal side of TM6 to the N-terminal side of TM8 in the cytoplasm and models our TM8 as a membrane spanning α–helix (designated TM 7 in their model), oriented with the N-terminal end near the cytoplasm and the C-terminal end at the extracellular membrane face. Their model is based on the following findings: 1) None of the cysteine substitutions created in GLT-1 between TM6 and their α-helical TM7 were reactive with BM in intact HeLa cells. 2) A few residues in this domain were labeled with BM after permeablization with streptolysin O, but only in an immature form of the carrier that was presumably located in an intracellular compartment and not in functional, mature carriers located at the cell surface. 3) An epitope (P695) spanning residues R372 through R386 in this region was not accessible to trypsin digestion after the carrier was reconstituted into proteoliposomes.

There are several possible explanations for why the model proposed in this study differs from the one presented by Grunewald et al. First, because we found only four cysteine substitutions (S366C, A367C, A395C and A414C) that were accessible to modification from TM6 through TM8, it may be that accessible cysteines exist in this region of GLT-1, but were not tested. It would be interesting to know if cysteines substituted for the comparable residues in GLT-1 (S364, A365, A393 and A412) are also reactive with BM or MTSEA-biotin in the absence of streptolysin O and with MTSET, SM or MTSES. Second, the accessibility of residues in the immature form of the carrier may not be the same as the accessibility of these residues in the mature, surface expressed transporter. Experimental analyses of the topological structures of two homologous water-selective channels (CHIP28 and MIWC) identified distinct topological structures for the channels when in the ER, but similar structures when at the plasma membrane (Shi et al., 1995). Third, the inaccessibility of the P695 epitope to trypsin digestion still allows for the possibility that this domain is extracellular and trypsin-insensitive due to secondary structure, protein-protein interactions or lipid bilayer interactions. Fourth, it may be that the seventh hydrophobic region (TM 7) is membrane-spanning and that the accessibilities of the S366 and A367 residues are dependent on environmental factors such as membrane potential, lipid composition, etc., such that the residues are not exposed under the conditions used in the study of GLT-1, whereas they are exposed under the conditions used here for EAAT1. Lastly, although EAAT1 and GLT-1 subunits are highly homologous, they may have inherently different topologies that may underlie some of the subtle variations observed in pharmacology and function.

Several residues in the last few domains are exposed to the extracellular milieu.

Although the topology of domains 9 and 10 (residues G424-T462) remains ambiguous, we were able to determine the membrane orientations of cysteines substituted for a number of

these residues. Hydropathy analysis of this region suggests the presence of two strongly hydrophobic domains (Figure 1), which have previously been modeled as two α-helical TMs, oriented from extracellular to intracellular (residues G424 to P444) and from intracellular to extracellular (residues Q445 to T462) (Slotbloom et al, 1995). However, the observed extracellular accessibility of a cysteine substituted for a residue at the end of domain 9 (G442) argues against this topology. Because all of the tested sulfhydryl reagents labeled G442C, it suggests that this residue is readily accessible and that it resides in the extracellular space rather than at the cytoplasmic side of the membrane, as was predicted by the hydropathy analysis. Grunewald et al. also found evidence that a residue close to G422 (S443C in GLT-1), was reactive with impermeant MTSET when substituted to cysteine (Grunewald et al., 1998). Interestingly, we could not label a cysteine substituted for the residue analogous to S443 with BM (data not shown) and although it is not known whether a cysteine substituted for the residue analogous to G442 can be labeled in GLT-1, these observations also suggest that subtle differences in the accessibilities of residues may exist between the two homologous transporters, as mentioned previously. Again, this may be due to differences inherent in the structures of the subunits themselves or to differences between the expression systems.

We identified two additional residues in domain 9 (T428 and T432) that were accessible to MTSEA-biotin when substituted with cysteine. Because these residues did not react with the larger BM, their accessibility appears to be somewhat restricted. T432C also appears to be electrostatically hindered, as unlike T428C, this residue did not react with MTSES or MTSET. Furthermore, an interesting pattern is found with eight consecutive residues in this region: residues from T428 to T434 alternate between threonine/serine and alanine/isolucine. These observations together with the highly hydrophobic nature of the domain suggests that this region may reside in the membrane as a β-strand with the hydroxyl-containing side chains lined up on one side facing into an aqueous vestibule and the hydrophobic side chains oriented in the opposite direction facing

into the lipid bilayer (Figure 9). Grunewald et al. modeled this domain of GLT-1 as two β-strands (from G423 to S443) based on the previously mentioned extracellular accessibility of S443C and on the supposedly intracellular localization of A431C (A433C in EAAT1) (Grunewald et al, 1998). Furthermore, they proposed that this region forms a re-entrant membrane loop similar to those found in ion channels. In contrast, Wahle and Stoffel modeled the region as part of a large extracellular loop (Wahle and Stoffel, 1996). In the absence of experimental evidence to formally link this region to the membrane, we can only postulate based on observations presented here including its high conservation and hydrophobicity, that the domain exists in the membrane as two β-strands.

There are a sufficient number of residues between G442 and T462 to propose that this region (domain 10) also forms two β-strands, however, the observation that a cysteine substituted for I453 was also accessible to all of the reagents, suggests that the middle of this region is exposed to the extracellular space. Plausible models to fit these data are that the residues participate in an extracellular loop (Wahle and Stoffel, 1996), or that they lie in parallel to the membrane at its interface with the extracellular space (Grunewald et al., 1998). A third and less likely model describes the region as a re-entrant loop with a pore size large enough to accommodate the maleimide derivatives. Again, experiments to address whether or not these residues are membrane associated are needed to resolve the topology of this domain.

Domain 11 is highly conserved and contains a number of charged and polar residues. We identified two residues in this region (T466C and R477C) that react with MTSEA-biotin and thus appear to be accessible to the extracellular environment. Furthermore, T466C reacts with all of the sulfhydryl compounds. The lack of reactivity of R477C with the large BM and SM compounds, and the smaller, charged MTSES and MTSET suggests that it has a more limited accessibility. Experimental models of the topology of GltT (Slotbloom et al., 1996) and GLT-1 (Grunewald et al., 1998) placed this region as the last TM and in the form of an amphipathic α-helix. The idea that this region

is very highly conserved and that the charged residues line up on one side of an α-helix are compelling reasons to model it as membrane-spanning. However, the domain could still have an important functional role, such as binding substrates, when modeled as an extracellular loop. Although we have not yet identified a residue beyond T466 that is accessible to the membrane impermeant compounds, it seems likely that the domain following this region (domain 12) forms the last TM because it is both hydrophobic and highly conserved.

The importance of domains 9-12 to transporter function is indicated both by their high degree of conservation and by the results of a study that implicated this region of the carrier in substrate interactions (Mitrovic et al., 1998). It is not possible to resolve by the methods used here, whether these domains are associated with the membrane or are extracellular. In either case, however, attractive models can be described that would support an important contribution of these domains to transporter function. If associated with the membrane, these domains may form several short membrane spanning segments that assemble to create one or more pores for substrate translocation and/or for the flux of uncoupled ions. Alternatively, if the domains are part of an extracellular loop, then they may form a structure that binds substrate similarly to what has been observed in the glutamine binding protein (QBP), a component of the bacterial glutamine transport system (Hsiao et al., 1996; Sun et al., 1998) and for the kainate binding domains of a rat ionotropic glutamate receptor (iGluR2) (Armstrong et al., 1998). In these proteins, two extracellular loops come together as lobes to form a binding pocket for substrate. Any one of the other conserved, extracellular loops in the glutamate carrier could interact with this C-terminal region to form the two lobes. This also implies that unless these lobes traverse the membrane, two cytoplasmic lobes would be required to act as a substrate binding domain during reverse transport and during exchange.

In conclusion, we propose that TMs 6 and 7 span the membrane, that residues in the loops following TMs 5, 7 and 8 are extracellular, and that TM 8 forms a re-entrant

loop. We have also identified several residues in the last conserved domains of the carrier (T428 to R477) that appear to be exposed to the extracellular milieu, however additional methods to determine whether or not residues in these regions are membrane associated will be required to more precisely establish their topology.

Experimental Procedures

Construction of Site-directed Mutants

Single cysteine substitution mutants were created using a PCR based mutagenesis strategy as previously described (Seal and Amara, 1998). Each mutant PCR product was re-subcloned into Cys(-)CMV5, for expression in COS-7 cells and sequenced by Dye Terminator Cycle Sequencing (ABI PRISM, Perkin Elmer).

Functional Characterization of the Cysteine Substitution Carriers

A maximum velocity (V_{max}) value for L-glutamate uptake was determined for each cysteine substitution mutant in COS-7 cells. Cells were transiently-transfected using the DEAE-dextran method and 48 hrs later a radiolabeled L-glutamate transport assay performed (Arriza et al., 1994). To establish a saturating concentration of substrate, cells were incubated for 10 min at RT with four concentrations of L-glutamate 10μM 100μM, 500μM, or 1000μM (100nM [^{3}H]-L-glutamate (24 Ci/mmol)), washed twice with ice cold PBS, solubilized in 0.1% SDS, and counted in a Beckman scintillation counter. Data were plotted and fitted by nonlinear regression analysis to the Michaelis-Menten equation to confirm saturation (Kaleidagraph, Synergy Software, Reading, PA.). Vmax values are expressed as a percent of Cys(-) Vmax.

Labeling of Cysteine Mutants with MTS-derivatives

COS-7 cells were distributed into 6-well plates and the next day transiently-transfected with the transporter mutants using the DEAE-dextran method. Forty-eight hours later, the transfected cells were washed twice with PBS and then incubated in the presence and absence of 1mM MTSET and 10mM MTSES (Toronto Research Chemicals Inc., North York, Ontario, Canada) for 5 min at RT. Compounds were solubilized in water as 50X stocks immediately prior to use. Cells were then washed three times with PBS and

incubated with 2mM MTSEA-biotin (Toronto Research Chemicals Inc.) for 20 minutes at RT. MTSEA-biotin was solubilized in DMSO at a final concentration of 0.5%. Cells were washed three times with PBS and then lysed on ice with 1ml of a 1% Triton X-100 buffer. After 1hr on ice, lysate was transferred to a 1.5 ml microfuge tube and spun at 14,000 rpm to pellet the insoluble material. Supernatants were transferred to a 1.5 ml microfuge tube, 150 µl of a 50% slurry of Ultralink™ Immobilized NeutrAvidin beads (Pierce, Rockford, IL) were added and the components incubated overnight at 4°C with mixing. The next day, the beads were washed three times with the lysis buffer, twice with the same buffer containing only 0.1% Triton X-100 and once with 50mM Tris pH 7.5. A 2X SDS loading buffer was added and then the samples were heated at 100°C for 3 minutes. The proteins were separated on an 8.5% polyacrylamide gel, transferred to Immobilon-P (Millipore Corp., Bedford, MA) and then probed with a polyclonal antibody raised to the C-terminus of EAAT1 (1:3,000 dilution). Proteins were visualized using a horseradish peroxidase (HRP)-conjugated secondary antibody (1:10,000; Amersham, Arlington Heights, IL) and chemiluminescence (Dupont NEN, Boston, MA).

Labeling of Cysteine Mutants with Maleimide Derivatives

Six-well plates containing COS-7 cells were transiently transfected by the DEAE-dextran method. Forty-eight hours later, the cells were washed twice with PBSCM and then incubated in the presence and absence of 0.2mM or 1mM stilbene disulfonate maleimide (Molecular Probes, Inc., Eugene, OR) for 30 minutes at RT. Cells were washed three times with PBSCM and then incubated with 0.2mM or 1mM biocytin maleimide (Molecular Probes, Inc., Eugene, OR) for 30 minutes at RT. Cells were washed three times with 2% β-mercaptoethanol in PBSCM and then three additional times with PBSCM. Cells were placed on ice and lysis buffer (150mM NaCl, 0.1% SDS, 1% NP-40, 0.5% Sodium deoxycholate, 0.02% NaN_3, 100µg/ml PMSF, 1µg/ml Aprotinin, 50mM Tris:Cl, pH 8.0) added. After 30 minutes on a rotating shaker, lysates were transferred to microcentrofuge

tube and spun 15 minutes at 15,000 x g at 4°C to remove the insoluble material. Supernant was transferred to a new tube and the volume brought to 1 ml with immunoprecipitation (IP) buffer (150mM NaCl, 0.1% NP-40, 1mM EDTA, 0.25% gelatin, 0.02% NaN3, 50mM Tris:HCl, pH 7.5). Immunoprecipitation was carried out at 4°C with the C-terminal antibody to EAAT1 (1:5,000 dilution) for 1hr with mixing and then protein A sepharose (Sigma) was added for an additional hr. Sepharose beads were washed two times at with IP buffer and one time with No Salt Wash buffer (0.1% NP-40, 10mM Tris:HCl, pH 7.5). After aspirating off all wash buffer, 2X SDS sample buffer was added, then samples were heated to 100°C for 3 minutes and separated on a 8% polyacrylamide gel. Gels were transferred to Immobilon-P (Millipore Corp., Bedford, MA) membrane for western blotting. After blocking with 2% BSA (Sigma), blots were incubated with strepavidin-HRP (1:10,000) and then developed by chemiluminescence (Dupont NEN, Boston, MA). Blots were reprobed with the C-terminal antibody to EAAT1 (1:5,000) and then visualized with an HRP-conjugated secondary antibody (1:10,000; Amersham, Arlington Heights, IL) and chemiluminescence (Dupont NEN, Boston, MA).

Application of MTS-derivatives and measurement of the transport activity. Cells were washed once with PBS before the MTS–derivatives were added at their final concentrations of 10mM (MTSES) and 1mM (MTSET) for 5 min at RT. The MTS-derivatives were solubilized immediately prior to use. Following the incubation, cells were washed 3X with PBS and assayed for uptake of 10μM radiolabeled L-glutamate (9.9μM non-labeled L-glutamate and 100nM [^{3}H]-L-glutamate (24 Ci/mmol) for 10 min at RT. The effect of the MTS-derivatives on uptake is expressed as the percent inhibition of uptake, which was calculated as PI = 100- (100*uptake after /uptake before).

Discussion and Conclusions

The EAA transporters have both a substrate translocation function that follows Michaelis-Menten kinetics and an associated ion conductance that has properties similar to ion channels. The idea that the carrier mediates both functions is supported by the fact that substrate transport and the anion conductance share the same ionic dependencies and pharmacological profiles (Picaud et al., 1995; Fairman et al., 1995; Wadiche et al., 1995a). Although much has been learned about these two processes, numerous questions remain with regard to the structural and functional relationships between the carrier and EAA substrates, co-transported ions and the anion flux. A clearer understanding of the molecular mechanisms of these transport activities will ultimately come from studies that resolve the transporter's structure and that identify the molecular determinants that underlie these functions, as well as from studies that evaluate both the macroscopic and microscopic properties of the currents generated by the EAA transporters.

A re-entrant loop domain participates in substrate and co-transported ion interactions and may form part of the permeation pathway.

One model that has been proposed to describe the mechanism that governs substrate transport and ion conductances through neurotransmitter transporters involves an alternating access strategy. In this scheme, one gating event at each face of the membrane controls in an alternating manner, the intracellular and extracellular accessibilities of the substrate and co-transported ions (Lester et al., 1994; Cammack et al., 1994; Sonders and Amara, 1996; Kavanaugh, 1998). Assuming that the anion channel is intrinsic to the carrier, the anion flux is modeled to occur when the gates are both open, which in the case of the EAA carriers occurs with a low probability (P_o~0.02) (Wadiche and Kavanaugh, 1998). An alternating access model for the mechanism of solute transport by ion pumps, in which subtle changes in conformation could explain the movement of substrates was

proposed by Jardetzky over 30 years ago (Jardetzky, 1966). Several issues arise with regard to this model for the EAA carriers. Do chloride ions travel through the same permeation pathway as substrates, and what are the residues that participate in forming this structure(s)? While a tight coupling between substrate and the co-transported ions, sodium, proton and potassium is required for the efficient transport of substrate against its concentration gradient (Zerangue and Kavanaugh, 1997), the flux of chloride ions is not coupled to substrate translocation (Fairman et al., 1995; Wadiche et al., 1995). In fact, it appears that chloride flux occurs in the absence of substrate (Otis and Jahr, 1998; Wadiche and Kavanaugh, 1998). Also, L-glutamate, although relatively the same size as other permeant anions, cannot substitute as the current carrying anion in the uncoupled anion conductance (Wadiche and Kavanaugh, 1998). Although it is quite likely that chloride ions and substrates move either through the same pathway, or through two separate pathways within the carrier, there is also a third, more remote possibility that the transporter and anion channel are two separate proteins. Our topological model of the transporter includes at least one re-entrant loop formed by a highly conserved region of the carrier that was also shown to participate in substrate and co-transported ion interactions. Because re-entrant loop domains have been identified as the pore regions of a number of voltage-gated and ligand-gated ion channels (MacKinnon, 1995), its presence suggests that this region may serve as part of the pathway for translocation of substrates and co-transported ions and/ or for the flux of uncoupled anions.

Re-entrant loops such as the P-loop of the voltage-gated potassium channel have been shown to extend into the permeation pathway and serve as the ion selectivity filter for potassium ions (Heginbotham et al., 1994; Doyle et al., 1998). The structure of the potassium channel is a tetramer, with each subunit folding into 6 α-helical TMs and a re-entrant P-loop. Residues of the signature sequence of this family of channels (GYG) that are located in the P-loop do not coordinate potassium ions via their side chains, but instead by the carbonyl backbone oxygen atoms (Doyle et al., 1998). The loop structure, unlike an

α-helix or β-sheet allows main chain atoms to be available for interaction with substrates and ions. Interestingly, potassium ions may interact with residues of the re-entrant loop in the EAA carriers. Loss of potassium counter-transport is observed upon individual mutation of two residues Y403 and E404 in GLT-1 (Y405 and E406 in TM8 of EAAT1) in this loop. These mutations also change the carriers from unidirectional transporters into exchangers (Kavanaugh et al., 1997, Zhang et al., 1998). Furthermore, mutation of the Y403 to phenylalanine or tryptophan increases the sodium affinity and changes the ion selectivity for sodium co-transport suggesting that this residue also senses sodium binding (Zhang et al., 1998). Our finding that sodium protects cysteines substituted for these residues from modification by sulfhydryl-reactive reagents further suggests that these residues interact in some way with the co-transported ions. A direct interaction of intracellular potassium with the side-chains or the main chain atoms of the Y403 (Y405 in EAAT1) and the E404 (E406 in EAAT1) would clearly support both our topological and functional model of a re-entrant loop domain. However, formal demonstration of a direct interaction rather than an allosteric effect with these two residues remains to be shown.

A re-entrant loop in a different C-terminal domain of the carrier (domain 9 in EAAT1) was proposed by Grunewald and colleagues (Grunewald et al., 1998). This domain is also highly conserved and hydrophobic and contains an interesting pattern of alternating serine/threonine residues and hydrophobic residues. Thus, it is attractive to model the domain as β-stranded within the membrane with the serine and threonine residues facing an aqueous pore and the hydrophobic residues facing the lipid bilayer. Unfortunately, experiments are still needed to address whether this domain or the domains that follow it are actually membrane associated, as neither the results from the study of GLT-1 nor from our study of EAAT1 adequately resolve this issue.

Identification of residues that are accessible from the extracellular milieu contributes to our understanding of the topology of EAA carriers.

The strength of the substituted cysteine accessibility method applied to topology is that residues, which are accessible to the extracellular space can be identified by their reactivity with impermeant sulfhydryl reagents. Findings based on this strategy have led to our model of the topology in which TMs 6 and 7 span the membrane, residues in the loops following TMs 5, 7 and 8 are extracellular and TM8 forms a re-entrant loop. Unfortunately, this method does not readily distinguish between residues that are in an aqueous pore within the membrane and residues that are extracellular. Because of this, it became somewhat problematic to model the topology of the last four conserved domains, where less is known of the functional significance of these residues and where hydropathy analyses fail to provide a first approximation. Fortunately some assumptions can be made regarding the location of the residues based on the size and charge of the reagents that react. Anion permeation experiments have determined that the size of the anion pore is at least 5 Å, the size of ClO_4 the largest permeant anion. Although the smaller MTS-derivatives (MTSEA, MTSES and MTSET) are approximately 6Å X 10Å (Javitch et al., 1995), the maleimide derivatives (BM and SM) are significantly larger. Thus, in the case where a residue is readily accessible to all of the reagents, showing neither steric nor electrostatic hindrance, we assume that it resides in the extracellular space.

Clearly, a more precise map of the C-terminal domain topology will require other techniques. One such strategy would be to evaluate the accessibility of the cysteine substitutions to impermeant reagents delivered to the cytoplasmic side of the membrane in inside-out excised patches. Although the substrate-elicited currents measured in the patch-clamp configuration are generated by the anion conductance (Wadiche and Kavanaugh, 1998), an effect on current amplitude upon application of the thiol-reactive compound would still indicate an intracellular accessibility. In this way, the number and orientation of transmembrane segments could be defined by a combination of both the intracellular and extracellular accessibilities. Moreover, examination of the anion conductance by the

substituted cysteine accessibility method could lead to new insights on the structural determinants that control its gating and permeation properties.

Monitoring conformational changes will provide important information about the mechanism of transport and the structure that underlies it.

Conformational changes of the EAA carrier are likely to participate in the mechanism of substrate translocation (Grunewald and Kanner, 1995), but how would they fit into the alternating access model that describes both a transport function and the anion conductance? Insight into the energy barriers required for the two transporter activities comes from a study of their temperature dependence. Measurements of the temperature dependence of the macroscopic substrate-elicited steady-state transport current and the substrate-activated anion conductance in EAAT1 demonstrate that, while the anion current (measured at +80mV) is relatively insensitive to temperatures (Q_{10}~1) consistent with what has been observed for the gating mechanisms of ion channels, the current representing substrate translocation (measured at -30mV) has a dependence that is much greater (Q_{10}~3), consistent with a mechanism that requires a conformational change with a relatively large energy barrier (Wadiche and Kavanaugh, 1998). How this temperature dependence fits into a model in which two relatively temperature-independent ion channel-like gates control substrate transport and the chloride conductance is not clear and will be an important issue to address in our understanding of the transport mechanism.

Transport by the Ca^{2}+ ATPase from sarcoplasmic reticulum, which operates by a primary active transport mechanism has been shown to be temperature-sensitive and that the temperature-sensitivity correlates with stabilization of conformational states of the pump (Pick and Karlish, 1982). These studies used a covalently attached fluorescent probe to measure conformational changes at various temperatures in the presence and absence of Ca^{2}+ and the inhibitor vanadate. Conformational changes using fluorescent probes have also been used to study the sodium-dependent glucose transporter (Loo et al., 1998) and

the *shaker* potassium channel (Cha and Bezanilla, 1997). Similar studies on EAA transporters could be carried out to examine the relationship between conformational changes and properties of the transporter including temperature and voltage-dependence.

Conformational changes could also be studied by monitoring changes in the accessibility of cysteine substitutions to modification as a function of voltage or another parameter (Horn, 1998). This approach may be useful to resolve a discrepancy that exists between the model proposed by Grunewald and colleagues (Grunewald et al., 1998) and our model for the region spanning from the end of TM6 to the middle of our TM8 (TM7 in GLT-1). We found that S366C and A367C are accessible to the extracellular space in EAAT1, whereas in GLT-1, the analogous residues were designated as part of an intracellular loop. Our model, which positions these residues at the extracellular membrane interface is consistent with both studies if the position of the residues relative to the membrane is either slightly different or if it changes as a function of some factor such as membrane voltage, composition or in association with other proteins. In this way, under the experimental conditions of the two studies, the residues of GLT-1 would be oriented so that their side-chains are not exposed, whereas the residues in EAAT1 are readily accessible. One avenue to address this would be to examine changes in accessibility of these residues in both EAAT1 and GLT-1, as a function of voltage or cell type.

The structural relationship of the anion conductance to the carrier and EAA substrates can be elucidated by applying the substituted cysteine accessibility method in *Xenopus* oocytes.

As has been already discussed here, the substituted cysteine accessibility method can be adapted to address a wide range of issues regarding structure and function. In this thesis, residues that participate in substrate and co-transported ion interactions with the carrier were identified in a region that was characterized as forming a re-entrant loop. Furthermore, the extracellular accessibility of several residues was demonstrated resulting

in a model for the topolog. These findings were achieved in COS-7 cells by evaluating the accessibility of cysteine substitutions using either radiolabeled substrate or by detecting biotin labeling with thiol-reactive compounds and transporter specific antibodies.

Initially, we had proposed that similar experimental paradigms be carried out in *Xenopus* oocytes with the aim of identifying residues important for the substrate binding and translocation, as well as the anion conductance (NIMH NRSA to R.P.S.) The *Xenopus* oocyte expression system allows both the current associated with uptake and the current generated by the anion conductance to be measured using the two-electrode voltage-clamp technique. In addition, radiolabeled uptake under voltage-clamp can be measured. Furthermore, because sodium binding and unbinding is thought to underlie an observed transient current (Wadiche and Kavanaugh, 1995), structural determinants of sodium ion binding could be identified using this system. Undoubtedly, mutations or modifications that change the properties of the chloride conductance, but not the transport activity would greatly increase our understanding of how the transporter functions. For example, altering the ion selectivity of the conductance would provide strong evidence that the channel is intrinsic to the carrier and would likely identify the location of the pore. Elimination of the anion conductance without altering transport could be used to study the physiological role of the anion conductance. Macroscopic recordings of the magnitude of the anion conductance could reflect either the kinetics of the substrate gating the anion channel or the anion's permeability. To differentiate between these possibilities, methods to evaluate the currents on a rapid time scale could be employed (Otis and Jahr, 1997). The effect of the anion conductance on glutamatergic transmission could be studied by creating "knock-in" mice (or drosophila) and then examining various glutamatergic synapses expressing the mutant carrier for changes in cell excitability, glutamate release, receptor activation and clearance rates.

Structural symmetry or lack of symmetry

The EAAT1 transporter appears to have a complex topology which includes at least six α-helical TMs, several β-stranded TMs and perhaps even non-periodic TMs. Most transporters, ligand-gated and voltage-gated ion channels and metabotropic receptors have been modeled as having more regular, consistent or symmetrical structures. Metabotropic receptors have seven α-helical TMs, the sodium and chloride-dependent superfamily of neurotransmitter transporters has 12 α-helical TMs. The voltage-gated possium, sodium, and calcium channels have four subunits arranged around a central pore with each subunit composed of six α-helical TMs and a P-loop. Maltoporin is a trimer of 18-stranded β-barrels. The family of neurotransmitter-gated ion channels has four TM α-helices, except for the glutamate receptors which have three α-helical TMs and one re-entrant loop. It will be interesting to see how closely the X-ray crystal structures of some of these proteins resemble the models that have been proposed based on hydropathy and lower resolution techniques. For example, the 3 dimensional crystal structure of the voltage-gated potassium channel validated much of the structural work that had been done previously (Doyle et al., 1998). Because of the regularity of so many other membrane protein structures, it will also be interesting to see if as the topology becomes more precisely mapped, a more regular structure develops for EAAT1.

dEAAT, a glutamate transporter from *Drosophila melanogaster*

In the appendix is a paper describing the cloning of an EAAT from Drosophila. Pharmacological and kinetic studies in COS-7 and *Xenopus* ooyctes shows that it has many of the same properties as the cloned mammalian EAA carriers including a micromolar affinity for EAAs, stereoselectivity for L-glutamate over D-glutamate, and an uncoupled chloride conductance. *In situ* studies show that it is expressed neuronally and that the pattern of staining could be consistent with expression in motor neurons, as the neuromuscular junction of invertebrates is glutamatergic. This may be the first demonstration of a pre-synaptically localized EAA transporter. We are currently generating

antibodies to the N-terminus in order to determine the localization of the dEAAT protein. If dEAAT is localized at the NMJ, we are interested in the kinetics of the carrier and how it affects transmission at a synapse that in mammals uses an enzyme (acetylcholinesterase) to degrade the neurotransmitter (ACh) with a considerably higher turnover rate then the EAA transporters show.

We would also like to investigate modulators of dEAAT activity in this system. It was reported that the last few amino acids in EAAT5 are capable (in a yeast two-hybrid screen) of mediating an interaction with the PDZ domain of proteins (PSD 93) that are known to cluster glutamate receptors at the membrane (Arriza et al., 1997). More recently, there have been reports of additional proteins that are thought to interact with the EAA carriers. Given the powerful genetic tool of Drosophila , it is of interest to isolate proteins that interact with dEAAT (yeast two-hybrid screen) and to investigate the purpose or consequence of the interaction in this system.

Finally, we isolated a second gene from Drosophila (dEAAT2) that shows significant homology to dEAAT and to the mammalian EAA transporters. In intial studies of this carrier expressed in COS-7 cells and *Xenopus* oocytes, we could not measure any transport or anion conductance activity upon application of EAAs or neutral amino acids. Placement of the green fluorescent protein (GFP) at the N-terminus allowed us to examine the subcellular distribution of dEAAT2 in COS-7 cells. It was observed that GFPdEAAT2 was not expressed significantly at the cell surface, but appears to reside mostly in the ER, Golgi and an unknown vesicular compartment. Studies to determine the factors that are required for its cell surface expression include expression in Drosophila cultured cells, co-expression of dEAAT2 with Drosophila mRNA in oocytes, application of compounds that generate second messenger cascades, and application of growth factors. Localization of dEAAT2 in drosophila may also provide clues on its role in Drosophila physiology and on possible mechanisms involved in its surface expresssion.

Conclusion

The aim of this thesis was to map the topology of the EAA carriers and to identify residues important to its transport function. To carry out these studies, numerous single cysteine mutants were created in a functional cysteine-less EAAT1 carrier. Functional mutants were evaluated for 1) altered transport activity after modification with MTS-derivatives in the presence and absence of substrates/inhibitors and co-transported ions and 2) extracellular accessibility as defined by modification with impermeant derivatives of methanethiosulfonates and maleimides. From these analyses, we identified several residues in a highly conserved region of the carrier (TM8) that appear to interact with substrates/inhibitors (A395C) and co-transported ions (Y405C, E406C). We also determined that many of the cysteine substitutions in this domain reside in an aqueous environment and form a re-entrant membrane loop structure that may participate in the permeation pathway. In addition to these function based findings, we also provide biochemical evidence to support the formation of the re-entrant loop. Furthermore, we propose that TM 6 (α-helix) and TM 7 (β-strand) span the membrane, residues in the loops following TMs 5, 7 and 8 are extracellular, and the C-terminal tail is intracellular. Although we have obtained some information regarding the extracellular accessibility of residues in the remaining four conserved domains, further studies are needed to more precisely map these regions of the carrier. By creating a multitude of functional single cysteine substitution mutants for these studies, we have generated the tools to carry out the analysis of many aspects of EAA transporter structure and function, including conformational changes, topological mapping, "helix-packing", and identifying the structural determinants that underlie substrate transport and the anion conductance.

Akabas, M.H., Stauffer, D.A., Xu, M., and Karlin, A. (1992). Acetylcholine receptor channel structure probed in cysteine-substitution mutants. Science 258, 307-10.

Akabas, M.H., Kaufmann, C., Archdeacon, P., and Karlin, A. (1994). Identification of acetylcholine receptor channel-lining residues in the entire M2 segment of the α subunit. Neuron 13, 919-27.

Amara, S.G., and Kuhar, M.J. (1993). Neurotransmitter transporters: recent progress. Annu Rev Neurosci. 16, 73-93.

Armstrong, N., Sun, Y., Chen, G.Q., and Gouaux, E. (1998). Structure of a glutamate-receptor ligand-binding core in complex with kainate. Nature 395, 913-7.

Arriza, J.L., Kavanaugh, M.P., Fairman, W.A., Wu, Y.-A., Murdoch, G.H., North, R.A., and Amara, S.G. (1993). Cloning and expression of a human neutral amino acid transporter with structural similarity to the glutamate transporter gene family. J. Biol. Chem. 268, 15329-32.

Arriza, J.L., Fairman, W.A., Wadiche, J., Murdoch, G.H., Kavanaugh, M.P., and Amara, S.G. (1994). Functional comparisons of three glutamate transporter subtypes cloned from motor cortex. J. Neurosci. 14, 5559-69.

Arriza, J.L., Eliasof, S., Kavanaugh, M.P., and Amaras, S.G. (1997). Excitatory amino acid transporter 5, a retinal glutamate transporter coupled to a chloride conductance. Proc. Natl. Acad. Sci. USA 94, 4155-60.

Attwell, D., Barbour, B., and Szatkowski, M. (1993). Nonvesicular release of neurotransmitter. Neuron 11, 401-7.

Attwell, D., Miller, B., and Sarantis, M. (1993). Arachidonic acid as a messenger in the central nervous system. Sem. Neurosci. 5, 159-69.

Balcar, V.J., and Johnston, G.A. (1972). The structural specificity of the high affinity uptake of L-glutamate and L-aspartate by rat brain slices. J. Neurochem. 19, 2657-66.

Barbour, B., Szatkowski, M., Ingledew, N., and Attwell, D. (1989). Arachidonic acid induces a prolonged inhibition of glutamate uptake into glial cells. Nature 342, 918-20.

Barbour, B., Brew, H., and Attwell, D. (1991). Electrogenic uptake of glutamate and aspartate into glial cells isolated from the salamander (Ambystoma) retina. J. Physiol. (Lond) 436, 169-93.

Barbour, B., Keller, B.U., Liano, I., and Marty, A. (1994). Prolonged presence of glutamate during excitatory synaptic transmission to cerebellar Purkinje cells. Neuron 12, 1331-43.

Barbour, B., and Hausser, M. (1997). Intersynaptic diffusion of neurotransmitter. Trends Neurosci. 20, 377-84.

Bennett, J.A., and Dingledine, R. (1995). Topology profile for a glutamate receptor: three transmembrane domains and a channel-lining reentrant membrane loop. Neuron 14, 373-84.

Bergles, D.E., and Jahr, C.E. (1997). Synaptic activation of glutamate transporters in hippocampal astrocytes. Neuron 19, 1297-308.

Bjørås, M., Gjesdal, O., Erickson, J.D., Torp, R., Levy, L.M., Ottersen, O.P., Degree, M., Storm-Mathisen, J., Seeberg, E., and Danbolt, N.C. (1996). Cloning and expression of a neuronal rat brain glutamate transporter. Mol. Brain Res. 36, 163-68.

Blitzblau, R., Gupta, S., Djali, S., Robinson, M.B., and Rosenberg, P.A. (1996). The glutamate transport inhibitor L-trans-pyrrolidine-2,4-dicarboxylate indirectly evokes NMDA receptor mediated neurotoxicity in rat cortical cultures. Eur. J. Neurosci. 8, 1840-52.

Bolton, E., Higginsson, B., Harrington, A., and O'Gara, G. (1986). Dicarboxylic acid transport in Rhizobium Meliloti: isolation of mutants and cloning of dicarboxylic acid transport genes. Arch Microbiol. 144, 142-46.

Breukel, A.I.M., Besselsen, E., Lopes da Silva, F.H., and Ghijsen, W.E.J.M. (1997). Arachidonic acid inhibits uptake of amino acids and potentiates PKC effects on glutamate, but not GABA, exocytosis in isolated hippocampal nerve terminals. Brain Res. 773, 90-97.

Bristol, L.A., and Rothstein, J.D. (1996). Glutamate transporter gene expression in amyotrophic lateral sclerosis motor cortex. Ann. Neurol. 39, 676-9.

Cammack, J.N., Rakhilin, S.V., and Schwartz, E.A. (1994). A GABA transporter operates asymetrically and with variable stoichiometry. Neuron 13, 949-60.

Cammack, J.N., and Schwartz, E.A. (1996). Channel behavior in a γ-aminobutyrate transporter. Proc. Natl. Acad. Sci. USA 93, 723-7.

Casado, M., Zafra, F., Aragón, C., and Giménez, C. (1991). Activation of high-affinity uptake of glutamate by phorbol esters in primary glial cell cultures. J. Neurochem. 57, 1185-90.

Casado, M., Bendahan, A., Zafra, F., Danbolt, N.C., Aragón, C., Giménez, C., and Kanner, B.I. (1993). Phosphorylation and modulation of brain glutamate transporters by protein kinase C. J. Biol. Chem. 268, 27313-17.

Cha A. and Benzanilla F. (1997). Characterizing voltage-dependent conformational changes in the *shaker* K^+ channel with fluorescence. Neuron 19, 1127-40.

Chamberlin, A.R., Koch, H.P., and Bridges, R.J. (1998). Design and synthesis of conformationally constrained inhibitors of high- affinity, sodium-dependent glutamate transporters. Methods Enzymol. 296, 175-89.

Chamberlin, R., and Bridges, R. (1993) Conformationally constrained acidic amino acids as probes of glutamate receptors and transporters. In: Drug Design for Neuroscience A. P. Kozikowski (New York: Raven Press Ltd.), 231-59

Clements, J.D. (1996). Transmitter timecourse in the synaptic cleft: its role in central synaptic function. Trends Neurosci. 19, 163-71.

Conradt, M., Storck, T., and Stoffel, W. (1995a). Localization of N-glycosylation sites and functional role of the carbohydrate units of GLAST-1, a cloned rat brain L-glutamate/L- aspartate transporter. Eur. J. Biochem. 229, 682-7.

Conradt, M., and Stoffel, W. (1995b). Functional analysis of the high affinity, Na(+)-dependent glutamate transporter GLAST-1 by site-directed mutagenesis. J. Biol. Chem. 270, 25207-12.

Conradt, M., and Stoffel, W. (1997). Inhibition of the high-affinity brain glutamate transporter GLAST-1 via direct phosphorylation. J. Neurochem. 68, 1244-51.

Davis, K.E., Straff, D.J., Weinstein, E.A., Bannerman, P.G., Correale, D.M., Rothstein, J.D., and Robinson, M.B. (1998). Multiple signaling pathways regulate cell surface expression and activity of the excitatory amino acid carrier 1 subtype of Glu transporter in C6 glioma. J. Neurosci. 18, 2475-85.

DeFelice, L.J., and Blakely, R.D. (1996). Pore models for transporters? Biophys. J. 70, 579-80.

Dehnes, Y., Chaudhry, F.A., Ullensvang, K., Lehre, K.P., Storm-Mathisen, J., and Danbolt, N.C. (1998). The glutamate transporter EAAT4 in rat cerebellar Purkinje cells: a glutamate-gated chloride channel concentrated near the synapse in parts of the dendritic membrane facing astroglia. J. Neurosci. 18, 3606-19.

Diamond, J.S., and Jahr, C.E. (1997). Transporters buffer synaptically released glutamate on a submillisecond time scale. J. Neurosci. 17, 4672-87.

Dougherty, D.A. (1996). Cation-pi interactions in chemistry and biology: a new view of benzene, Phe, Tyr, and Trp. Science 271, 163-8.

Dowd, L.A., and Robinson, M.B. (1996). Rapid stimulation of EAAC1-mediated Na^+-dependent L-glutamate transport activity in C6 glioma cells by phorbol ester. J. Neurochem. 67, 508-16.

Doyle, D.A., Cabral, J.M., Pfuetzner, R.A., Kuo, A., Gulbis, J.M., Cohen, S.L., Chait, B.T., and MacKinnon, R. (1998). The structure of the potassium channel: molecular basis of K+ conduction and selectivity. Science 280, 69-77.

Drejer, J., Benveniste, H., Diemer, N.H., and Schousboe, A. (1985). Cellular origin of ischemia-induced glutamate release from brain tissue in vivo and in vitro. J. Neurochem. 45, 145-51.

Dumuis, A., Sebben, M., Haynes, L., Pin, J.-P., and Bockaert, J. (1988). NMDA receptors activate the arachidonic acid cascade system in striatal neurons. Nature 336, 68-70.

Eliasof, S., and Werblin, F. (1993). Characterization of the glutamate transporter in retinal cones of the tiger salamander. J. Neurosci. 13, 402-11.

Eliasof, S., and Jahr, C.E. (1996). Retinal glial cell glutamate transporter is coupled to an anionic conductance. Proc. Natl. Acad. Sci. U S A 93, 4153-8.

Eliasof, S., Arriza, J.L., Leighton, B.H., Kavanaugh, M.P., and Amara, S.G. (1998). Excitatory amino acid transporters of the salamander retina: identification, localization, and function. J. Neurosci. 18, 698-712.

Engelke, T., Jording, D., Kapp, D., and Puhler, A. (1989). Identification and sequence analysis of the Rhizobium meliloti dctA gene encoding the C4-dicarboxylate carrier. J. Bacteriol. 171, 5551-60.

Erecinska, M., Wantorsky, D., and Wilson, D.F. (1983). Aspartate transport in synaptosomes from rat brain. J. Biol. Chem. 258, 9069-77.

Fagg, G.E., and Foster, A.C. (1983). Amino acid neurotransmitters and their pathways in the mammalian central nervous system. Neuroscience 9, 701-19.

Fairman, W.A., Vandenberg, R.J., Arriza, J.L., Kavanaugh, M.P., and Amara, S.G. (1995). An excitatory amino-acid transporter with properties of a ligand-gated chloride channel. Nature 375, 599-603.

Fairman, W.F., Sonders, M.S., Murdoch, G.H., and Amara, S.G. (1998). Arachidonic acid elicits a substrate-gated proton current associated with the glutamate transporter EAAT4. Nature Neurosci. 1, 105-13.

Ferkany, J., and Coyle, J.T. (1986). Heterogeneity of sodium-dependent excitatory amino acid uptake mechanisms in rat brain. J. Neurosci. Res. 16, 491-503.

Fletcher, E.J., and Johnston, G.A. (1991). Regional heterogeneity of L-glutamate and L-aspartate high-affinity uptake systems in the rat CNS. J. Neurochem. 57, 911-4.

Fong, J.C., Chen, C.-C., Liu, D., Chai, S.-P., Tu, M.-S., and Chu, K.-Y. (1996). Arachidonic acid stimulates the intrinsic activity of ubiquitous glucose transporter (GLUT1) in 3T3-L1 adipocytes by a protein kinase C-independent mechanism. Cell Signal 8, 179-83.

Gaal, L., Roska, B., Picaud, S.A., Wu, S.M., Marc, R., and Werblin, F.S. (1998). Postsynaptic response kinetics are controlled by a glutamate transporter at cone photoreceptors. J. Neurophysiol. 79, 190-6.

Ganel, R., and Crosson, C.E. (1998). Modulation of human glutamate transporter activity by phorbol ester. J. Neurochem. 70, 993-1000.

Gemba, T., Oshima, T., and Ninomiya, M. (1994). Glutamate efflux via the reversal of the sodium-dependent glutamate transporter caused by glycolytic inhibition in rat cultured astrocytes. Neuroscience 63, 789-95.

Gilbert, W., Marchionni, M., and McKnight, G. (1986). On the antiquity of introns. Cell 46, 151-4.

Goh, J.W., Ho-Asjoe, M., and Sastry, B.R. (1986). Tetanic stimulation-induced changes in [3H]glutamate binding and uptake in rat hippocampus. Gen. Pharmacol. 17, 537-42.

Grant, G.B., and Werblin, F.S. (1996). A glutamate-elicited chloride current with transporter-like properties in rod photoreceptors of the tiger salamander. Vis. Neurosci.13, 135-44.

Grunewald, M., and Kanner, B. (1995). Conformational changes monitored on the glutamate transporter GLT-1 indicate the existence of two neurotransmitter-bound states. J. Biol. Chem. 270, 17017-24.

Grunewald, M., Bendahan, A., and Kanner, B.I. (1998). Biotinylation of single cysteine mutants of the glutamate transporter GLT-1 from rat brain reveals its unusual topology. Neuron 21, 623-32.

Hansson, E., and Ronnback, L. (1989). Regulation of glutamate and GABA transport by adrenoceptors in primary astroglial cell cultures. Life Sci. 44, 27-34.

Harada, T., Harada, C., Watanabe, M., Inoue, Y., Sakagawa, T., Nakayama, N., Sasaki, S., Okuyama, S., Watase, K., Wada, K., and Tanaka, K. (1998). Functions of the two glutamate transporters GLAST and GLT-1 in the retina. Proc. Natl. Acad. Sci. U S A 95, 4663-6.

Haugeto, O., Ullensvang, K., Levy, L.M., Chaudhry, F.A., Honoré, T., Nielsen, M., Lehre, K.P., and Danbolt, N.C. (1996). Brain glutamate transporter proteins from homomultimers. J. Biol. Chem. 271, 27715-22.

Hofmann, K., Duker, M., Fink, T., Lichter, P., and Stoffel, W. (1994). Human neutral amino acid transporter ASCT1: structure of the gene (SLC1A4) and localization to chromosome 2p13-p15. Genomics 24, 20-6.

Hollmann, M., Maron, C., and Heinemann, S. (1994). N-glycosylation site tagging suggests a three transmembrane domain topology for the glutamate receptor GLuR1. Neuron 13, 1331-43.

Holmgren, M., Lui, Y., Xu, Y., and Yellen, G. (1996). On the use of thiol-modifying agents to determine channel topology. Neuropharmacology 35, 797-804.

Hsiao, C.D., Sun, Y.J., Rose, J., and Wang, B.C. (1996). The crystal structure of glutamine-binding protein from Escherichia coli. J. Mol. Biol. 262, 225-42.

Inoue, K., Sakaitani, M., Shimada, S., and Tohyama, M. (1995). Cloning and expression of a bovine glutamate transporter. Brain Res. Mol. Brain Res. 28, 343-8.

Isaacson, J.S., and Nicoll, R.A. (1993a). The uptake inhibitor L-trans-PDC enhances responses to glutamate but fails to alter the kinetics of excitatory synaptic currents in the hippocampus. J. Neurophysiol. 70, 2187-91.

Isaacson, J.S., Solis, J.M., and Nicoll, R.A. (1993b). Local and diffuse synaptic actions of GABA in the hippocampus. Neuron 10, 165-75.

Jardetzky, O. (1996) Simple allosteric model for membrane pumps. Nature (London) 211, 969-70.

Javitch J.A., Fu, D. Chen J., and Karlin, A. (1995). Mapping the binding-site crevice of the dopamine D2 receptor by the substituted-cysteine accessibility method. Neuron 14, 825-31.

Javitch, J.A. (1998) Probing structure of neurotransmitter transporters by substituted-cysteine accessibility method. In: Methods Enzymol. S. G. Amara (San Diego, California: Academic Press), 296, 331-46

Jording, D., and Puhler, A. (1993). The membrane topology of the Rhizobium meliloti C4-dicarboxylate permease (DctA) as derived from protein fusions with Escherichia coli K12 alkaline phosphatase (PhoA) and beta-galactosidase (LacZ). Mol. Gen. Genet. 241, 106-14.

Kanai, Y., and Hediger, M.A. (1992). Primary structure and functional characterization of a high-affinity glutamate transporter. Nature 360, 467-71.

Kanai, Y., Bhide, P.G., DiFiglia, M., and Hediger, M.A. (1995a). Neuronal high-affinity glutamate transport in the rat central nervous system. Neuroreport 6, 2357-62.

Kanai, Y., Nussberger, S., Romero, M.F., Boron, W.F., Hebert, S.C., and Hediger, M.A. (1995b). Electrogenic properties of the epithelial and neuronal high affinity glutamate transporter. J. Biol. Chem. 270, 16561-8.

Kanner, B.I., and Sharon, I. (1978). Active transport of L-glutamate by membrane vesicles isolated from rat brain. Biochemistry 17, 3949-53.

Kanner, B.I., and Bendahan, A. (1982). Binding order of substrates to the sodium and potassium ion coupled L-glutamic acid transporter from rat brain. Biochemistry 21, 6327-30.

Kapus, A., Romanek, R., and Grinstein, S. (1994). Arachidonic acid stimulates the plasma membrane H+ conductance of macrophages. J. Biol. Chem. 269, 4736-45.

Karlin, A., and Akabas, M.H. (1998) Substituted-cysteine accessibility method. In Methods Enzymol. Vol. 293, P. Michael Conn. ed. (San Diego, California: Academic Press), 1-24

Kataoka, Y., Morii, H., Watanabe, Y., and Ohmori, H. (1997). A postsynaptic excitatory amino acid transporter with chloride conductance functionally regulated by neuronal activity in cerebellar Purkinje cells. J. Neurosci. 17, 7017-24.

Kavanaugh, M.P., Bendahan, A., Zerangue, N., Zhang, Y., and Kanner, B.I. (1997). Mutation of an amino acid residue influencing potassium coupling in the glutamate transporter GLT-1 induces obligate exchange. J. Biol. Chem. 272, 1703-8.

Kavanaugh, M.P. (1998) Neurotransmitter transport: Models in flux. Commentary in Proc. Natl. Acad. Sci. U.S.A. 95, 12737-8.

Kawakami, H., Tanaka, K., Nakayama, T., Inoue, K., and Nakamura, S. (1994). Cloning and expression of a human glutamate transporter. Biochem. Biophys. Res. Commun. 199, 171-6.

Kirschner, M.A., Arriza, J.L., Copeland, N.G., Gilbert, D.J., Jenkins, N.A., Magenis, E., and Amara, S.G. (1994a). The mouse and human excitatory amino acid transporter gene (EAAT1) maps to mouse chromosome 15 and a region of syntenic homology on human chromosome 5. Genomics 22, 631-3.

Kirschner, M.A., Copeland, N.G., Gilbert, D.J., Jenkins, N.A., and Amara, S.G. (1994b). Mouse excitatory amino acid transporter EAAT2: isolation, characterization, and proximity to neuroexcitability loci on mouse chromosome 2. Genomics 24, 218-24.

Klöckner, U., Storck, T., Conradt, M., and Stoffel, W. (1993). Electrogenic L-glutamate uptake in *Xenopus laevis* oocytes expressing a cloned rat brain L-glutamate/L-aspartate transporter (GLAST-1). J. Biol. Chem. 268, 14594-6.

L'hirondel, M., Chéramy, A., Godeheu, G., and Glowinski, J. (1995). Effects of arachidonic acid on dopamine synthesis, spontaneous release, and uptake in striatal synaptosomes from the rat. J. Neurochem. 64, 1406-9.

Lebrun, B., Sakaitani, M., Shimamoto, K., Yasuda-Kamatani, Y., and Nakajima, T. (1997). New β–hydroxyaspartate derivatives are competitive blockers for the bovine glutamate/aspartate transporter. J. Biol. Chem. 272, 20336-20339.

Lehre, K.P., and Danbolt, N.C. (1998). The number of glutamate transporter subtype molecules at glutamatergic synapses: chemical and stereological quantification in young adult rat brain. J. Neurosci .18, 8751-7.

Lehre, K.P., Levy, L.M., Ottersen, O.P., Storm-Mathisen, J., and Danbolt, N.C. (1995). Differential expression of two glial glutamate transporters in the rat brain: Quantitative and immunocytochemical observations. J. Neurosci. 15, 1835-53.

Lester, H.A., Mager, S., Quick, M.W., and Corey, J.L. (1994). Permeation properties of neurotransmitter transporters. Annu. Rev. Pharmacol. Toxicol. 34, 219-49.

Lester, R.A., Clements, J.D., Westbrook, G.L., and Jahr, C.E. (1990). Channel kinetics determine the time course of NMDA receptor-mediated synaptic currents. Nature 346, 565-7.

Li, S., Mallory, M., Alford, M., Tanaka, S., and Masliah, E. (1997). Glutamate transporter alterations in Alzheimer disease are possibly associated with abnormal APP expression. J. Neuropathol. Exp. Neurol. 56, 901-11.

Lin, C.L., Bristol, L.A., Jin, L., Dykes-Hoberg, M., Crawford, T., Clawson, L., and Rothstein, J.D. (1998). Aberrant RNA processing in a neurodegenerative disease: the cause for absent EAAT2, a glutamate transporter, in amyotrophic lateral sclerosis. Neuron 20, 589-602.

Linden, D.J. (1995). Phospholipase A2 controls the induction of short-term versus long-term depression in the cerebellar Purkinje neuron in culture. Neuron 15, 1393-401.

Loo, D.D., Hirayama, B.A, Gallardo, E.M, Lam, J.T, Turk, E., and Wright, E.M. (1998). Conformational changes couple Na+ and glucose transport. Proc. Natl. Acad. Sci. 95, 7789-94.

Loo, T.W., and Clarke, D.M. (1995). Membrane topology of a cysteine-less mutant of human P-glycoprotein. J Biol Chem 270, 843-8.

Lundy, D.F., and McBean, G.J. (1995). Pre-incubation of synaptosomes with arachidonic acid potentiates inhibition of [^{3}H]D-aspartate transport. Eur. J. Pharmacol. 291, 273-9.

Lundy, D.F., and McBean, G.J. (1996). Inhibition of the high-affinity uptake of D-[^{3}H]aspartate in rat brain by L-alpha-aminoadipate and arachidonic acid. J. Neurol. Sci. 139, 1-9.

MacKinnon, R. (1995). Pore loops: an emerging theme in ion channel structure. Neuron 14, 889-92.

Maeno-Hikichi, Y., Tanaka, K., Shibata, T., Watanabe, M., Inoue, Y., Mukainaka, Y., and Wada, K. (1997). Structure and functional expression of the cloned mouse neuronal high- affinity glutamate transporter. Brain Res Mol Brain Res 48, 176-80.

Mager, S., Min, C., Henry, D., Chavkin, C., Hoffman, B., Davidson, N., and Lester, H. (1994). Conducting states of a mammalian serotonin transporter. Neuron 12, 845-59.

Mager, S., Cao, Y., and Lester, H.A. (1998). Measurement of transient currents from neurotransmitter transporters expressed in Xenopus oocytes. In Methods Enzymol. Vol 296, Susan G. Amara, ed. (San Diego, California: Academic Press), 551-66.

Maki, R., Robinson, M.B., and Dichter, M.A. (1994). The glutamate uptake inhibitor L-*Trans*-pyrrolidine-2,4-dicarboxylate depresses excitatory synaptic transmission via a presynaptic mechanism in cultured hippocampal neurons. J. Neurosci. 14, 6754-62.

Martin, L.J., Brambrink, A.M., Lehmann, C., Portera-Cailliau, C., Koehler, R., Rothstein, J., and Traystman, R.J. (1997). Hypoxia-ischemia causes abnormalities in glutamate transporters and death of astroglia and neurons in newborn striatum. Ann. Neurol. 42, 335-48.

Masliah, E. (1998). Mechanisms of synaptic pathology in Alzheimer's disease. J. Neural Transm. Suppl. 53, 147-58.

Meldrum, B.S. (1994). The role of glutamate in epilepsy and other CNS disorders. Neurology 44 (suppl 8), S14-S23.

Mennerick, S., and Zorumski, C.F. (1994). Glial contributions to excitatory neurotransmission in cultured hippocampal cells. Nature 368, 59-62.

Mennerick, S., Dhond, R.P., Benz, A., Xu, W., Rothstein, J.D., Danbolt, N.C., Isenberg, K.E., and Zorumski, C.F. (1998). Neuronal expression of the glutamate transporter GLT-1 in hippocampal microcultures. J. Neurosci. 18, 4490-9.

Miller, H.P., Levey, A.I., Rothstein, J.D., Tzingounis, A.V., and Conn, P.J. (1997). Alterations in glutamate transporter protein levels in kindling-induced epilepsy. J. Neurochem. 68, 1564-70.

Mitrovic, A.D., Amara, S.G., Johnston, G.A., and Vandenberg, R.J. (1998). Identification of functional domains of the human glutamate transporters EAAT1 and EAAT2. J. Biol. Chem. 273, 14698-706.

Mukainaka, Y., Tanaka, K., Hagiwara, T., and Wada, K. (1995). Molecular cloning of two glutamate transporter subtypes from mouse brain. Biochim. Biophys. Acta. 1244, 233-7.

Murrin, L.C., Lewis, M.S., and Kuhar, M.J. (1978). Amino acid transport: alterations due to synaptosomal depolarization. Life Sci. 22, 2009-16.

Nakayama, T., Kawakami, H., Tanaka, K., and Nakamura, S. (1996). Expression of three glutamate transporter subtype mRNAs in human brain regions and peripheral tissues. Mol. Brain Res. 36, 189-192.

Nonaka, M., Kohmura, E., Yamashita, T., Shimada, S., Tanaka, K., Yoshimine, T., Tohyama, M., and Hayakawa, T. (1998). Increased transcription of glutamate-aspartate transporter (GLAST/GluT-1) mRNA following kainic acid-induced limbic seizure. Mol. Brain Res. 55, 54-60.

Obrenovitch, T.P., Zilkha, E., and Urenjak, J. (1998). Effects of pharmacological inhibition of glutamate-uptake on ischaemia- induced glutamate efflux and anoxic depolarization latency. Naunyn Schmiedebergs Arch Pharmacol. 357, 225-31.

Oshima, T., Rossi, D., and Attwell, D. (1998). Release of glutamate by reversed uptake during ischaemia of rat hippocampal cultures. Eur J Neurosci. 10, 205-10.

Otis, T.S., Wu, Y.C., and Trussell, L.O. (1996). Delayed clearance of transmitter and the role of glutamate transporters at synapses with multiple release sites. J. Neurosci. 16, 1634-44.

Otis, T.S., Kavanaugh, M.P., and Jahr, C.E. (1997). Postsynaptic glutamate transport at the climbing fiber-Purkinje cell synapse. Science 277, 1515-8.

Otori, Y., Shimada, S., Tanaka, K., Ishimoto, I., Tano, Y., and Tohyama, M. (1994). Marked increase in glutamate-aspartate transporter (GLAST/GluT-1) mRNA following transient retinal ischemia. Mol. Brain Res. 27, 310-4.

Peghini, P., Janzen, J., and Stoffel, W. (1997). Glutamate transporter EAAC-1-deficient mice develop dicarboxylic aminoaciduria and behavioral abnormalities but no neurodegeneration. EMBO J. 16, 3822-32.

Perez-Garcia, M.T., Chiamvimonvat, N., Marban, E., and Tomaselli, G.F. (1996). Structure of the sodium channel pore revealed by serial cysteine mutagenesis. Proc. Natl. Acad. Sci. USA 93, 300-4.

Picaud, S.A., Larsson, H.P., Grant, G.B., Lecar, H., and Werblin, F.S. (1995a). Glutamate-gated chloride channel with glutamate-transporter-like properties in cone photoreceptors of the tiger salamander. J. Neurophysiol. 74, 1760-71.

Picaud, S., Larsson, H.P., Wellis, D.P., Lecar, H., and Werblin, F. (1995b). Cone photoreceptors respond to their own glutamate release in the tiger salamander. Proc. Natl. Acad. Sci. USA 92, 9417-21.

Pick U. and Karlish, S.J. D. (1982) Regulation of the conformational transition in the Ca-ATPase from sarcoplasmic reticulum by pH, temperature, and calcium ions. J. Biol. Chem. 257, 6120-6.

Pines, G., Danbolt, N.C., Bjoras, M., Zhang, Y., Bendahan, A., Eide, L., Koepsell, H., Storm-Mathisen, J., Seeberg, E., and Kanner, B.I. (1992). Cloning and expression of a rat brain L-glutamate transporter. Nature 360, 464-7.

Pines, G., Zhang, Y., and Kanner, B.I. (1995). Glutamate 404 is involved in the substrate discrimination of GLT-1, a (Na+ + K+)-coupled glutamate transporter from rat brain. J. Biol. Chem. 270, 17093-7.

Pullan, L.M., Olney, J.W., Price, M.T., Compton, R.P., Hood, W.F., Michel, J., and Monahan, J.B. (1987). Excitatory amino acid receptor potency and subclass specificity of sulfur-containing amino acids. J. Neurochem. 49, 1301-7.

Roberts, D.D., Lewis, S.D., Ballou, D.P., Olson, S.T., and Shafer, J.A. (1986). Reactivity of small thiolate anions and cysteine-25 in papain toward methyl methanthiosulfonate. Biochemistry 25, 5595-601.

Robinson, M.B., Hunter-Ensor, M., and Sinor, J. (1991). Pharmacologically distinct sodium-dependent L-[3H]glutamate transport processes in rat brain. Brain Res 544, 196-202.

Robinson, M.B., Sinor, J.D., Dowd, L.A., and Kerwin, J.F., Jr. (1993). Subtypes of sodium-dependent high-affinity L-[3H]glutamate transport activity: pharmacologic specificity and regulation by sodium and potassium. J Neurochem 60, 167-79.

Robinson, M.B. (1998). Examination of glutamate transporter heterogeneity using synaptosomal preparations. In Methods Enzymol Vol. 296, Susan G. Amara, ed. (San Diego, California: Academic Press), 189-202.

Roettger, V.R., and Lipton, P. (1996). Mechanism of glutamate release from rat hippocampal slices during in vitro ischemia. Neuroscience 75, 677-85.

Rothstein, J.D., Martin, L.J., and Kuncl, R.W. (1992). Decreased glutamate transport by the brain and spinal cord in amyotrophic lateral sclerosis [see comments]. N. Engl J. Med. 326, 1464-8.

Rothstein, J.D., Martin, L., Levey, A.I., Dykes-Hoberg, M., Jin, L., Wu, D., Nash, N., and Kuncl, R.W. (1994). Localization of neuronal and glial glutamate transporters. Neuron 13, 713-25.

Rothstein, J.D., Van Kammen, M., Levey, A.I., Martin, L.J., and Kuncl, R.W. (1995a). Selective loss of glial glutamate transporter GLT-1 in amyotrophic lateral sclerosis. Ann. Neurol. 38, 73-84.

Rothstein, J.D. (1995b) Excitotoxic mechanisms in the pathogenesis of amyotrophic lateral sclerosis. In: Pathogenesis and Therapy of Amyotrophic Lateral Sclerosis Vol. 68, G. Serratrice & T. Munsat (Philadelphia: Lippincott-Raven Publishers), 7-20.

Rothstein, J.D., Dykes-Hoberg, M., Pardo, C.A., Bristol, L.A., Jin, L., Kuncl, R.W., Kanai, Y., Hediger, M.A., Wang, Y., Schielke, J.P., and Welty, D.F. (1996). Knockout of glutamate transporters reveals a major role for astroglial transport in excitotoxicity and clearance of glutamate. Neuron 16, 675-86.

Sarantis, M., Everett, K., and Attwell, D. (1988). A presynaptic action of glutamate at the cone output synapse. Nature 332, 451-3.

Sather, W.A., Yang, J., and Tsien, R.W. (1994). Structural basis of ion channel permeation and selectivity. Curr. Opin. Neurobiol. 4, 313-23.

Schwartz, E., and Tachibana, M. (1990). Electrophysiology of glutamate and sodium co-transport in a glial cell of the salamander retina. J. Physiol. 426, 43-80.

Seal, R.P., Daniels, G.M., Wolfgang, W.J., Forte, M.A., and Amara, S.G. (1998a). Identification and characterization of a cDNA encoding a neuronal glutamate transporter from Drosophila melanogaster. Receptors Channels 6, 51-64.

Seal, R.P., and Amara, S.G. (1998b). A re-entrant loop domain in the glutamate carrier EAAT1 participates in substrate binding and translocation. Neuron 21, 1-20.

Shafqat, S., Tamarappoo, B.K., Kilberg, M.S., Puranam, R.S., McNamara, J.O., Guadano-Ferraz, A., and Fremeau, R.T., Jr. (1993). Cloning and expression of a novel Na(+)-dependent neutral amino acid transporter structurally related to mammalian Na+/glutamate cotransporters. J. Biol. Chem. 268, 15351-5.

Shashidharan, P., Huntley, G.W., Murray, J.M., Buku, A., Moran, T., Walsh, M.J., Morrison, J.H., and Plaitakis, A. (1997). Immunohistochemical localization of the neuron-specific glutamate transporter EAAC1 (EAAT3) in rat brain and spinal cord revealed by a novel monoclonal antibody. Brain Res. 773, 139-48.

Shayakul, C., Kanai, Y., Lee, W.S., Brown, D., Rothstein, J.D., and Hediger, M.A. (1997). Localization of the high-affinity glutamate transporter EAAC1 in rat kidney. Am. J. Physiol. 273, 1023-9.

Shi, L.B., Skach, W.R., Ma, T., and Verkman, A.S. (1995). Distinct biogenesis mechanisms for the water channels MIWC and CHIP28 at the endoplasmic reticulum. Biochemistry 34, 8250-6.

Shimamoto, K., LeBrun, B., Yasuda-Kamatani, Y., Sakaitani, M., Shigeri, Y., Yumoto, N., and Nakajima, T. (1998). DL-*threo*-β-benzyloxyaspartate, a potent blocker of excitatory amino acid transporter. Mol. Pharmacol. 53, 195-201.

Slotboom, D.J., Lolkema, J.S., and Konings, W.N. (1996). Membrane topology of the C-terminal half of the neuronal, glial, and bacterial glutamate transporter family. J. Biol. Chem. 271, 31317-21.

Sonders, M.S., and Amara, S.G. (1996). Channels in transporters. Curr. Opin. Neurobiol. 6, 294-302.

Sonders, M.S., Zhu, S.-J., Zahniser, N.R., Kavanaugh, M.P., and Amara, S.G. (1997). Multiple ionic conductances of human dopamine transporter: The actions of dopamine and psychostimulants. J. Neurosci. 17, 960-74.

Stallcup, W.B., Bulloch, K., and Baetge, E.E. (1979). Coupled transport of glutamate and sodium in a cerebellar nerve cell line. J. Neurochem. 32, 57-65.

Stauffer, D.A., and Karlin, A. (1994). Electrostatic potential of the actylcholine binding sites in the nicotinic receptors probed by reactions of binding-site cyteines with charged methanethiosulfonates. Biochemistry 33, 6840-6849.

Stern-Bach, Y., Bettler, B., Hartley, M., Sheppard, P.O., O'Hara, P.J., and Heinemann, S.F. (1994). Agonist selectivity of glutamate receptors is specified by two domains structurally related to bacterial amino acid-binding proteins. Neuron 13, 1345-57.

Stoffel, W., Sasse, J., Düker, M., Müller, R., Hofmann, K., Fink, T., and Lichter, P. (1996). Human high affinity, Na^+-dependent L-glutamate/L-aspartate transporter GLAST-1 (EAAT-1): gene structure and localization to chromosome 5p11-p12. FEBS Lett. 386, 189-193.

Storck, T., Schulte, S., Hoffman, K., and Stoffel, W. (1992). Structure, expression and functional analysis of a Na^+-dependent glutamate/aspartate transporter from rat brain. Proc. Natl. Acad. Sci. USA 89, 10955-9.

Su, A., Mager, S., Mayo, S.L., and Lester, H.A. (1996). A multi-substrate single-file model for ion-coupled transporters. Biophys. J. 70, 762-77.

Sun, Y.J., Rose, J., Wang, B.C., and Hsiao, C.D. (1998). The structure of glutamine-binding protein complexed with glutamine at 1.94 A resolution: comparisons with other amino acid binding proteins. J. Mol. Biol. 278, 219-29.

Sun, Z.P., Akabas, M.H., Goulding, E.H., Karlin, A., and Siegelbaum, S.A. (1996). Exposure of residues in the cyclic nucleotide-gated channel pore: P region structure and function in gating. Neuron 16, 141-9.

Sutherland, M.L., Delaney, T.A., and Noebels, J.L. (1995). Molecular characterization of a high-affinity mouse glutamate transporter. Gene 162, 271-4.

Szatkowski, M., and Attwell, D. (1994). Triggering and execution of neuronal death in brain ischaemia: two phases of glutamate release by different mechanisms. Trends Neurosci. 17, 359-65.

Szatkowski, M., Barbour, B., and Attwell, D. (1990). Non-vesicular release of glutamate from glial cells by reversed electrogenic glutamate uptake. Nature 348, 443-5.

Takahashi, M., Sarantis, M., and Attwell, D. (1996). Postsynaptic glutamate uptake in rat cerebellar Purkinje cells. J Physiol (Lond) 497, 523-30.

Takahashi, M., Billups, B., Rossi, D., Sarantis, M., Hamann, M., and Attwell, D. (1997). The role of glutamate transporters in glutamate homeostasis in the brain. J Exp Biol 200, 401-9.

Tanaka, K. (1993). Cloning and expression of a glutamate transporter from mouse brain. Neurosci Lett 159, 183-6.

Tanaka, K., Watase, K., Manabe, T., Yamada, K., Watanabe, M., Takahashi, K., Iwama, H., Nishikawa, T., Ichihara, N., Kikuchi, T., Okuyama, S., Kawashima, N., Hori, S., Takimoto, M., and Wada, K. (1997). Epilepsy and exacerbation of brain injury in mice lacking the glutamate transporter GLT-1. Science 276, 1699-702.

Tanaka, J., Ichikawa, R., Watanabe, M., Tanaka, K., and Inoue, Y. (1997). Extra-junctional localization of glutamate transporter EAAT4 at excitatory Purkinje cell synapses. Neuroreport 8, 2461-4.

Tang, C.M., Dichter, M., and Morad, M. (1989). Quisqualate activates a rapidly inactivating high conductance ionic channel in hippocampal neurons. Science 243, 1474-7.

Tolner, B., Poolman, B., and Konings, W.N. (1992). Characterization and functional expression in Escherichia coli of the sodium/proton/glutamate symport proteins of Bacillus stearothermophilus and Bacillus caldotenax. Mol. Microbiol. 6, 2845-56.

Tolner, B., Poolman, B., Wallace, B., and Konings, W.N. (1992). Revised nucleotide sequence of the gltP gene which encodes the proton-glutamate-aspartate transport protein of Escherichia Coli K-12. J. Bacteriol. 174, 2391-3.

Tong, G., and Jahr, C.E. (1994). Block of glutamate transporters potentiates postsynaptic excitation. Neuron 13, 1195-203.

Torp, R., Danbolt, N.C., Babaie, E., Bjoras, M., Seeberg, E., Stormmathisen, J., and Ottersen, O.P. (1994). Differential expression of two glial glutamate transporters in the rat brain: An in situ hybridization study. Eur. J. Neurosci. 6, 936-42.

Tzingounis, A.V., Lin, C.L., Rothstein, J.D., and Kavanaugh, M.P. (1998). Arachidonic acid activates a proton current in the rat glutamate transporter EAAT4. J. Biol. Chem. 273, 17315-7.

Umbach, J.A., Coady, M.J., and Wright, E.M. (1990). Intestinal Na+/glucose cotransporter expressed in Xenopus oocytes is electrogenic. Biophys. J. 57, 1217-24.

Utsunomiya-Tate, N., Endou, H., and Kanai, Y. (1996). Cloning and functional characterization of a system ASC-like Na+- dependent neutral amino acid transporter. J. Biol. Chem. 271, 14883-90.

Vandenberg, R.J., Arriza, J.L., Amara, S.G., and Kavanaugh, M.P. (1995). Constitutive ion fluxes and substrate binding domains of human glutamate transporters. J. Biol. Chem. 270, 17668-71.

Vandenberg, R.J., Mitrovic, A.D., Chebib, M., Balcar, V.J., and Johnston, G.A.R. (1997). Contrasting modes of action of methylglutamate derivatives on the excitatory amino acid transporters, EAAT1 and EAAT2. Mol. Phamracol. 51, 809-15.

Velaz-Faircloth, M., McGraw, T.S., Malandro, M.S., Fremeau, R.T., Jr., Kilberg, M.S., and Anderson, K.J. (1996). Characterization and distribution of the neuronal glutamate transporter EAAC1 in rat brain. Am. J. Physiol. 270, C67-C75.

Volterra, A., Bezzi, P., Rizzini, B.L., Trotti, D., Ullensvang, K., Danbolt, N.C., and Racagni, G. (1996). The competitive transport inhibitor L-trans-pyrrolidine-2,4-dicarboxylate triggers excitotoxicity in rat cortical neuron-astrocyte co-cultures via glutamate release rather than uptake inhibition. Eur. J. Neurosci. 8, 2019-28.

Wadiche, J.I., Amara, S.G., and Kavanaugh, M.P. (1995a). Ion fluxes associated with excitatory amino acid transport. Neuron 15, 721-8.

Wadiche, J.I., Arriza, J.L., Amara, S.G., and Kavanaugh, M.P. (1995b). Kinetics of a human glutamate transporter. Neuron 14, 1019-27

Wadiche, J.I., and Kavanaugh, M.P. (1998). Macroscopic and microscopic properties of a cloned glutamate transporter/chloride channel. J. Neurosci. 18, 7650-61.

Wahle, S., and Stoffel, W. (1996). Membrane topology of the high-affinity L-glutamate transporter (GLAST-1) of the central nervous system. J. Cell Biol. 135, 1867-77.

Watase, K., Hashimoto, K., Kano, M., Yamada, K., Watanabe, M., Inoue, Y., Okuyama, S., Sakagawa, T., Ogawa, S., Kawashima, N., Hori, S., Takimoto, M., Wada, K., and Tanaka, K. (1998). Motor discoordination and increased susceptibility to cerebellar injury in GLAST mutant mice. Eur. J. Neurosci 10, 976-88.

Willis, C.L., Humphrey, J.M., Koch, H.P., Hart, J.A., Blakely, T., Ralston, L., Baker, C.A., Shim, S., Kadri, M., Chamberlin, A.R., and Bridges, R.J. (1996). L-trans-2,3-pyrrolidine dicarboxylate: characterization of a novel excitotoxin. Neuropharmacology 35, 531-9.

Wo, Z.G., and Oswald, R.E. (1994). Transmembrane topology of two kainate receptor subunits revealed by N-glycosylation. Proc. Natl. Acad. Sci. USA 91, 7154-8.

Yamada, K., Watanabe, M., Shibata, T., Tanaka, K., Wada, K., and Inoue, Y. (1996). EAAT4 is a post-synaptic glutamate transporter at Purkinje cell synapses. Neuroreport 7, 2013-7.

Yan, Y.P., Yin, K.J., and Sun, F.Y. (1998). Effect of glutamate transporter on neuronal damage induced by photochemical thrombotic brain ischemia. Neuroreport 9, 441-6.

Yellen, G., Jurman, M.E., Abramson, T., and MacKinnon, R. (1991). Mutations affecting internal TEA blockade identify the probable pore- forming region of a K+ channel. Science 251, 939-42.

Yin, K.J., Yan, Y.P., and Sun, F.Y. (1998). Altered expression of glutamate transporter GLAST mRNA in rat brain after photochemically induced focal ischemia. Anat. Rec. 251, 9-14.

Yu, A.C., Chan, P.H., and Fishman, R.A. (1986). Effects of arachidonic acid on glutamate and gamma-aminobutyric acid uptake in primary cultures of rat cerebral cortical astrocytes and neurons. J. Neurochem. 47, 1181-9.

Zarbiv, R., Grunewald, M., Kavanaugh, M.P., and Kanner, B.I. (1998). Cysteine scanning of the surroundings of an alkali-ion binding site of the glutamate transporter GLT-1 reveals a conformationally sensitive residue. J. Biol. Chem. 273, 14231-7.

Zerangue, N., Arriza, J.L., Amara, S.G., and Kavanaugh, M.P. (1995). Differential modulation of human glutamate transporter subtypes of arachidonic acid. J. Biol. Chem. 270, 6433-5.

Zerangue, N., and Kavanaugh, M.P. (1996). Flux coupling in a neuronal glutamate transporter. Nature 383, 634-7.

Zhang, Y., Pines, G., and Kanner, B.L. (1994). Histidine 326 is critical for the function of GLT-1, a ($Na^+ + K^+$)-coupled glutamate transporter from rat brain. J. Biol. Chem. 269, 19573-7.

Zhang, Y., Bendahan, A., Zarbiv, R., Kavanaugh, M.P., and Kanner, B.I. (1998). Molecular determinant of ion selectivity of a ($Na^+ + K^+$)-coupled rat brain glutamate transporter. Proc. Natl. Acad. Sci. USA 95, 751-5.

Identification and Characterization of a cDNA Encoding a Neuronal Glutamate Transporter from *Drosophila melanogaster*

Rebecca P. Seal[‡§], Gwynn M. Daniels[†§], William J. Wolfgang[§], Michael A. Forte[§] and Susan G. Amara[¶§#].

[‡]Program in Neuroscience, [†]Department of Cell and Developmental Biology, [¶]Howard Hughes Medical Institute and [§]Vollum Institute for Advanced Biomedical Research, Oregon Health Sciences University, Portland, OR 97201 U.S.A.

Running Title: *Drosophila* sodium-dependent glutamate transporter

25 Manuscript Pages
6 Figures
2 Tables

Keywords: Glutamate, transport, chloride conductance, *Drosophila*

[#]Correspondence address:
Vollum Institute and Howard Hughes Medical Institute
Oregon Health Sciences University, L-474
3181 S.W. Sam Jackson Park Rd.
Portland, Oregon 97201 U.S.A
Telephone: (503) 494-6721
Fax: (503) 494-2285
E-mail: amaras@ohsu.edu

Published in Receptors and Channels 6, 51-64 (1998)

Summary

Sodium-dependent glutamate transporters influence neurotransmission in the central nervous system by removing synaptically released glutamate from the extracellular space and by maintaining extracellular glutamate concentrations below neurotoxic levels. In insects, glutamate also serves as the neurotransmitter at the neuromuscular junction, but the mechanism for neurotransmitter clearance at this synapse has not been well-established. Here we report the cloning and characterization of a sodium-dependent glutamate transporter, dEAAT, from *Drosophila melanogaster*. The 479 amino acid dEAAT gene product is 40-50% homologous to mammalian members of this carrier family. A 3.3 kilobase (kb) transcript for dEAAT was detected in adult fly heads and to a lesser extent in bodies by Northern blot analysis and was also localized to neurons in the central nervous system by *in situ* hybridization. The transport activity observed following expression of dEAAT in *Xenopus* oocytes or COS-7 cells shows a high affinity for L-glutamate, L-aspartate and D-aspartate, an absolute dependence on external sodium ions, and considerable stereoselectivity for the transport of L-glutamate over D-glutamate. As has been observed for the human carriers, EAAT4 and EAAT5, a significant component of the current activated by L-glutamate application to dEAAT-expressing oocytes appears to arise from the activation of a chloride channel associated with the carrier.

Introduction

Glutamate is a major excitatory neurotransmitter in the mammalian central nervous system that has been implicated in many important physiological processes such as developmental plasticity and long-term potentiation, as well as in pathological conditions such as ischemia and ALS (Zorumski and Olney, 1993; Choi, 1994; Rothstein, 1995; Bristol and Rothstein, 1996). In the vertebrate central nervous system (CNS), extracellular concentrations of excitatory amino acids are regulated by high affinity sodium-dependent glutamate transporters present on neurons and glial cells. Furthermore, glutamate transporters have been thought to contribute to the termination of signaling by limiting the extracellular lifetime of neurotransmitter molecules following exocytotic release into the synaptic cleft (Barbour et al., 1994; Tong and Jahr, 1994; Mennerick and Zorumski, 1994; Otis et al., 1996). In *Drosophila melanogaster* and other invertebrates, glutamate acts as a neurotransmitter at the neuromuscular junction (NMJ) (Lea and Usherwood, 1973; Jan and Jan, 1976), as well as in the central nervous system, but whether glutamate transport serves to maintain the signaling capacity at these fast excitatory synapses remains to be established. A distinct mechanism operates at the vertebrate NMJ, where the precise temporal and spatial action of acetylcholine is maintained by acetylcholinesterase (AChE), a highly catalytic enzyme which metabolizes acetylcholine to choline and acetate (Taylor and Radic, 1994). Because no evidence exists for the enzymatic inactivation of glutamate at the invertebrate NMJ, it is of interest to determine whether glutamate carriers contribute to clearance at this synapse and how the kinetic properties of these carriers compare to those of AChE acting at the mammalian NMJ.

Several sodium-dependent glutamate transporter subtypes have been cloned and characterized from vertebrates (Pines et al., 1992; Storck et al., 1992; Kanai and Hediger, 1992; Arriza et al., 1994; Fairman et al., 1995; Arriza et al., 1997). These carriers use the electrochemical gradient for sodium ions to drive the unidirectional transport of glutamate

against its concentration gradient, with a stoichiometry of two or three sodium ions and one proton cotransported and one potassium ion counter-transported (Kanner and Bendahan, 1982; Erecinska et al., 1983; Barbour et al., 1988; Amato et al., 1994; Zerangue and Kavanaugh, 1996a). This results in a coupled influx of at least one, and as many as two, positive charges for each glutamate molecule transported. Additionally, each of the cloned human carriers appears to mediate a substrate-elicited chloride conductance which is thermodynamically uncoupled from substrate translocation (Fairman et al., 1995; Wadiche et al., 1995a; Arriza et al., 1997). Thus, substrate induced steady-state currents measured under two-electrode voltage-clamp are the sum of both the transport mediated currents and the chloride conductance. The relative magnitude of the chloride conductance appears to vary among the cloned carriers and in the case of EAAT 4 and EAAT5, appears to comprise greater than 95% of the observed steady-state current (Fairman et al., 1995; Arriza et al., 1997). The activation of this chloride conductance during excitatory amino acid transport suggests additional contributions of glutamate transporters to cellular signaling and provides support for the contention that transporters may serve as sensors of extracellular glutamate concentrations as has been proposed to occur in retinal photoreceptors (Eliasof and Werblin, 1993; Picaud et al., 1995a; Picaud et al., 1995b; Grant and Werblin, 1996).

To further understand the role of sodium-dependent glutamate carriers at glutamatergic synapses in invertebrates and during development, we have identified and characterized a high affinity sodium-dependent glutamate transporter from the fruit fly, *Drosophila melanogaster*, as this organism has proven to be a powerful system for the genetic and developmental analyses of protein function.

Results

Isolation of dEAAT cDNA from Drosophila melanogaster To further understand the functional impact of sodium-dependent glutamate transporters on glutamatergic transmission, we isolated cDNAs encoding members of this carrier family from *D. melanogaster*, by using an approach based on sequence similarities. Degenerate oligonucleotides designed from two conserved regions of the human glutamate transporters were used to prime PCR reactions containing cDNA from *drosophila* embryos (24 hr). A 200bp DNA fragment exhibiting high homology to cloned glutamate transporters was generated and used to isolate a longer cDNA clone from a *drosophila* head cDNA library. Oligonucleotides designed against the start and stop regions of the 1437 bp open reading frame (ORF) present in this clone were used to amplify additional clones from head and body cDNA by PCR. This resulted in the isolation of several identical clones, one of which was chosen for further characterization and termed "dEAAT".

The deduced amino acid sequence of dEAAT predicts a 479 amino acid residue protein exhibiting approximately 40-50% identity to the five human glutamate transporters, EAATs 1-5. The greatest sequence conservation exists in the C-terminal half of the molecule which includes a domain implicated in the interaction of substrates and inhibitors with the carrier (Fig. 1) (Conradt and Stoffel, 1995; Vandenberg et al., 1995; Pines et al., 1995; Kavanaugh et al., 1997). Much less homology (33-35%) is observed between dEAAT and the sodium-dependent neutral amino acid (ASC) transporters, which also belong to this carrier family (Shafqat et al., 1993; Arriza et al., 1993; Kekuda et al., 1996; Utsunomiya-Tate et al., 1996). Hydropathy analysis, carried out using the Goldman, Engleman, Steitz algorithm (Engleman et al., 1986), revealed 8-10 hydrophobic stretches identical to those observed in EAATs 1-5. Studies to evaluate the transmembrane topology of these carriers indicate that the N- and C-termini are located within the cytoplasm, but the exact number of segments that span the membrane remains unclear (Slotboom et al., 1996,

Wahle and Stoffel, 1996). Two consensus sites for glycosylation are encoded by the dEAAT sequence, one is located within the first putative extracellular loop and the other in the large loop between putative TMDs 3 and 4 (Fig. 1). Glycosylation in the large loop has been demonstrated for GLAST1, but its significance has yet to be demonstrated, as it appears not to be essential for either targeting to the plasma membrane or for substrate translocation (Conradt et al., 1995). The dEAAT protein has several putative consensus sites for phosphorylation by Cam Kinase II and cyclic AMP-dependent Protein Kinase in the C-terminal half of the molecule. A serine residue in GLT-1, the rat homolog of EAAT2, is proposed to serve as a site for phosphorylation by Protein Kinase C (Casado et al., 1993), but this residue is not present in the analogous position in dEAAT .

Expression of dEAAT mRNA and Chromosomal Localization of the dEAAT gene- The spatial and temporal pattern of dEAAT expression during early stages of *drosophila* development was assessed by *in situ* hybridization (Fig. 2). Hybridization of antisense RNA probes to whole embryos detected no transcripts until stage 16, a point when embryonic development is essentially complete. At this time, transcripts were localized exclusively to cell bodies within the central nervous system, with no detectable staining in peripheral sensory neurons or in somatic or visceral muscles. Control embryos hybridized with sense RNA probes had no detectable staining at any embryonic stage. In the CNS, positively stained cells were generally observed in discrete clusters within larger groups of unstained cells. In abdominal neuromeres, a stereotyped repeating pattern was observed in each neuromere composed of a single small ventral midline cluster, a single midline cluster at the level of the longitudinal connectives, two small lateral clusters within each hemi-neuromere, and a single large medial cluster dorsal to the connectives within each hemi-neuromere (Fig. 2A). Clusters of cell bodies were also stained in thoracic neuromeres as well as in the brain (Fig. 2B). This overall pattern is consistent with the expression of dEAAT mRNA in motor neurons and other neuronal cell types within the embryonic nervous system.

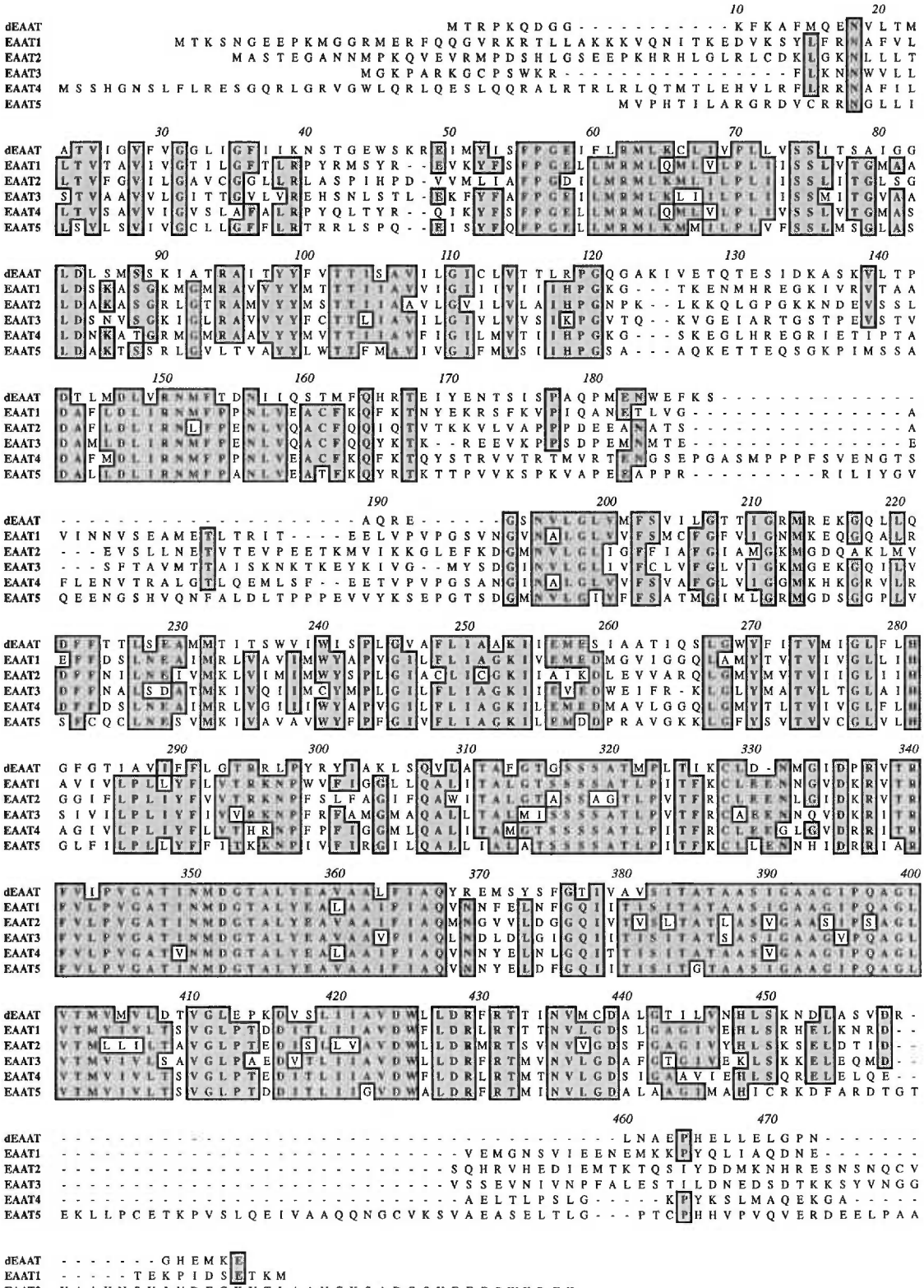
dEAAT
EAAT1
EAAT2
EAAT3
EAAT4
EAAT5

FIG. 1. Amino acid sequence of dEAAT aligned with the human glutamate transporters EAATs 1-5. Residues which are conserved in four of the six transporters are boxed and shaded. The percent identity of the dEAAT protein with the human EAATs is as follows: EAAT1 = 46%, EAAT2 = 45%, EAAT3 = 47%, EAAT4 = 42%, and EAAT5 = 40%.

The expression of dEAAT mRNA in adult *drosophila* heads and bodies was examined by Northern-blot analysis. Total RNA was isolated from these regions and probed with the coding sequence of dEAAT. A single transcript of approximately 3.3 kb was abundantly expressed in fly heads and was also detectable in bodies, but to a much lesser extent (Fig. 3). This difference in the expression levels of dEAAT mRNA is consistent with the results obtained from the *in situ* hybridization study.

In situ hybridization to *drosophila* polytene chromosomes indicates that the gene encoding dEAAT is located at position 30A on the left arm of the second chromosome. Further mapping to P1 clones from this region is consistent with this chromosomal location.

Expression of dEAAT in COS-7 cells - In addition to the high primary sequence homology, several functional properties were evaluated to ascertain whether or not the isolated clone belongs to the sodium-dependent glutamate transporter family. All assays were carried out by measuring the uptake of radiolabeled substrates into COS-7 cells that had been transiently transfected with pCMV5-dEAAT cDNA or the vector pCMV5 DNA. COS-7 cells expressing dEAAT displayed a 3-4 fold increase in the accumulation of radiolabeled L-glutamate over vector transfected cells. Radiolabeled substrates were transported with high affinity in a concentration-dependent and saturable manner. Transport activity by dEAAT showed considerable stereoselectivity for L-glutamate over D-glutamate, and the K_m values determined for L-glutamate, L-aspartate and D-aspartate were comparable to those determined for EAATs 1-3 in this system (Table 1). The sodium-dependence of dEAAT-mediated glutamate uptake was evaluated by measuring the transport of radiolabeled glutamate after reducing the extracellular concentration of sodium ions from 153 mM to 16 mM, using choline as the sodium substitute. Under these conditions, uptake of radiolabeled L-glutamate was essentially abolished (Fig. 4).

A

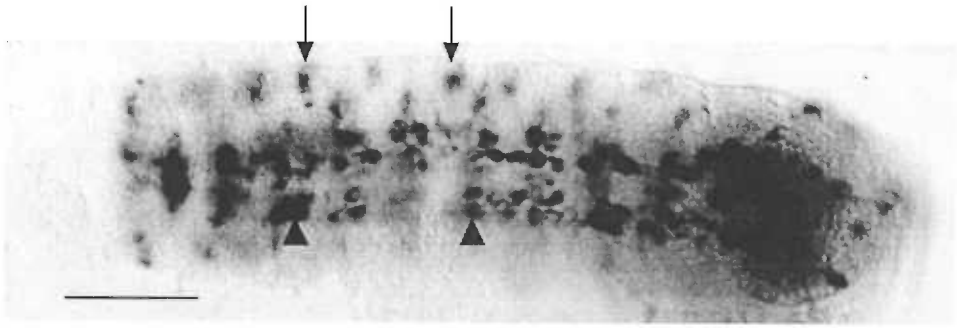

B

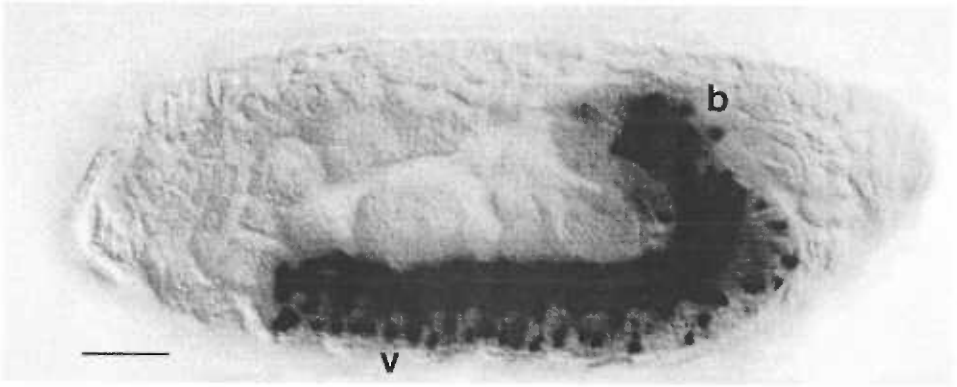

FIG. 2. In situ hybridization to dEAAT transcripts in stage 16 *drosophila* embryos. A, Ventral view showing cell body clusters in abdominal neuromeres. The apparent asymmetry around the mid-line results from contralateral cells out of the plane of focus. B, Lateral view showing cell clusters in the brain and thoracic ganglia. Note the absence of any hybridization in the muscles or peripheral nervous system. b, brain; v, ventral ganglia; arrow, lateral cell cluster; arrow head, medial cell cluster. Bar = 50μm.

Expression of dEAAT in Xenopus oocytes - Members of the sodium-dependent glutamate transporter family are electrogenic based on their overall substrate stoichiometry which results in the net influx of one or two positive charges per transport cycle. Additional current is generated by the activation of substrate-gated chloride conductances associated with the carriers. Thus, it is possible to functionally characterize members of this family in *Xenopus* oocytes not only by assaying radiolabeled substrate transport, but also by measuring substrate-induced steady-state currents using two-electrode voltage-clamp techniques. Moreover, this system allows for the measurement of radiolabeled uptake at fixed membrane potentials.

Application of 100 μM [^{3}H]-L-glutamate to dEAAT cRNA-injected oocytes held at -60 mV resulted in a 4-fold greater accumulation of radiolabeled substrate than non-injected oocytes (24.1 ± 2.6 pmoles versus 6.1 ± 0.2 pmoles, n = 4). Uptake was concentration-dependent and saturable, with an apparent transport affinity for L-glutamate of 26 ± 5 μM (Fig. 5A). L-glutamate applied to oocytes expressing dEAAT, elicited currents that were both concentration-dependent and saturable, but had no affect on uninjected oocytes over the voltage range of -100 mV to +40 mV (Fig. 5B).

The sodium-dependence of the substrate-elicited currents was examined by substituting choline chloride for sodium chloride in the recording solution. Under these conditions, no currents were detected over the voltage range of -100 mV to +40 mV upon application of glutamate (Fig. 5C). This is consistent with the observed sodium-dependence of dEAAT-mediated transport in COS-7 cells.

When the current-voltage relationship for the substrate-elicited steady-state currents of dEAAT were evaluated from -100 mV to +40 mV, the currents were inward at negative potentials and reversed at -2 +/- 7 mV. For a sodium-coupled cotransporter, substrate-elicited steady-state currents would not be expected to reverse during electrogenic transport of substrates in the presence of an inwardly directed sodium gradient. However, reversal of substrate-elicited currents has been observed in oocytes expressing EAATs 1-5, and has

Table 1. Kinetic parameters of uptake in COS-7 cells

Substrate	$K_m(\mu M)$	V_{max} [a]
L-Glutamate	72±3	117±3
L-Aspartate	31±4	47±2
D-Glutamate	-	0 [b]
D-Aspartate	92±9	126±8

[a] pmol/well/min.
[b] No uptake observed with application of > 5mM.

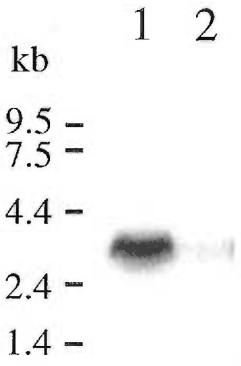

FIG. 3. Northern-blot analysis of glutamate transporter transcripts. Total RNA (25 μg) isolated from *D. melanogaster* heads (lane 1) and bodies (lane 2) was separated on a formaldehyde-agarose gel, blotted, and hybridized with a dEAAT cDNA probe. The size of hybridizing mRNA species were determined using RNA standards run in parallel.

Expression of dEAAT in Xenopus oocytes - Members of the sodium-dependent glutamate transporter family are electrogenic based on their overall substrate stoichiometry which results in the net influx of one or two positive charges per transport cycle. Additional current is generated by the activation of substrate-gated chloride conductances associated with the carriers. Thus, it is possible to functionally characterize members of this family in *Xenopus* oocytes not only by assaying radiolabeled substrate transport, but also by measuring substrate-induced steady-state currents using two-electrode voltage-clamp techniques. Moreover, this system allows for the measurement of radiolabeled uptake at fixed membrane potentials.

Application of 100 μM [^{3}H]-L-glutamate to dEAAT cRNA-injected oocytes held at -60 mV resulted in a 4-fold greater accumulation of radiolabeled substrate than non-injected oocytes (24.1 ± 2.6 pmoles versus 6.1 ± 0.2 pmoles, n = 4). Uptake was concentration-dependent and saturable, with an apparent transport affinity for L-glutamate of 26 ± 5 μM (Fig. 5A). L-glutamate applied to oocytes expressing dEAAT, elicited currents that were both concentration-dependent and saturable, but had no affect on uninjected oocytes over the voltage range of -100 mV to +40 mV (Fig. 5B).

The sodium-dependence of the substrate-elicited currents was examined by substituting choline chloride for sodium chloride in the recording solution. Under these conditions, no currents were detected over the voltage range of -100 mV to +40 mV upon application of glutamate (Fig. 5C). This is consistent with the observed sodium-dependence of dEAAT-mediated transport in COS-7 cells.

When the current-voltage relationship for the substrate-elicited steady-state currents of dEAAT were evaluated from -100 mV to +40 mV, the currents were inward at negative potentials and reversed at -2 +/- 7 mV. For a sodium-coupled cotransporter, substrate-elicited steady-state currents would not be expected to reverse during electrogenic transport of substrates in the presence of an inwardly directed sodium gradient. However, reversal of substrate-elicited currents has been observed in oocytes expressing EAATs 1-5, and has

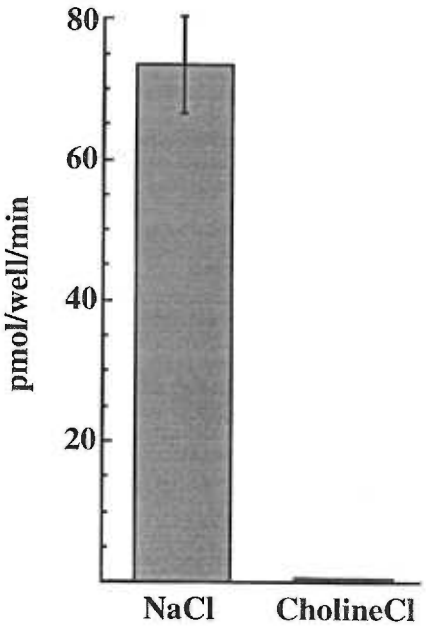
80
60
40
20
pmol/well/min
NaCl
CholineCl

FIG. 4. Sodium dependence of L-glutamate uptake in COS-7 cells expressing dEAAT. Uptake of 500 μM L-glutamate with 100 nM [^{3}H]-L-glutamate for 10 min. at 20°C. Values are the mean ± SD from a single representative experiment done in triplicate. The sodium ion concentration was reduced from 153 mM to 16 mM by replacement of sodium chloride in the buffer with an equimolar concentration of choline chloride.

Table 2. Functional properties of dEAAT in *Xenopus* oocytes

Substrate	*n*	$K_m(\mu M)$	I_{max} *
L-Glutamate	4	24±3	1
L-Aspartate	5	21±2	1.4±0.2
D-Glutamate	5	>5000	-
D-Aspartate	5	90±6	1.4±0.2
L-Cysteine	4	2600±300	1.1±0.1
THA	6	22±2	1.1±0.1

Inhibitor	*n*	K_i (μM)
L-*trans* -PDC	4	11±3
Kainate	5	>1000

* I_{max} values are normalized to the I_{max} of L-Glutamate in the same oocyte.

been shown to be an uncoupled, substrate-activated chloride conductance associated with these carriers (Fairman et al., 1995; Wadiche et al., 1995a; Arriza et al., 1997). To determine whether a substrate-activated chloride conductance underlies reversal of the steady-state current mediated by dEAAT, chloride ions were replaced by gluconate in the recording solution. Under these conditions, the glutamate-elicited steady-state currents no longer reversed when the current-voltage relationship was evaluated at voltages as positive as +40 mV (Fig. 6A). This is consistent with an outward current generated by an inward movement of chloride ions. Although a slight reduction in the amplitude of the currents was observed at membrane potentials more negative than -24mV, the chloride equilibrium potential (E_{Cl}) in the oocyte (Barish, 1983), when chloride ions were absent, the amount of radiolabeled L-glutamate accumulated did not differ significantly at a membrane potential of -60mV (10.2 ± 0.8 pmoles in the absence of extracellular chloride versus 14.0 ± 1.5 pmoles, $P<0.07$).

To examine the effect of both internal and external chloride on the substrate-activated currents, chloride ions were replaced with gluconate by dialyzing dEAAT-expressing oocytes for at least 40 hours in chloride-free recording solution. In the absence of chloride ions, the currents were completely abolished over the voltage range of -100 mV to +40 mV (Fig. 6B). In an oocyte held at -60mV in normal recording solution we estimate that coupled transport accounts for one to two of the approximately five net charges that move with each glutamate molecule transported and thus ~20-40% of the current measured should reflect the transport of substrates. The absence of a measurable current in the dialyzed oocyte suggests that glutamate transport may also be substantially reduced by chloride removal. Consistent with this finding, uptake of [^{3}H]-L-glutamate was abolished following dialysis in chloride-free recording solution. As a control experiment, oocytes from the same batch were used to express a human glutamate transporter, EAAT1. In EAAT1-expressing oocytes a large transport current could still be measured even after

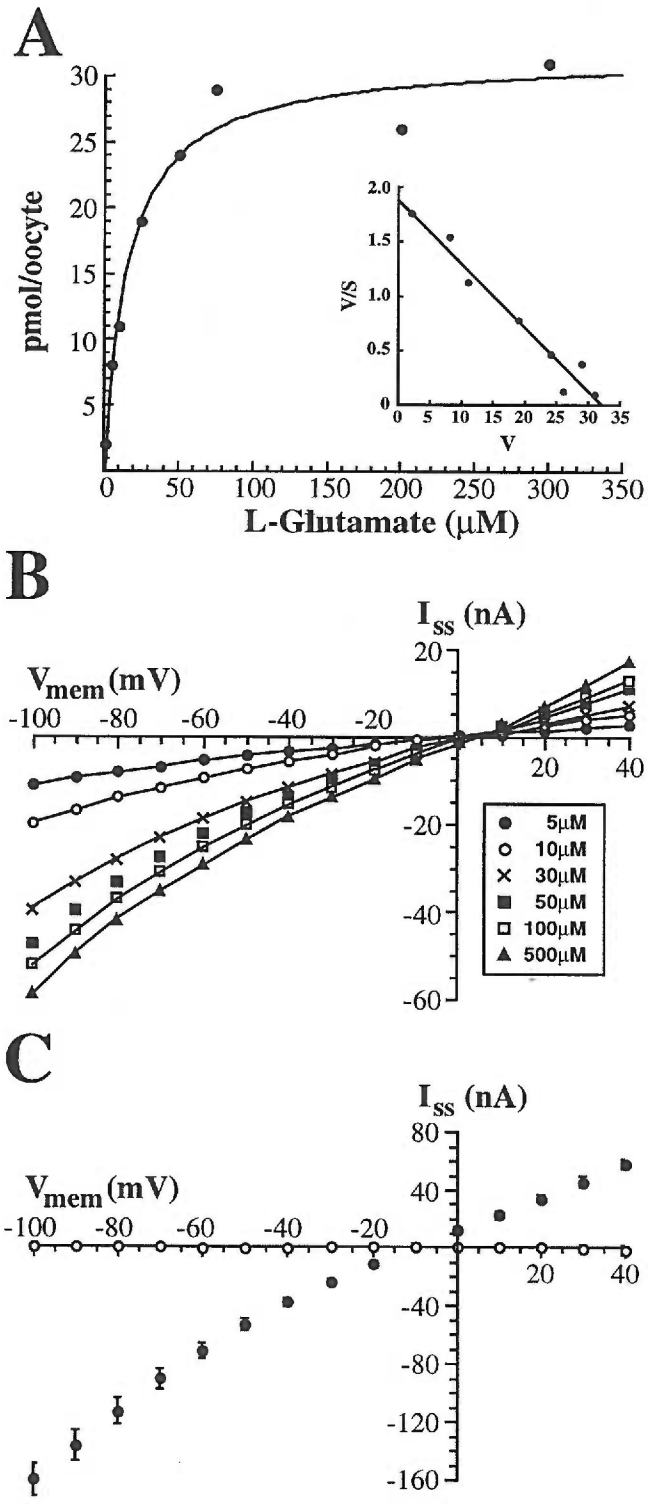
A
pmol/oocyte
L-Glutamate (μM)
V/S
V
B
I_{ss} (nA)
V_{mem} (mV)
5μM
10μM
30μM
50μM
100μM
500μM
C
I_{ss} (nA)
V_{mem} (mV)

FIG. 5. Kinetic properties of L-glutamate uptake in *Xenopus laevis* oocytes expressing dEAAT. A, Uptake velocity (in pmol/oocyte) was measured using 100 nM [^{3}H]-L-glutamate and increasing concentrations of unlabeled L-glutamate in oocytes injected with synthetic dEAAT RNA. The data presented are the mean of triplicate determinations from a single representative experiment. Individual determinations for each point do not vary from the mean by >12.5%. The K_m value was calculated from the Eadie-Hofstee plot (inset), and represents the mean ± S.E.M. B, Current-voltage relationships of steady-state currents elicited by increasing concentrations of glutamate show dose- and concentration-dependence. Plotted curves represent one oocyte expressing dEAAT. C, Steady-state currents (I_{ss}) elicited by 100 μM L-glutamate over the voltage range of -100 mV to +40 mV (filled circles) are abolished when external sodium is replaced with equimolar choline (open circles). Data is the average of 4 cells ± S.E.M.

dialysis indicating that under these conditions oocytes retain the capacity for sodium-coupled transport.

The K_m values for several well-known substrates of sodium-dependent glutamate transporters were determined by measuring substrate-induced steady-state currents. L-glutamate, L-aspartate, D-aspartate and DL-threo-B-hydroxyaspartate (THA) were all high affinity substrates of the transporter, while D-glutamate and L-cysteine were poor substrates (Table 2). The apparent affinity of the dEAAT transporter for L-glutamate, derived by measuring the transport of radiolabeled L-glutamate in oocytes (K_m=26 ± 5 μM), is consistent with the affinity constant obtained by measuring L-glutamate-elicited steady-state currents (K_m=24 ± 3 μM). Quisqualate, a glutamate receptor agonist, did not elicit a current when applied at a concentration of 100 μM.

The sensitivity of dEAAT to compounds known to inhibit sodium-dependent glutamate transporters was also evaluated. Although L-*trans*-Pyrrolidine-2,4-dicarboxylate (L-*trans*-PDC) applied alone elicited an inward current at very negative potentials (-100 mV), the I_{max} was less than 5% of the I_{max} for L-glutamate (data not shown). Therefore, we measured the ability of L-*trans*-PDC to inhibit the current elicited by 100 μM L-glutamate (K_i = 11 ± 3 μM, Table 2). Kainate, a structural analog of glutamate, was a poor inhibitor of dEAAT (K_i >1 mM). Ibotenate, a high affinity agonist at the H-receptor, a glutamate-gated chloride channel in invertebrates, neither elicited a current nor blocked a glutamate elicited current over a voltage range of -100 mV to +40 mV (data not shown). Additionally, 100 μM picrotoxin, a blocker of ligand-gated chloride channels, had no affect on the current elicited by 100 μM L-glutamate.

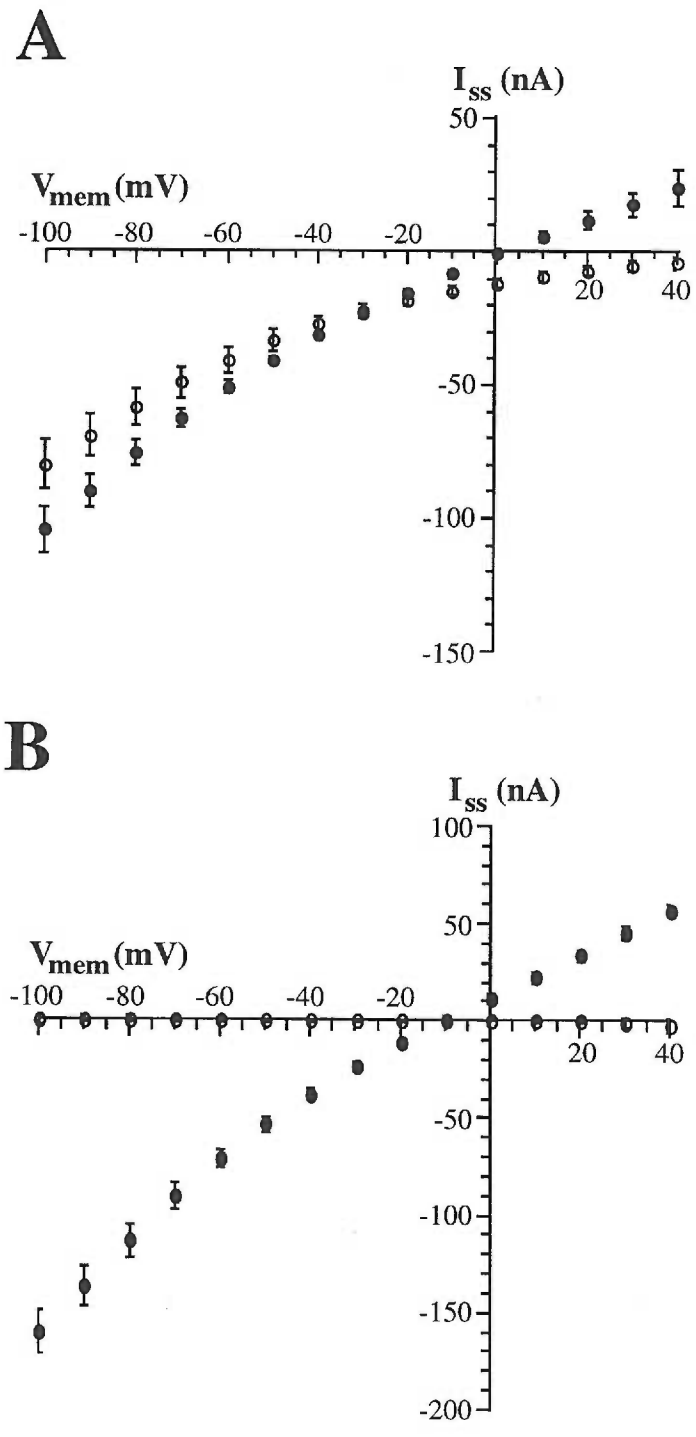
A
I_{ss} (nA)
50
V_{mem} (mV)
-100 -80 -60 -40 -20
20 40
-50
-100
-150
B
I_{ss} (nA)
100
50
V_{mem} (mV)
-100 -80 -60 -40 -20
20 40
-50
-100
-150
-200

FIG. 6. Effect of chloride ions on dEAAT-mediated currents. A, Steady-state currents elicited by 100 μM L-glutamate (filled circles) were reduced at membrane potentials more negative than -24 mV and did not reverse at potentials up to +40 mV, when external chloride ions were replaced with an equimolar concentration of gluconate (open circles). Data is the average of 4 cells ± S.E.M. B, When both external and internal chloride ions were replaced with gluconate (open circles), steady-state currents elicited by 100 μM L-glutamate (filled circles) were abolished over the voltage range of -100 mV to +40 mV. Currents shown are the average of 4 cells ± S.E.M.

Discussion

We have identified a cDNA from *Drosophila melanogaster* that encodes a protein showing high homology (40-50%) to mammalian members of the high affinity sodium-dependent glutamate transporter family, which also includes the sodium-dependent neutral amino acid carriers. Thus far, five subtypes of glutamate transporters and two subtypes of ASC carriers have been cloned from vertebrates. Analysis of the amino acid sequence of dEAAT indicates that it shares the highest homology with EAAT 1 (46%) and EAAT 3 (47%). dEAAT is the first member of this family to be cloned from *drosophila.*

In both transiently transfected COS-7 cells and in oocytes injected with dEAAT cRNA, the expressed carrier exhibits functional properties characteristic of sodium-dependent glutamate transporters. Exogenously applied excitatory amino acids are transported in a sodium-dependent manner and the uptake velocity is both concentration-dependent and saturable. The substrate selectivities for dEAAT are also similar to mammalian carriers; the transport activity encoded by dEAAT shows high apparent affinities for L-glutamate, and L- and D-aspartate, and low affinity for D-glutamate. L-cysteine, which is poorly transported by EAATs 1, 2, and 4, but is a better substrate for EAAT3 (Zerangue and Kavanaugh, 1996b), is a poor substrate for dEAAT (K_m = 2.6 ± 0.3 mM). THA applied alone elicits a current and has an apparent transport affinity (K_m=22 +/- 2μM) similar to the values reported for EAATs 1-4. The calculated inhibition constant (K_i = 11 ± 3 μM) for L-*trans*-PDC is also similar to that observed for EAATs 1-5. Overall, with the exception of the low apparent affinity for transport of L-cysteine, the transport and inhibition constants determined for dEAAT are most similar to those reported for EAAT3 (Arriza et al., 1994). Differences in the K_m values for L-glutamate and L-aspartate are observed when a comparison is made between expression in oocytes and the transfected COS-7 cell system, but similar discrepancies are also observed with mammalian EAATs examined in these two systems (Arriza et al., 1994). Several possible reasons

could account for these disparities, including differences in the ionic composition of the uptake buffers, distinct cell membrane lipid compositions or the differential influences of accessory or modulatory proteins.

As has been observed in oocytes expressing the human carriers EAATs 1-5, a substrate-activated chloride conductance appears to underlie the reversal of the steady-state current mediated by dEAAT. The chloride conductance mediated by dEAAT contributes significantly to the steady-state currents and as has been noted with EAAT4 and EAAT5, may be larger in magnitude than the current generated by substrate transport. The chloride conductances associated with glutamate transporters are not directly coupled to the transport of substrates (Fairman et al., 1995; Wadiche et al., 1995a; Arriza et al., 1997) and transport mediated by these carriers does not depend on chloride ions. In the absence of external chloride ions, the substrate-elicited outward currents mediated by dEAAT are abolished, consistent with the notion that the outward current is due to the passive flux of chloride ions. The amplitude of the inwardly directed steady-state currents also appear reduced. This slight decrease in amplitude is likely the result of a decrease in the chloride efflux rather than a reduction in the coupled transport component of the current, as the amount of radiolabeled L-glutamate accumulated is not significantly different. In the case where both external and internal chloride ions have been replaced with gluconate, a dramatic reduction is observed in both the amplitude of the transport-mediated current and in the uptake of radiolabeled L-glutamate. This effect appears to be specific to dEAAT, as EAAT1-expressing oocytes that were treated in parallel were still able to elicit a large substrate-activated steady-state current in the absence of both internal and external chloride ions. Several factors could underly the apparent loss in glutamate transport activity observed under these conditions including a down-regulation of dEAAT molecules at the membrane surface or an alteration in the ion gradients that support transport. It is also possible that gluconate mediates the observed decrease in transport. This effect, however,

may otherwise suggest that, in contrast to EAATs 1-5, the presence of chloride ions is required for transport activity of dEAAT.

The relevance of the glutamate-gated chloride channel activity of dEAAT to neurotransmission in flies remains to be established, but there are a number of possible role that it could serve. The changes in chloride permeability mediated by the carrier could modulate cellular excitability, they could serve as a mechnism for sensing extracellular glutamate concentrations or alternatively, a chloride current could counterbalance the depolarization associated with electrogenic transport. In invertebrates, several studies have confirmed that glutamate acts as both an inhibitory and excitatory neurotransmitter at and adjacent to the NMJ due to the presence of both anion conducting (H-type) and cation conducting (D-type) glutamate receptors (Cull-Candy, 1976; Wafford and Sattelle, 1989). H-receptors, the hyperpolarizing extrajunctional glutamate receptors that were initially identified in arthropod muscle (Lea & Usherwood, 1973) are gated by L-glutamate, ibotenate, and the antiparasitic agent avermectin. This class of glutamate-activated chloride channel are also weakly blocked by picrotoxin, an inhibitor of ligand-gated chloride channels. D-type receptors are activated by quisqualate and AMPA and appear to have pharmacological profiles distinct from those found in mammals. Although glutamate transporters serve dual functions as ligand-gated chloride channels and carrier proteins in several vertebrate species (Fairman et al., 1995; Arriza et al., 1997; Wadiche et al., 1995a; Grant & Werblin, 1996; Grant and Dowling, 1995; Eliasof and Jahr, 1996; Billups et al., 1996), the structure, functional properties and distribution of dEAAT confirm that it is unrelated to the H-receptor glutamate- and avermectin-gated chloride channel isoform that was recently cloned from *drosophila* (Cully et al., 1996)

The neuronal localization of dEAAT mRNA alao supports the idea that this carrier might influence glutamatergic signaling in *Drosophila*. The expression of dEAAT mRNA appears to be limited to neurons of the central nervous system, including abdominal and thoracic neuromeres, and was not detected in somatic or visceral muscles. To date, the two

glutamate carrier subtypes, EAAT3 and EAAT4, demonstrated to be in mammalian CNS neurons are present on the soma and dendrites of neurons, rather than on axons or at presynaptic terminals (Rothstein et al., 1994; Yamada et al., 1996). However, in the vertebrate retina some carrier subtypes such as Glt-1 (EAAT2) (Rauen et al., 1996) and salamander EAAT5A (Eliasof et al, 1998) do appear to be located at the presynaptic terminals of cells that release glutamate. Taken together these data suggest that neuronal glutamate transporters, with their roles in clearing neurotransmitter and in modulating cellular excitability through their associated chloride conductances, could regulate glutamate concentrations in the synaptic cleft from either side of synapse. The localization of dEAAT mRNA in the embryo is consistent with the expression of dEAAT in motorneurons, making it plausible that this transporter could function in the presynaptic uptake of glutamate at the neuromuscular junction. Formal confirmation of this hypothesis will await the development of antibodies directed against dEAAT to examine more precisely its localization within these neuronal populations.

Although the NMJ of *drosophila* has been studied extensively by a variety of methods, the mechanisms of signal termination at this synapse have not been well-characterized. It is reasonable to hypothesize that EAATs may be the major route for glutamate clearance in a manner analogous to their function in the mammalian CNS, because enzymes that catalyze the breakdown of glutamate have not been identified at the NMJ in invertebrates. A comparison of the kinetics and distribution of AChE at the vertebrate NMJ to what is known for CNS glutamate transporters, however, suggests fundamental differences between the two mechanisms of neurotransmitter inactivation. In the mammalian CNS glutamate transporters are relatively abundant but have a slow turnover rate (1 to 250 msec per molecule of glutamate (Schwartz and Tachibana, 1990; Danbolt et al., 1990; Wadiche et al., 1995b). It has been proposed that the presence of a large number of transporters may enhance the decay rate of glutamate by serving as binding sites that buffer the concentration of free glutamate (Tong & Jahr, 1994; Wadiche et al.,

1995b). In contrast, at the vertebrate NMJ, AChE has a higher turnover rate (100μsec per molecule of ACh (Lawler, 1961; Wilson and Harrison, 1961) but is less abundant than the ACh receptors (AChRs) which are clustered postsynaptically at sites of release. At this synapse neurotransmitter is utilized with high efficiency; most of the ACh is available for binding to and activating receptors and only a small fraction of the released ACh is binding to the local AChE sites. Futher analyses of dEAAT, including its precise subcellular localization and density relative to glutamate release sites, will be important for understanding the differences in the clearance of neurotransmitter at the vertebrate and invertebrate NMJ and at excitatory CNS synapses. A more indepth analysis of the functional properties of dEAAT, including the targeted disruption of the dEAAT gene, should provide further insight into the contribution of this carrier to the termination of glutamate signaling in the invertebrate nervous system.

Materials and Methods

cDNA cloning, sequence analysis and plasmid construction - Degenerate oligonucleotides complementary to highly conserved regions of the human excitatory amino acid transporters (EAAT1-4) were used to amplify a partial sequence from *D. melanogaster* embryo (24 hr.) cDNA. The primer sequences were 5'-CGCGGGTACCGCNGCNRTN-TTYATHGCNCA-3' and 5'-CGCGTCTAGATCNARNARCCARTCNACNGCNA-3', which correspond to amino acid residues 361 to 367 and 422 to 428 of dEAAT. A 200 basepair (bp) product was generated by polymerase chain reaction (PCR) with 25 cycles of denaturation (94°C, 30 sec), annealing (50°C, 30 sec), and extension (72°C, 30 sec). The resulting PCR product was labeled with [α-^{32}P]dCTP (New England Nuclear) by the random priming method (Boehringer Mannheim), and used to probe a cDNA library prepared from *D. melanogaster* heads (Quan et al., 1993). $5x10^5$ plaques were immobilized on duplicate on nylon filters (Colony/Plaque Screen; DuPont), and hybridized with 1 x 10^6 cpm/ml ^{32}P-labeled probe in 7% SDS, 0.5 M $NaPO_4$, pH 7.2 at 60°C. Filters were washed extensively in 1% SDS, 2X SSPE (0.3 M NaCl, 20 mM $NaPO_4$, 2 mM EDTA, pH 7.4) at 60°C and exposed to film (Kodak X-OMAT AR) overnight at -70°C. After secondary screening several inserts were excised with EcoR1 and subcloned into pBluescript II SK- (Stratagene). Plasmids were sequenced on both strands using double-stranded template, synthetic oligonucleotide primers and Amplitaq DNA polymerase (ABI). Sequence data analysis was performed using MACVECTOR (IBI; New Haven, CT). One plasmid contained a cDNA insert of 1.6 kb, including a 1437 nucleotide coding sequence beginning with an initiator methionine located within a sequence that fits well with the Kozak concensus sequence for initiation of transcription.

The coding sequence was amplified from the cDNA clone by PCR using 25 cycles of denaturation (94°C, 1 min), annealing (50°C, 1 min), and extension (72°C, 2 min). The oligonucleotide primer sequences were 5'-CGCGGAATTCACCATGACGCGAC-

CCAAACAGG-3' and 5'-CGCGTCTAGATCATTCCTTCATCTCGTGTCC-3', which incorporated unique flanking EcoR1 and Xba1 restriction enzyme sites. The PCR product was digested with EcoR1 and Xba1, subcloned into pBluescript and sequenced on both strands as described above. The nucleotide sequence was found to be identical to that of the clone isolated from the cDNA library. The PCR-generated coding sequences were also subcloned into pCMV5 (Andersson et al., 1989) for transfection into COS-7 cells, and into pOTV (Arriza et al., 1994) for expression in *Xenopus laevis* oocytes. The resulting expression plasmids are termed pCMV5-dEAAT and pOTV-dEAAT.

Northern blot analysis - Total RNA was isolated from adult fly heads and bodies with TRI REAGENT™ (Sigma) following the protocol provided with this reagent. RNA (25 μg) was size fractionated on a denaturing formaldehyde gel and transferred to nylon membrane. The coding sequence of dEAAT was excised and labeled with [α-^{32}P]dCTP by the random priming method. The membrane was hybridized with 1 x10^6 cpm/ml ^{32}P-labeled probe in 50% formamide, 5% SDS, 400 mM $NaPO_4$, 1 mM EDTA, 1 mg/ml BSA, pH 7.0 at 42°C. Filters were washed in 0.1% SDS, 2X SSPE at 42°C, and exposed to film overnight at -70°C.

Chromosomal mapping and in situ hybridization - *In situ* hybridization to polytene chromosomes was done as previously described (Quan et al., 1993). Subsequent analysis using dEAAT probes further localized the position of the dEAAT gene to P1 clones DS03809 and DS06931 (provided by the Berkeley Drosophila Genome Project) in the 30A region. *Drosophila* embryos were hybridized with sense and antisense RNA probes representing the entire coding sequence of dEAAT as described (Demchyshyn et al., 1994).

Cell transfections and transport assays - COS-7 cells were maintained in DMEM (GIBCO) supplemented with 10% FCS (GIBCO), 10 U/ml penicillin, and 10 μg/ml streptomycin, in 5% CO_2. dEAAT was expressed by DEAE dextran-mediated transfection of COS-7 cells with pCMV5-dEAAT (Lopeta et al., 1994). COS-7 cells were plated at a density of ~100,000 cells per well in 12-well tissue culture dishes and transfected the

following day with 0.5 μg of plasmid DNA per well essentially as described for this method. Two days post-transfection the cells were assayed for uptake activity as described (Arriza et al., 1994). The cells were washed with 0.5 ml room temperature PBS-d (GIBCO), and uptake was initiated by the addition of 100 nM [^{3}H]-L-glutamate (22 Ci/mmole, New England Nuclear-DuPont) with varying concentrations of cold substrate. In the sodium substitution experiment, sodium chloride was replaced with an equimolar concentration of choline chloride. Assays were terminated after 10 minutes by washing the cells three times in ice cold PBS-d. The cells were solubilized in 0.5 ml of 0.1N NaOH, 0.1% SDS prior to scintillation counting in 4.5 ml ScintiVerse (Fisher Scientific). Background uptake in pCMV5 transfected COS-7 cells was subtracted from total uptake in pCMV5-dEAAT transfected cells to give dEAAT-specific uptake. K_m values were calculated from a least-squares fit to the Michaelis-Menten equation and an Eadie-Hofstee transformation using KALEIDAGRAPH (Synergy Software).

Expression of dEAAT in Xenopus oocytes Messenger RNA was transcribed from the pOTV-dEAAT plasmid, which had been linearized with BamH1, by following the protocol of the mMessage mMachine Kit (Ambion). Fifty nanoliters of cRNA was injected into defolliculated stage IV *Xenopus laevis* oocytes and assayed for transport activity two to three days later, either by uptake of radiolabeled substrates or by two-electrode voltage-clamp recordings. A GeneClamp 500 amplifier and a Digidata 1200 interface (both from Axon Instruments) were used for the two-electrode voltage-clamp recordings. Oocytes were clamped at -60 mV and continuously superfused in ND96 recording solution (96mM NaCl, 2mM KCl, 1.8mM $CaCl_2$, 1mM $MgCl_2$, 5mM HEPES, pH 7.5). The profile generated by plotting current amplitude as a function of substrate concentration was fitted by least squares (KALEIDAGRAPH) to $I = (I_{max}[S])/(K_m+[S])$ where I_{max} is the maximum current amplitude and K_m is the Michaelis constant, representing the apparent affinity of the transporter for substrate. Values of K_m and I_{max} are expressed as the mean ± the standard error of the mean (SEM) for at least 4 oocytes. The K_m values were

determined by normalizing each curve to its I_{max} and averaging the values at each concentration. The I_{max} value for each substrate was normalized to the I_{max} for L-glutamate in the same oocyte. K_i values for inhibitors of transport were calculated from IC_{50} values using the method of Cheng and Prusoff (Cheng and Prusoff, 1973). For the sodium substitution experiments, sodium chloride was replaced with an equimolar concentration of choline chloride, and for the chloride substitution experiments, all chloride salts were replaced with equimolar gluconate salts (Sigma, St. Louis, MO). Voltage-clamped uptake of radiolabeled L-glutamate was performed by perfusing 80 nM [^{3}H]-L-glutamate and 100 μM unlabeled L-glutamate onto oocytes clamped at -60 mV for 120 seconds, followed by a 120 second washout period. Oocytes were immediately solubilized in 1% SDS and counted in a scintillation counter as described above.

Acknowledgments

We thank Sarah Smolik for analysis of polytene chromosomes and Sue Povlock for insightful comments on the manuscript. This work was supported by the Howard Hughes Medical Institute and a grant from the National Institutes of Health.

References

Amato A, Barbour B, Szatkowski M, Attwell D (1994) J Physiol **479** 371-80.

Andersson S, Davis DL, Dahlback H, Jornvall H, Russel DW (1989) J Biol Chem **264** 8222-8229.

Arriza JA, Eliasof S, Kavanaugh MP, Amara SG (1997) Proc Natl Acad Sci USA **94** 4155-4160.

Arriza JL, Fairman WA, Wadiche JI, Murdoch GH, Kavanaugh MP, Amara SG (1994) J Neurosci **14** 5559-69.

Arriza JL, Kavanaugh MP, Fairman WA, Wu Y-A, Murdoch GH, North RA, Amara SG (1993) J Biol Chem **268** 15329-15332.

Barbour B, Brew H, Attwell D (1988) Nature **335** 433-435.

Barbour B, Keller BU, Liano I, Marty A (1994) Neuron **12** 1331-1343.

Barish ME (1983) J Physiol **342** 309-325.

Billups B, Sarantis M, Attwell D (1996) J Physiol **494** 85.

Bristol LA, Rothstein JD (1996) Ann Neurol **39** 676-9.

Casado M, Bendahan A, Zafra F, Danbolt NC, Aragón C, Giménez C, Kanner BI (1993) J Biol Chem **268** 27313-27317.

Cheng Y-C, Prusoff WH (1973) Biochem Pharmacol **22** 3099-3108.

Choi D (1994) Prog Brain Res **100** 47-51.

Conradt M, Stoffel W (1995) J Biol Chem **270** 25207-25212.

Conradt M, Storck T, Stoffel W (1995) Eur J Biochem **229** 682-687.

Cull-Candy SG (1976) J Physiol **255** 449-464.

Cully DF, Paress PS, Liu KK, Schaffer JM, Arena JP (1996) J Biol Chem **271** 20187-20191.

Danbolt NC, Pines G, Kanner BI (1990) Biochemistry **29** 6734-6740.

Demchyshyn LL, Pristupa ZB, Sugamori KS, Barker EL, Blakely RD, Wolfgang WJ, Forte MA, Niznik HB (1994) Proc Natl Acad Sci USA **91** 5158-5162.

Eliasof S, Arriza JL, Leighton BH, Kavanaugh MP, Amara SG (1997) J Neurosci **18**(2) 698-712

Eliasof S, Jahr CE (1996) Proc Natl Acad Sci USA **93** 4153-8.

Eliasof S, Werblin F (1993) J Neurosci. **13** 402-11.

Engleman DM, Steitz TA, Goldman A (1986) Annu Rev Biophys Biophys Chem **15** 321-353.

Erecinska M, Wantorsky D, Wilson DF (1983) J Biol Chem **258** 9069-9077.

Fairman WA, Vandenberg RJ, Arriza JL, Kavanaugh MP, Amara SG (1995) Nature **375** 599-603.

Grant GB, Dowling JE (1995) J Neurosci **15** 3852-62.

Grant GB, Werblin FS (1996) Vis Neurosci **13** 135-144.

Jan LY, Jan YN (1976) J Physiol **262** 215-236.

Kanai Y, Hediger MA (1992) Nature **360** 467-471.

Kanner BI, Bendahan A (1982) Biochemistry **21** 6327-6330.

Kavanaugh MP, Bendahan A, Zerangue N, Zhang Y, Kanner BI (1997) J Biol Chem **272** 1703-1708.

Kekuda R, Prasad PD, Fei Y-J, Torres-Zamorano V, Sinha S, Yang-Feng TL, Leibach FH, Ganapathy V (1996) J Biol Chem **271** 18657-18661.

Lawler HC (1961) J Biol Chem **236** 2296-2301.

Lea TJ, Usherwood PNR (1973) Comp gen Pharmac **4** 333-350.

Lopeta M, Cleveland D, Sollner-Webb B (1994) Nucleic Acids Res **12** 5707-5717.

Mennerick S, Zorumski CF (1994) Nature **368** 59-62.

Otis TS, Wu YC, Trussell LO (1996) J Neurosci **16** 1634-1644.

Picaud S, Larsson HP, Wellis DP, Lecar H, Werblin F (1995a) Proc. Natl Acad Sci USA **92** 9417-21.

Picaud SA, Larsson HP, Grant GB, Lecar H, Werblin FS (1995b) J Neurophysiol **74** 1760-1771.

Pines G, Danbolt NC, Bjoras M, Zhang Y, Bendahan A, Eide L, Koepsell H, Storm-

Mathisen J, Seeberg E, Kanner BI (1992) Nature **360** 464-467.

Pines G, Zhang Y, Kanner BI (1995) J Biol Chem **270** 17093-17097.

Quan F, Wolfgang W, Forte M (1993) Proc Nat Acad Sci **90** 4236-4240.

Rauen T, Rothstein JD, Wassle H (1996) Cell TIssue Res **286** 325-336.

Rothstein JD (1995) In: Pathogenesis and Therapy of Amyotrophic Lateral Sclerosis (G. Serratrice & T. Munsat, Ed.), pp. 7-20. Philadelphia: Lippincott-Raven Publishers.

Rothstein JD, Martin L, Levey AI, Dykes-Hoberg M, Jin L, Wu D, Nash N, Kuncl RW (1994) Neuron **13** 713-25.

Schwartz EA, Tachibana M (1990) J Physiol **426** 43-80.

Shafqat S, Tamarappoo BK, Kilberg MS, Puranam RS, Mcnamara JO, Guadaño-Ferraz A, Fremeau RT, Jr. (1993) J Biol Chem **268** 15351-15355.

Slotboom DJ, Lolkema JS, Konings WN (1996) J Biol Chem **271** 31317-31321.

Storck T, Schulte S, Hofmann K, Stoffel W (1992) Proc Natl Acad Sci USA **89** 10955-10959.

Taylor P, Radic Z (1994) Annu Rev Pharmacol Toxicol **34** 281-320.

Tong G, Jahr CE (1994) Neuron **13** 1195-203.

Utsunomiya-Tate N, Endou H, Kanai Y (1996) J Biol Chem **271** 14883-14890.

Vandenberg RJ, Arriza JL, Amara SG, Kavanaugh MP (1995) J Biol Chem **270** 17668-17671.

Wadiche JI, Amara SG, Kavanaugh MP (1995a) Neuron **15** 721-728.

Wadiche JI, Arriza JL, Amara SG, Kavanaugh MP (1995b) Neuron **14** 1019-27.

Wafford KA, Sattelle DB (1989) J Exp Biol **144** 449-462.

Wahle S, Stoffel W (1996) J Cell Biol **135** 1867-1877.

Wilson IB, Harrison MA (1961) J Biol Chem **236** 2292-2295.

Yamada K, Watanabe M, shibata T, Tanaka K, Wada K, Inoue Y (1996) Neuroreport **7** 2013-2017.

Zerangue N, Kavanaugh MP (1996a) Nature **383** 634-637.

Zerangue N, Kavanaugh MP (1996b) J Physiol **493 (2)** 419-423.

Zorumski CF, Olney JW (1993) Pharmacol Ther **59** 145-162.